ISSN 2686-7575 (Online)

ТОНКИЕ ХИМИЧЕСКИЕ ТЕХНОЛОГИИ

Fine Chemical Technologies

- Theoretical Bases of Chemical Technology
- Chemistry and Technology of Organic Substances
- Chemistry and Technology of Medicinal Compounds and Biologically Active Substances
- Biochemistry and Biotechnology
- Synthesis and Processing of Polymers and Polymeric Composites
- Chemistry and Technology of Inorganic Materials
- Analytical Methods in Chemistry and Chemical Technology
- Mathematical Methods and Information Systems in Chemical Technology

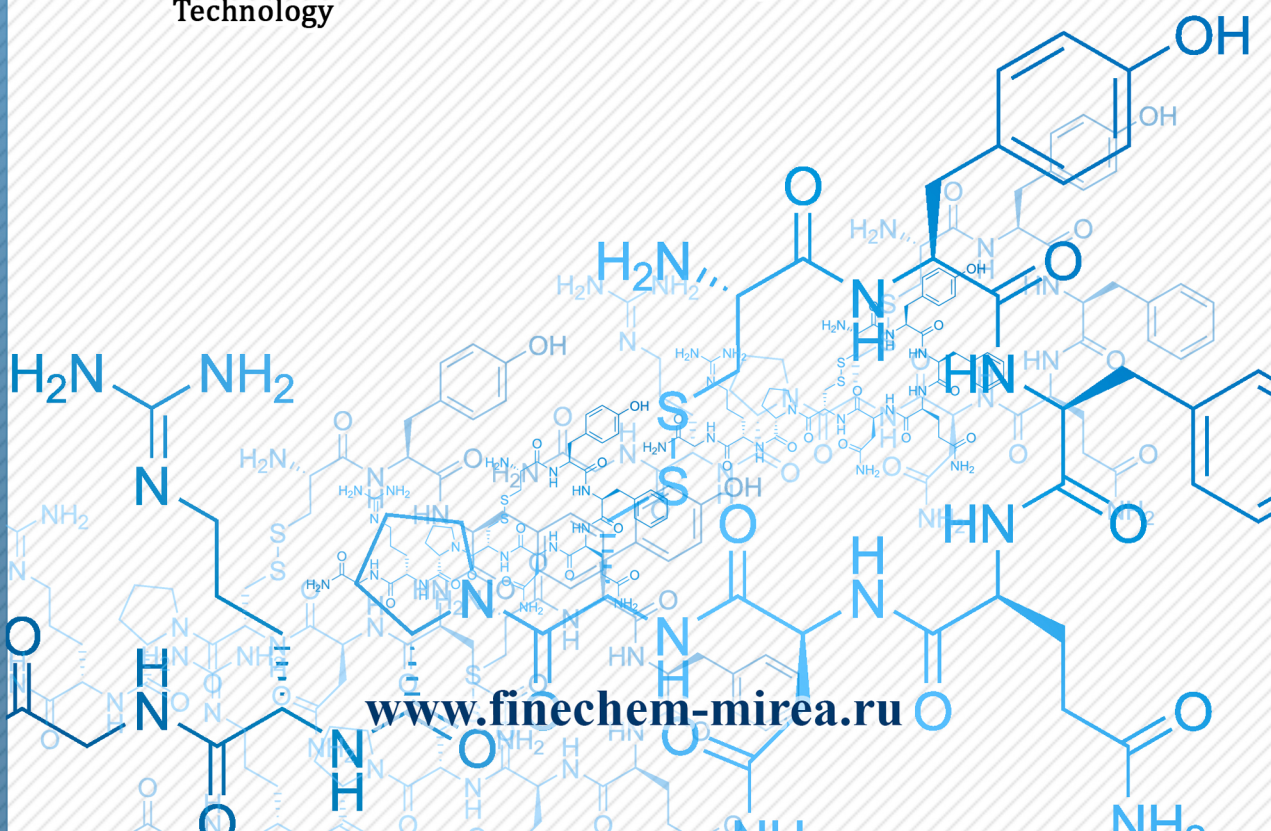

19(2)
2024

www.finechem-mirea.ru

ISSN 2686-7575 (Online)

ТОНКИЕ ХИМИЧЕСКИЕ ТЕХНОЛОГИИ

Fine Chemical Technologies

- Theoretical Bases of Chemical Technology
- Chemistry and Technology of Organic Substances
- Chemistry and Technology of Medicinal Compounds and Biologically Active Substances
- Biochemistry and Biotechnology
- Synthesis and Processing of Polymers and Polymeric Composites
- Chemistry and Technology of Inorganic Materials
- Analytical Methods in Chemistry and Chemical Technology
- Mathematical Methods and Information Systems in Chemical Technology

Tonkie Khimicheskie Tekhnologii = Fine Chemical Technologies.
Vol. 19, No. 2, 2024

Тонкие химические технологии = Fine Chemical Technologies.
Том 19, № 2, 2024

https://doi.org/10.32362/2410-6593-2024-19-2
www.finechem-mirea.ru

**Tonkie Khimicheskie Tekhnologii =
Fine Chemical Technologies
2024, Vol. 19, No. 2**

The peer-reviewed scientific and technical journal Fine Chemical Technologies highlights the modern achievements of fundamental and applied research in the field of fine chemical technologies, including theoretical bases of chemical technology, chemistry and technology of medicinal compounds and biologically active substances, organic substances and inorganic materials, biochemistry and biotechnology, synthesis and processing of polymers and polymeric composites, analytical and mathematical methods and information systems in chemistry and chemical technology.

Founder and Publisher

Federal State Budget
Educational Institution of Higher Education
"MIREA – Russian Technological University"
78, Vernadskogo pr., Moscow, 119454, Russian Federation.
Publication frequency: bimonthly.
The journal was founded in 2006. The name was Vestnik MITHT until 2015 (ISSN 1819-1487).

The journal is included into the List of peer-reviewed science press of the State Commission for Academic Degrees and Titles of the Russian Federation.

The journal is indexed: SCOPUS, DOAJ, Chemical Abstracts, Science Index, RSCI, Ulrich's International Periodicals Directory

86, Vernadskogo pr., Moscow, 119571, Russian Federation.
Phone: +7 (499) 600-80-80 (#31288)
E-mail: *seredina@mirea.ru*

The registration number ПИ № ФС 77–74580 was issued in December 14, 2018 by the Federal Service for Supervision of Communications, Information Technology, and Mass Media of Russia

The subscription index of *Pressa Rossii*: **36924**

**Тонкие химические технологии =
Fine Chemical Technologies
2024, том 19, № 2**

Научно-технический рецензируемый журнал «Тонкие химические технологии» освещает современные достижения фундаментальных и прикладных исследований в области тонких химических технологий, включая теоретические основы химической технологии, химию и технологию лекарственных препаратов и биологически активных соединений, органических веществ и неорганических материалов, биохимию и биотехнологию, синтез и переработку полимеров и композитов на их основе, аналитические и математические методы и информационные системы в химии и химической технологии.

Учредитель и издатель

федеральное государственное бюджетное
образовательное учреждение высшего образования
«МИРЭА – Российский технологический университет»
119454, РФ, Москва, пр-т Вернадского, д. 78.
Периодичность: один раз в два месяца.
Журнал основан в 2006 году. До 2015 года издавался под названием «Вестник МИТХТ» (ISSN 1819-1487).

Журнал входит в Перечень ведущих рецензируемых научных журналов ВАК РФ.

Индексируется: SCOPUS, DOAJ, Chemical Abstracts, РИНЦ (Science Index), RSCI, Ulrich's International Periodicals Directory

119571, Москва, пр. Вернадского, 86, оф. Л-119.
Тел.: +7 (499) 600-80-80 (#31288)
E-mail: *seredina@mirea.ru*

Регистрационный номер и дата принятия решения о регистрации СМИ: ПИ № ФС 77-74580 от 14.12.2018 г. СМИ зарегистрировано Федеральной службой по надзору в сфере связи, информационных технологий и массовых коммуникаций (Роскомнадзор)

Индекс по Объединенному каталогу «Пресса России»: **36924**

EDITORIAL BOARD

РЕДАКЦИОННАЯ КОЛЛЕГИЯ

Contents

СОДЕРЖАНИЕ

Tonkie Khimicheskie Tekhnologii = Fine Chemical Technologies.
2024;19(2):95–103 ISSN 2686-7575 (Online)

Theoretical bases of chemical technology
Теоретические основы химической технологии

UDC 66.03
https://doi.org/10.32362/2410-6593-2024-19-2-95-103

RESEARCH ARTICLE

Preparation of fine suspensions using stirred media bead mill

Larisa S. Elinevskaya, Danil V. Dzardanov, Olga V. Ulybina, Roman N. Ivanov✉
Firma August, Moscow, 129515 Russia
✉ *Corresponding author, e-mail: r.ivanov@avgust.com*

Abstract

Objectives. To determine the change patterns for the main physical properties of suspensions after their grinding in bead mills, with the prospect of optimizing the preparation technology and extending the results obtained to other dispersed phases.

Methods. The study used the Fraunhofer laser diffraction method to determine particle size. The obtained data on the particle size distribution of suspensions were qualitatively verified by optical microscopy. The Brookfield relative viscosity method was used to evaluate the rheological properties of the resulting suspensions. The density of the resulting suspensions was measured by the hanging method using a calibrated pycnometer.

Results. The dependencies of the change in the particle size distribution after grinding in a bead mill were established. The viscosity of the suspensions was observed to increase following grinding. Common regularities of changes in the density of the considered suspensions were established.

Conclusions. The conducted studies showed that the physical and mechanical properties of suspensions are affected by the type and the filling ratio of the grinding media; the residence time of the suspension in the grinding chamber; the number of grinding operations; mill designs.

Keywords

bead mill, stirred media mill, grinding, particle size distribution, suspensions, disperse systems, Fraunhofer diffraction, suspension viscosity

Submitted: 01.03.2023
Revised: 12.05.2023
Accepted: 14.03.2024

For citation

Elinevskaya L.S., Dzardanov D.V., Ulybina O.V., Ivanov R.N. Preparation of fine suspensions using stirred media bead mill. *Tonk. Khim. Tekhnol. = Fine Chem. Technol*. 2024;19(2):95–103. https://doi.org/10.32362/2410-6593-2024-19-2-95-103

НАУЧНАЯ СТАТЬЯ

Приготовление тонкодисперсных суспензий с использованием бисерных мельниц

Л.С. Елиневская, Д.В. Дзарданов, О.В. Улыбина, Р.Н. Иванов✉

Фирма Август, Москва, 129515 Россия

✉ *Автор для переписки, e-mail: r.ivanov@avgust.com*

Аннотация

Цели. Изучение закономерностей изменения основных физических свойств суспензий после их измельчения в бисерных мельницах с перспективой оптимизации технологии приготовления и распространения полученных результатов на другие дисперсионные фазы.

Методы. Размеры частиц определяли с помощью лазерной дифракции Фраунгофера. Полученные данные по дисперсному составу суспензий качественно проверяли оптической микроскопией. Для оценки реологических свойств полученных суспензий использовали метод определения кажущейся динамической вязкости по Брукфильду. Плотность полученных суспензий измеряли навесным методом с помощью калиброванного пикнометра.

Результаты. Установлены зависимости изменения дисперсного состава после измельчения суспензий в бисерной мельнице. Было обнаружено увеличение вязкости суспензий после процесса размола. Установлены общие закономерности изменения плотности рассматриваемых суспензий.

Выводы. Проведенные исследования показали, что на физико-механические свойства суспензий влияют вид и степень загрузки используемого бисера, время пребывания суспензии в размольной камере, количество операций измельчения, конструкции мельницы.

Ключевые слова

бисерная мельница, диспергирование, размер частиц, суспензии, функции распределения частиц, микрогетерогенные дисперсные системы, дифракция Фраунгофера, вязкость суспензий

Поступила: 01.03.2023
Доработана: 12.05.2023
Принята в печать: 14.03.2024

Для цитирования

Елиневская Л.С., Дзарданов Д.В., Улыбина О.В., Иванов Р.Н. Приготовление тонкодисперсных суспензий с использованием бисерных мельниц. *Тонкие химические технологии*. 2024;19(2):95–103. https://doi.org/10.32362/2410-6593-2024-19-2-95-103

INTRODUCTION

Heterogeneous systems in the form of suspensions are widely applicable and convenient products in many areas of production and human activity. Depending on the application and the physicochemical properties of their constituent components, suspensions vary greatly in terms of their quality characteristics and the methods used to produce them. This present work sets out to examine the process of obtaining finely dispersed products using bead mills.

Bead mills have become widespread in recent years in such areas as the production of plant protection chemicals, paints, pharmaceuticals and food products, as well as in the production of building materials, extraction of natural resources, etc. Compared with other dispersion devices, bead mills typically have lower energy costs for the grinding process [1]. However, despite the fairly wide distribution of such devices, the regularities of their operation have so far been poorly studied [2]. This, in particular, can be due to the complexity of the processes occurring in them during grinding, which involve a significant number of parameters [3] that affect the actual grinding of dispersion phase particles. In addition to purely technological characteristics, such as the size, hardness and degree of filling of the grinding bodies, suspension flow rate, mill design, etc., it is also worth noting the ongoing increase in the active surface area of the ground components. This, in turn, can be associated with various surface phenomena affecting the final product. In addition, the very concept of quality is determined by a different combination of physical and chemical characteristics depending on its intended purpose. Among these characteristics, in addition to particle size before and after grinding, it is also worth noting the rheological behavior of suspensions, their aggregation and sedimentation stability, as well as the uniformity of distribution of particles of the dispersion phase, etc.

The construction of a single algorithm based on available theories and capable of including all of the

above parameters for working with a bead mill often appears as a more labor-intensive and complex than the grinding itself. For this reason, the operating modes of such devices are typically selected on an *ad hoc* basis [2, 4]. However, this results in a lack of numerical data on the process of grinding suspensions in bead mills. Approaches to the theoretical description of the operating patterns of bead mills are presented in [1, 3, 5–14] together with some data obtained from experimental studies.

The purpose of the present work is to refine the above-mentioned theoretical basis, experimentally study the influence of the main technological parameters of bead mills on the physical and mechanical properties of the resulting suspensions (disperse composition, viscosity, and density), as well as to identify possible regularities for their further extension to other systems and practical application in production processes.

MATERIALS AND METHODS

The objects of study were aqueous suspensions of chalk and kaolin, which are used in the production of a number of products: plant protection agents, fine fillers, building materials and building mixtures, paper and glass products, paints, cosmetics, etc. The process of grinding suspensions in bead mills is directly associated with colloidal phenomena. In particular, the surface area of the solid phase, which increases during grinding, can interact differently with the dispersion medium, which does not exclude the formation of aggregates from the resulting crushed particles. The studied water suspensions of chalk and kaolin have sufficient aggregative stability, which makes it possible to neglect the influence of surface phenomena on the grinding process.

Experiments were carried out on LabStar (*Netzsch*, Germany) and MultiLab (*WAB*, Switzerland) laboratory mills. These machines differ in terms of the size of the grinding chambers, the types of mixing devices on the rotor, and the systems for separating beads from the product. The LabStar mill grinding chamber has a volume of 0.9 L, an internal diameter of 90 mm, and a length of 187.9 mm. A mesh cartridge with a centrifugal bead ejection system is used as a system for separating beads from the product. In the LabStar mill, ZetaBeads (*Netzsch*, Germany) 0.6 ceramic beads with a load of 61.7 vol % were used as grinding media.

The MultiLab grinding chamber has a volume of 0.561 L, an internal diameter of 77 mm, and a length of 150 mm. A slot classifier (*WAB*, Switzerland) was used as a system for separating beads from the product. Glass beads SL 7505 (*Sigmund Lindner GmbH*, Germany) with a load of 80 vol % were used as grinding media in this mill.

During the experiments, chalk of MTD-2 grade (*MelStrom*, Russia), dry enriched kaolin from the Chekmakul deposit (GOST 19608-84[1], *Novokaolinovyi GOK*, Russia) was used with distilled water according to GOST R 58144-2018[2]. The solid content phase in the chalk suspension was 40 wt %, while in the aqueous suspension of kaolin, it was 25 wt %. The experiments were carried out on a laboratory installation as depicted in Fig. 1. The suspension was prepared in beaker B_1. A paddle mixer was used for mixing. A predetermined amount of chalk or kaolin was added into a given amount of water with continuous stirring. After loading all the components, the resulting suspension was additionally stirred for 10–15 min. Then a sample of the resulting suspension was taken to measure its initial dispersion, viscosity, and density.

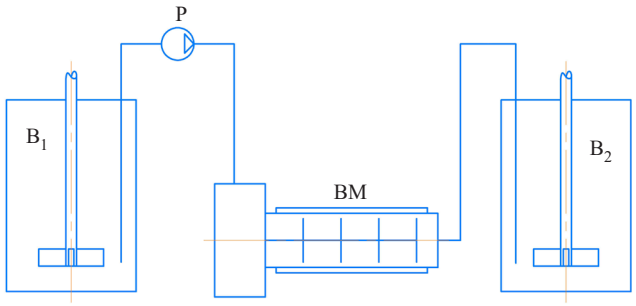

Fig. 1. Scheme of the laboratory assembly: B_1 and B_2 are chemical beakers with an overhead stirrer; P is a peristaltic pump; BM is an agitator bead mill

After preparing the initial suspension and setting certain experimental parameters, the suspension was ground in a continuous mode. The initial suspension was fed into a bead mill (BM) using a peristaltic pump (H) equipped with a supply hose with a diameter of 13 × 2.5 mm. Filling of the mills was typically performed at a pump rotor speed of 15 rpm. A mill rotor speed for the LabStar mill was 1000 rpm, while for the MultiLab mill, filling was carried out in rotor-off mode. In all the experiments, the pump rotor speed during the grinding process was 50 rpm, which corresponds to a volumetric flow rate of V = 350 mL/min for the LabStar mill and V = 195 mL/min for the MultiLab mill. In all the experiments, the rotor speed ω of the LabStar mill was 3000 rpm, while that of the MultiLab was 2986 rpm. Immediately after the suspension in B_1 ran out, the grinding process was stopped. Next, in order

[1] GOST 19608-84. State Standard of the USSR. Enriched kaolin for rubber and plastic products, artificial leather and fabrics. Technical conditions. Moscow: USSR State Committee for Standards; 1984.

[2] GOST R 58144-2018. National Standard of the Russian Federation. Distilled water. Technical conditions. Moscow: Russian Institute of Standardization; 2022.

to average the properties, the resulting suspension was stirred in beaker B_2 for 10–15 min. Then a sample was taken to measure the dispersion, viscosity, and density of the finished product. Finally, beakers B_2 and B_1 were swapped, and additional sampling passes were carried out.

The mill jackets were connected to a liquid thermostat. The latter was set at 3°C and filled with a water-glycol solution. During each experiment, technological parameters were recorded, and analysis of the dispersed composition, viscosity and density of the resulting suspensions—the most general characteristic properties of suspensions—was carried out.

The dispersed composition of the suspensions under study was measured using a Mastersizer 2000 laser particle analyzer (*Malvern Instruments*, UK). A sample of the suspension in an amount of 1 g was added to 30 g of distilled water and stirred for 2 min by a glass rod with a rubber tip. After placing the resulting suspension in a measuring cell, the particle size was measured. To assess the dispersed composition of the crushed materials, the following characteristics were selected [15]:

- percentage of particles with the size less than 5 μm, a_5;
- weighted average volume diameter of particles, $d(4,3)$[3].

The density of the initial suspensions was measured by the hanging method using a pycnometer according to GOST 319992.1[4]. The apparent dynamic viscosity of suspensions η was measured on a Brookfield viscometer (*AMETEK Brookfield*, USA) in accordance with GOST 25271-93[5] at three different spindle speeds, n: 20, 60 and 100 rpm.

RESULTS AND DISCUSSION

From the data presented in Figs. 2 and 3, the distribution peak for the suspensions of chalk and kaolin shifts to the left after one pass—to the region of lower particle sizes. In this case, the distribution of particles has become more monomodal.

The $d(4.3)$ value for chalk suspensions in one pass changed from 9.76 to 2.25 μm, for kaolin—from 23.55 to 17.09 μm. The change in the viscosity of the resulting suspensions associated with a decrease in the particle size of the solid phase can be seen in the graphs shown in Fig. 4. According to the dependencies, the apparent dynamic viscosity at low rotation speeds of the viscometer spindle after one pass increases about 200-fold for chalk suspensions and almost 4-fold for kaolin suspensions. Here it is worth noting that the viscosity of the finished suspensions depends not only on the particle size, but also on the physicochemical properties of the dispersed phase and the dispersion medium. The main substance in kaolin suspensions—kaolinite—can swell in water, thus forming fragile structures. Thus, despite the higher $d(4.3)$, these dispersed systems have a higher viscosity than more loaded chalk suspensions. At increased rotation speed of the viscometer spindle, the shear rate in the test sample also increases. Thus, it can be argued on the basis of the dependencies shown in Fig. 4 that all the suspensions under consideration are pseudoplastic fluids.

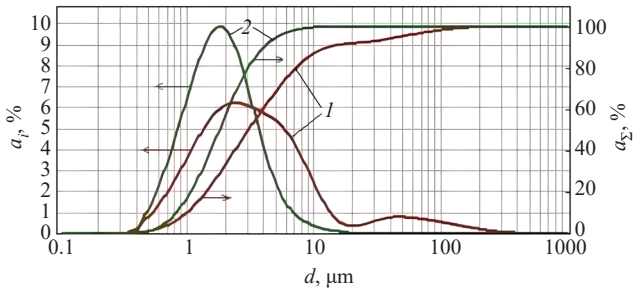

Fig. 2. Differential a_i and integral a_Σ size distribution functions of the chalk suspension particles in water for different number of passes:
(*1*) initial suspension;
(*2*) one pass

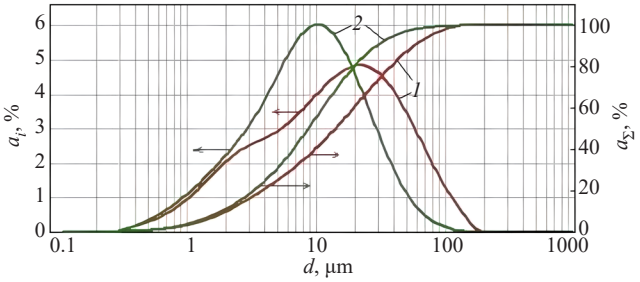

Fig. 3. Differential a_i and integral a_Σ size distribution functions of the kaolin suspension particles in water for different number of passes:
(*1*) initial suspension;
(*2*) one pass

From the data given in Table 1 it can be seen that the density of chalk and kaolin suspensions after grinding increases and is close to the density calculated using the formula for the additivity of specific volumes of solid and liquid phases. Apparently, this is due to the fact that

[3] $d(4,3)$—De Broecker or Harden average diameter—weighted average by mass or volume (average diameter of a sphere of equivalent volume), is the center of mass for density distribution functions in volume/mass units.

[4] GOST 319992.1. Interstate Standard. Paint and varnish materials. Method for determining density. Part 1. Pycnometric method. Moscow: Standartinform; 2013.

[5] GOST 25271-93. Interstate Standard. Plastics. Liquid resins, emulsions or dispersions. Determination of apparent viscosity according to Brookfield. Minsk: Interstate Council for Standardization, Metrology and Certification; 1993.

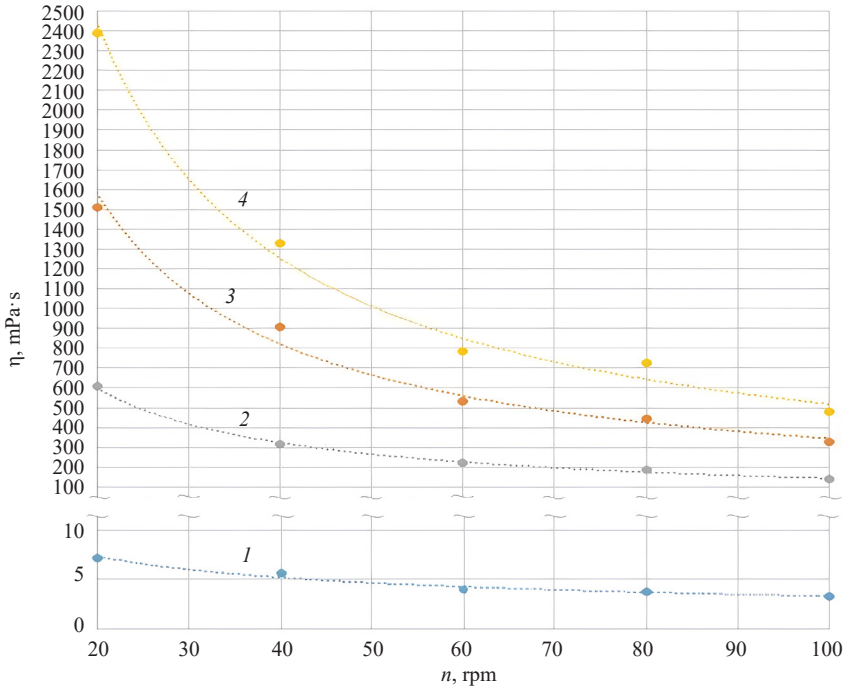

Fig. 4. Dependence of the relative viscosity of suspensions on the frequency of rotation of the viscometer spindle (LabStar mill):
(*1*) the initial suspension of chalk;
(*2*) the initial suspension of kaolin;
(*3*) the suspension of chalk after one pass;
(*4*) the suspension of kaolin after one pass

Table 1. Density of the studied suspensions depending on the degree of grinding

Suspension	Density of suspension after grinding, kg/m^3	Density of suspension after one pass grinding, kg/m^3	Calculated density of suspension, kg/m^3
40% chalk in water	1316	1333	1341
25% kaolin in water	1162	1180	1182

during the grinding process, air contained in aggregates and agglomerates of solid phase particles is released.

When studying the multi-pass grinding mode using chalk suspensions as an example, the distribution peak was observed to shift to the left and the suspension become monodisperse as the number of passes increases (Fig. 5). After three passes, the value of the weighted average volumetric diameter $d(4.3)$ changed from 9.76 to 1.77 μm. It is clear from the dependencies shown in Fig. 6 that the viscosity of the resulting suspensions increases with the number of passes. Over three grinding cycles, the viscosity index at a viscometer spindle speed of 20 rpm increased by approximately 500 times.

An optical microscope (*Olympus*, Japan) was additionally used for studying the dispersed composition of the initial and resulting suspensions. Figure 7 depicts samples of such suspensions. In particular, the photo of the initial suspensions (Fig. 7a) reveals rather large crystalline particles of the solid phase. Following three

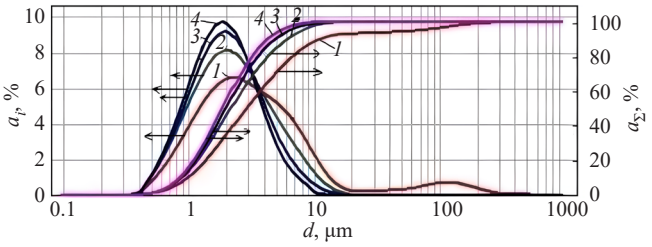

Fig. 5. Particle size distribution of chalk suspension particles in water with different number of passes (LabStar mill):
(*1*) initial suspension;
(*2*) one pass;
(*3*) two passes;
(*4*) three passes

grinding operations, all dispersed phase particles are smaller and more uniform in size (Fig. 7b).

The results show that, at the same number of passes, the particles with the size less than 5 μm for a chalk

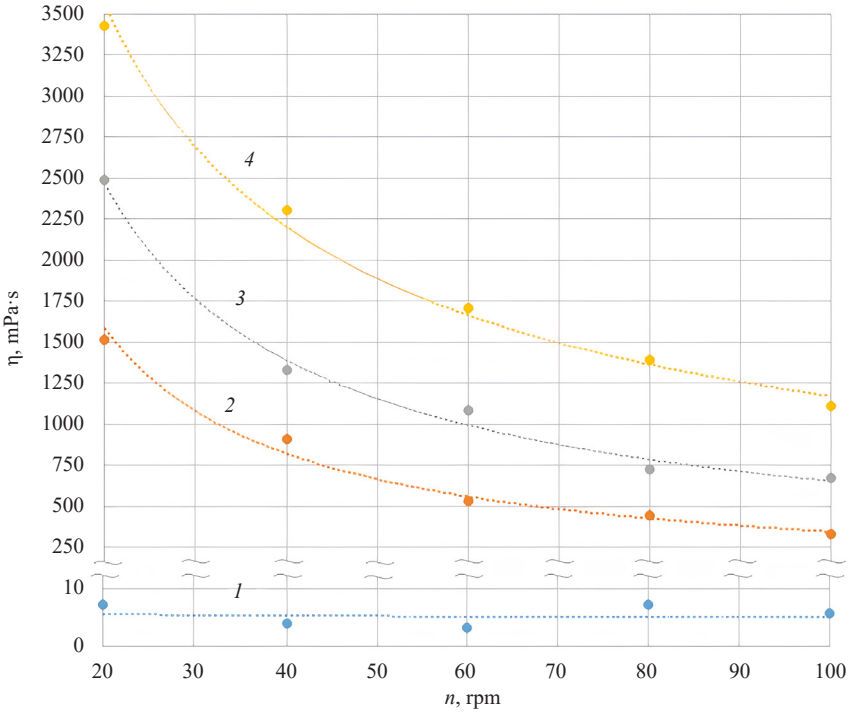

Fig. 6. Dependence of the relative viscosity of chalk suspensions on the speed of rotation of the viscometer spindle:
(*1*) initial suspension;
(*2*) one pass;
(*3*) two passes;
(*4*) three passes

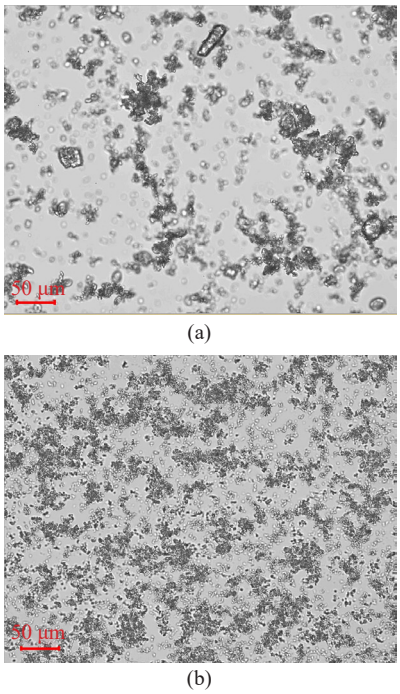

Fig. 7. Image of the initial suspension of chalk (a)
and the suspension after three passes (b)
(optical microscope)

suspension under experimental conditions is better ground in a LabStar mill than in a MultiLab mill (Fig. 8). Parameter a_5 changed in three passes from 68 to 94.1% for MultiLab and from 68 to 99.9% for LabStar. The weighted average volumetric diameter $d(4.3)$ changed in 3 passes from 9.76 to 2.27 μm for MultiLab and from 9.76 to 1.77 μm for LabStar.

As noted in [3], the average residence time of suspension particles in bead mills can be calculated using the formula (1):

$$\overline{\tau} = \frac{V_{fr} - V_b}{V}, \quad (1)$$

where V_{fr} is the free volume of the grinding chamber without beads, m^3; V_b is the total volume of bead particles, m^3; V is the volumetric flow rate of the suspension, m^3/s.

Calculation using formula (1) showed that the average residence time is 98 s for the LabStar mill and 87 s for the MultiLab mill. Thus, it will take a few seconds longer to process the solid particles in the grinding chamber of the LabStar mill.

It was proposed in [5] to introduce two parameters in order to estimate the specific energy E_m expended on the grinding process in bead mills: *SN* (number of stress events)—the number of grinding events; and *SI* (stress intensity)—collision intensity (formulas (2) and (3)):

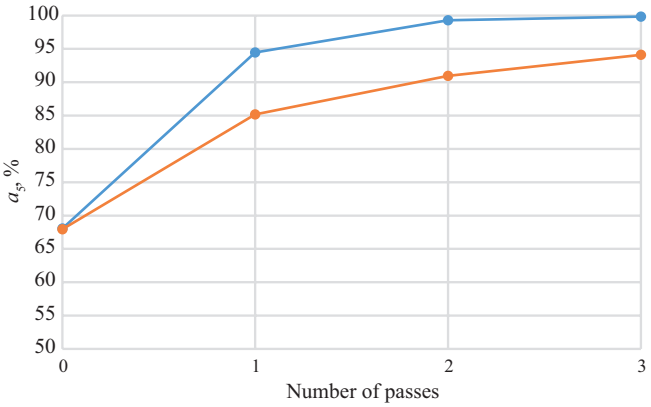

Fig. 8. Dependence of parameter a_5 for chalk suspension on the number of passes:
(*1*) MultiLab mill;
(*2*) LabStar mill

$$SN \propto \frac{\varphi_b(1-\varepsilon)}{(1-\varphi_b(1-\varepsilon))x_V} \cdot \frac{\omega\tau}{d_b^2}, \quad (2)$$

where ω is the rotation speed of the mill rotor, rpm; τ is mill operating time, s; φ_b is the volume fraction of beads in the grinding chamber; ε is bead porosity; d_b is the diameter of beads, m; x_V is the volume fraction of the solid phase in the suspension.

$$SI \propto d_b^3 \rho_b \upsilon_r^2 , \quad (3)$$

where d_b is the diameter of the beads, m; ρ_b is the bead density, kg/m^3; υ_r is the maximum linear speed of the mill rotor, m/s.

When calculating the *SN* parameters using dependence (2), it was found that the number of grinding events for the LabStar mill is approximately 3.6 times higher than for the MultiLab mill (Table 2). When calculating the *SI* parameters using dependence (3), the intensity of bead collision in the MultiLab mill was found to be approximately 5.6 times higher than in the LabStar mill (Table 2), although the peripheral rotation speeds of the mill rotors υ are quite close: for MultiLab, υ was 10.00 m/s, and for LabStar, 9.73 m/s.

When estimating the expended specific energy E_m, the following expression can also be used [5] (formula (4)):

$$E_m \propto SI \cdot SN , \quad (4)$$

Calculations using dependence (4) showed that the specific energy spent on the grinding process in the MultiLab mill is approximately 1.5 times higher than in the LabStar mill (Table 2).

Table 2. Results of the analysis of experimental data

Agitator bead mill	$\bar{\tau}$, s	*SN*	*SI*	*SI* · *SN*
LabStar (Netzsch)	98	$3.41 \cdot 10^{10}$	$1.56 \cdot 10^{-4}$	$5.32 \cdot 10^{6}$
MultiLab (WAB)	87	$0.947 \cdot 10^{10}$	$8.74 \cdot 10^{-4}$	$8.28 \cdot 10^{6}$

CONCLUSIONS

The dependencies of the basic physicochemical properties of aqueous suspensions of chalk and kaolin on the parameters of their grinding in bead mills were studied. It was established that the type of differential and integral curves following the grinding process changes in the same manner for different suspensions: both the weighted average volume diameter and the dispersion of particle sizes decrease. The viscosity of suspensions was also found to increase after grinding; this occurred regardless of the nature of the dispersion phase and its ability to form associates. The density of the suspensions under study tends to increase during the preparation process and with approaches that are calculated by the additivity rule. It was shown that changes in the main parameters of suspensions after grinding can be influenced by the properties and degree of filling of the beads and the residence time of the suspension in the grinding chamber. According to the results of a numerical assessment of the energy consumed, grinding in the LabStar mill turned out to be more energy efficient under experimental conditions than in the MultiLab mill.

Acknowledgments

The work was carried out using raw materials and equipment of the R&D department of *Firma August*. The authors thank the company's management for supporting scientific and research activities in the field of wet grinding technologies.

Authors' contributions

L.S. Elinevskaya—research idea, planning experiments, analyzing and discussing the results, and editing the text of the article.

D.V. Dzardanov—development of a methodology for conducting an experiment, participation in experimental work, and discussion of the results.

O.V. Ulybina—participation in experiments, processing of the obtained data, and participation in editing the text of the article.

R.N. Ivanov—search for scientific publications on the topic of the article, formation of a list of references, setting up and conducting experiments, processing the data obtained, and writing and formatting the text of the article.

The authors declare no conflict of interest.

REFERENCES

1. Stehr N. *Zerkleinerung und Materialtransport in einer Rührwerkskugelmühle*. Dissertation. Braunschweig: Techn. Univ.; 1982. 199 p.
2. Ostrovskii G.M. *Novyi spravochnik khimika i tekhnologa. Protsessy i apparaty khimicheskikh tekhnologii* (*New Handbook of Chemist and Technologist. Processes and Apparatuses of Chemical Technologies*). St. Petersburg: Professional; 2004. Part 1. 848 p. (in Russ.).
3. Schwedes J., Bunge F. Comminution and transport behaviour in agitated ball mills. *Adv. Powder Technol*. 1992;3(1):55–70. https://doi.org/10.1016/s0921-8831(08)60689-5
4. Aksyonov A.V., Vasiliev A.A., Okhotin V.N., Shvets A.A. Application of ultrafine grinding for mineral raw materials processing. *Izvestiya. Non-Ferrous Metallurgy*. 2014;2:20–25 (in Russ.). https://doi.org/10.17073/0021-3438-2014-2-20-25
5. Kwade A., Schwedes J. Breaking characteristics of different materials and their effect on stress intensity and stress number in stirred media mills. *Powder Technol*. 2002;122(2–3):109–121. https://doi.org/10.1016/s0032-5910(01)00406-5
6. Blecher L., Kwade A., Schwedes J. Motion and stress intensity of grinding beads in a stirred media mill. Part 1: Energy density distribution and motion of single grinding beads. *Powder Technol*. 1996;86(1):59–68. https://doi.org/10.1016/0032-5910(95)03038-7
7. Kwade A. Determination of the most important grinding mechanism in stirred media mills by calculating stress intensity and stress number. *Powder Technol*. 1999;105(1–3):382–388. https://doi.org/10.1016/s0032-5910(99)00162-x
8. Weit H., Schwedes J. Scale-up of power consumption in agitated ball mills. *Chem. Eng. Technol.* 1987;10(1):398–404. https://doi.org/10.1002/ceat.270100149
9. Austin L.G. Understanding Ball Mill Sizing. *Ind. Eng. Chem. Process Des. Dev.* 1973;12(2):121–129. https://doi.org/10.1021/i260046a001
10. Kwade A., Schwedes J. Chapter 6. Wet Grinding in Stirred Media Mills. *Handbook of Powder Technology*. 2007;12:251–382. https://doi.org/10.1016/S0167-3785(07)12009-1
11. Sterling D., Breitung-Faes S., Kwade A. Experimental evaluation of the energy transfer within wet operated stirred media mills. *Powder Technol*. 2023;425:118579. https://doi.org/10.1016/j.powtec.2023.118579
12. Böttcher A.-C., Schilde C., Kwade A. Experimental assessment of grinding bead velocity distributions and stressing conditions in stirred media mills. *Adv. Powder Technol.* 2021;32(2):413–423. https://doi.org/10.1016/j.apt.2020.12.022
13. Nöske M., Müller J., Nowak C., Li K., Xu X., Breitung-Faes S., Kwade A. Multicomponent Comminution within a Stirred Media Mill and Its Application for Processing a Lithium-Ion Battery Slurry. *Processes*. 2022;10(11):2309. https://doi.org/10.3390/pr10112309
14. Fragnière G., Naumann A., Schrader M., Kwade A., Schilde C. Grinding Media Motion and Collisions in Different Zones of Stirred Media Mills. *Minerals*. 2021;11(2):185. https://doi.org/10.3390/min11020185
15. Rawle A. Basic of principles of particle-size analysis. *Surf. Coatings Int. Part A: Coatings J.* 2003;86(2):58–65.

About the authors

Larisa S. Elinevskaya, Cand. Sci. (Chem.), Head of the Department for the Development of Preparative Forms, Firma August (6, Tsandera ul., Moscow, 129515, Russia). E-mail: l.elinevskaya@avgust.com. Scopus Author ID 56423694700, https://orcid.org/0009-0001-0859-9017

Danil V. Dzardanov, Head of the Department for the Development of Solid and Combined Preparative Forms, Firma August (6, Tsandera ul., Moscow, 129515, Russia). E-mail: d.dzardanov@avgust.com. Scopus Author ID 36962497300, RSCI SPIN-code 3795-1236, https://orcid.org/0000-0002-7122-6731

Olga V. Ulybina, Head of the Department for the Development of Liquid Preparative Forms, Firma August (6, Tsandera ul., Moscow, 129515, Russia). E-mail: o.ulybina@avgust.com. Scopus Author ID 36847255500, https://orcid.org/0000-0002-1529-5855

Roman N. Ivanov, Senior Researcher, Department for the Development of Solid and Combined Preparative Forms, Firma August (6, Tsandera ul., Moscow, 129515, Russia). E-mail: r.ivanov@avgust.com. ResearcherID HKF-3424-2023, RSCI SPIN-code 1923-5088, https://orcid.org/0000-0002-1664-0980

Об авторах

Елиневская Лариса Степановна, к.х.н., начальник департамента разработки препаративных форм, АО Фирма «Август» (129515, Россия, Москва, ул. Цандера, д. 6). E-mail: l.elinevskaya@avgust.com. Scopus Author ID 56423694700, https://orcid.org/0009-0001-0859-9017

Дзарданов Данил Валентинович, начальник отдела разработки твердых и комбинированных препаративных форм, АО Фирма «Август» (129515, Россия, Москва, ул. Цандера, д. 6). E-mail: d.dzardanov@avgust.com. Scopus Author ID 36962497300, SPIN-код РИНЦ 3795-1236, https://orcid.org/0000-0002-7122-6731

Улыбина Ольга Вячеславовна, начальник отдела разработки жидких препаративных форм, АО Фирма «Август» (129515, Россия, Москва, ул. Цандера, д. 6). E-mail: o.ulybina@avgust.com. Scopus Author ID 36847255500, https://orcid.org/0000-0002-1529-5855

Иванов Роман Николаевич, старший научный сотрудник, отдел разработки твердых и комбинированных препаративных форм, АО Фирма «Август» (129515, Россия, Москва, ул. Цандера, д. 6). E-mail: r.ivanov@avgust.com. ResearcherID HKF-3424-2023, SPIN-код РИНЦ 1923-5088, https://orcid.org/0000-0002-1664-0980

Translated from Russian into English by M. Povorin
Edited for English language and spelling by Thomas A. Beavitt

Tonkie Khimicheskie Tekhnologii = Fine Chemical Technologies.
2024;19(2):104–110 ISSN 2686-7575 (Online)

UDC 547.464.7
https://doi.org/10.32362/2410-6593-2024-19-2-104-110

RESEARCH ARTICLE

Dichlorocarbenation of polar olefins in conditions of microwave irradiation

Yulianna G. Borisova✉, Airat I. Musin, Rimma M. Sultanova, Simon S. Zlotskii
Ufa State Petroleum Technological University, Ufa, 450064 Russia
✉ *Corresponding author, e-mail: yulianna_borisova@mail.ru*

Abstract

Objectives. To evaluate the influence and efficiency of using microwave irradiation on the dichlorocarbenation of polar olefins. To determine the conditions (reaction time and process temperature) under which the maximum yield of target *gem*-dichlorocyclopropanes is achieved.

Methods. The target compounds were obtained by classical methods of organic synthesis — acetalization of polyols and dichlorocarbenation of unsaturated compounds. The preparation of *gem*-dichlorocyclopropanes was carried out using the microwave activation method on a Sineo device (microwave system for organic synthesis, made in China). In order to determine the qualitative and quantitative composition of the reaction masses, gas–liquid chromatography (using the Kristall 2000 hardware complex), mass-spectroscopy (using Chromatek-Kristall 5000M device with NIST 2012), and nuclear magnetic resonance spectroscopy (using Bruker AM-500 device with operating frequencies of 500 and 125 MHz) were carried out.

Results. Under microwave irradiation at 25°C for 2 h with the maximum yield (92–98%), the target substituted *gem*-dichlorocyclopropanes were obtained: 2-(2,2-dichloro-3-methylcyclopropyl)-1,3-dioxolane, 2-(2,2-dichloro-3-phenylcyclopropyl)-1,3-dioxolane, 8,8-dichloro-4-isopropyl-3,5-dioxabicyclooctane, diethyl-2,2-dichloro-3-phenylcyclopropane-1,1-dicarboxylate, and diethyl-2,2-dichloro-3-isopropylcyclopropane-1,1-dicarboxylate.

Conclusions. Under the conditions herein proposed, the use of the microwave stimulation method in the dichlorocarbenation of double C=C bonds containing polar substituents allows the reduce the temperature and reaction time to be significantly reduced, and the yield of target *gem*-dichlorocyclopropanes to be increased.

Keywords
dichlorocarbenation, Mokosh method, microwave radiation, olefins, phase transfer catalysis

Submitted: 07.07.2023
Revised: 01.09.2023
Accepted: 11.03.2024

For citation
Borisova Yu.G., Musin A.I., Sultanova R.M., Zlotskii S.S. Dichlorocarbenation of polar olefins in conditions of microwave irradiation. *Tonk. Khim. Tekhnol. = Fine Chem. Technol.* 2024;19(2):104–110. https://doi.org/10.32362/2410-6593-2024-19-2-104-110

НАУЧНАЯ СТАТЬЯ

Дихлоркарбенирование полярных олефинов в условиях микроволнового излучения

Ю.Г. Борисова✉, А.И. Мусин, Р.М. Султанова, С.С. Злотский

Уфимский государственный нефтяной технический университет, Уфа, 450064 Россия

✉ *Автор для переписки, e-mail: yulianna_borisova@mail.ru*

Аннотация

Цели. Оценить влияние и эффективность использования микроволнового излучения на дихлоркарбенирование полярных олефинов; определить условия (продолжительность реакции и температуру проведения процесса), при которых достигается максимальный выход целевых *гем*-дихлорциклопропанов.

Методы. Целевые соединения были получены классическими методами органического синтеза — ацетализацией полиолов и дихлоркарбенированием непредельных соединений. *Гем*-дихлорциклопропаны были получены методом микроволновой активации с помощью микроволновой системы для проведения органических синтезов «Sineo» (Китай). Для определения качественного и количественного состава реакционных масс использовались газожидкостная хроматография (на аппаратно-программном комплексе «Кристалл 2000»), масс-спектроскопия (на приборе «Хроматэк-Кристалл 5000М» с базой NIST 2012) и спектроскопия ядерного магнитного резонанса (на приборе «BrukerAM-500» с рабочими частотами 500 и 125 МГц).

Результаты. В условиях микроволнового излучения при 25°С за 2 ч с максимальным выходом (92–98%) получены целевые замещенные *гем*-дихлорциклопропаны: 2-(2,2-дихлор-3-метилциклопропил)-1,3-диоксолан, 2-(2,2-дихлор-3-фенилциклопропил)-1,3-диоксолан, 8,8-дихлоро-4-изопропил-3,5-диоксабициклооктан, диэтил-2,2-дихлоро-3-фенилциклопропан-1,1-дикарбоксилат и диэтил-2,2-дихлоро-3-изопропилциклопропан-1,1-дикарбоксилат.

Выводы. В предложенных условиях использование метода микроволновой активации при дихлоркарбенировании двойных С=С связей, содержащих полярные заместители, позволяет существенно снизить температуру, уменьшить продолжительность реакции и повысить выход целевых *гем*-дихлорциклопропанов.

Ключевые слова

дихлоркарбенирование, метод Макоши, микроволновое излучение, олефины, межфазный катализ

Поступила: 07.07.2023
Доработана: 01.09.2023
Принята в печать: 11.03.2024

Для цитирования

Борисова Ю.Г., Мусин А.И., Султанова Р.М., Злотский С.С. Дихлоркарбенирование полярных олефинов в условиях микроволнового излучения. *Тонкие химические технологии*. 2024;19(2):104–110. https://doi.org/10.32362/2410-6593-2024-19-2-104-110

INTRODUCTION

Polyfunctional *gem*-dichlorocyclopropanes find application in the synthesis of low-tonnage products, reagents, and biologically active compounds [1–5]. In addition, molecules containing the *gem*-dichlorocyclopropane fragment are important intermediates which can be modified into more complex structures exhibiting a variety of properties [6]. The main method for the preparation of compounds of this class is dichlorocarbenation of double C=C bonds using the Mokosh method [7–10].

The aim of this work is to determine the effect of microwave radiation (MWR) on the multiple bond attachment of dichlorocarbenes, since under such conditions a high yield can be achieved in a short time [11].

MATERIALS AND METHODS

Using the hardware-software complex Chromatek-Crystal 5000M (*Chromatek*, Russia) with NIST 2012 database (*National Institute of Standards and Technology*, USA), reaction masses were analyzed and mass spectra of compounds were recorded. The conditions of analysis were as follows: capillary quartz column — 30-m long; analysis duration, 20 min; ion source temperature, 260°C; transition line temperature, 300°C; scanning range, 30–300 Da; pressure, 37–43 mTorr; and carrier gas—helium; heating rate, 20 deg/min). The electron impact ionization method, 70 eV, was used to obtain mass spectra of the compounds. ^{1}H and ^{13}C nuclear magnetic resonance (NMR) spectra were recorded on a Bruker AM-500 spectrometer (*Bruker Corporation*, USA) with operating frequencies of 500 and 125 MHz, respectively. The solvent used was $CDCl_3$ (Russia). Chemical shifts are given on the δ scale (ppm) relative to tetramethylsilane as internal standard. Spin-spin interaction constants (*J*) are given in Hz.

The basic methodology of dichlorocarbenization under thermal conditions is presented in [9].

Synthesis of compounds 2a-b and 4a,b under microwave radiation conditions

A mixture of 0.01 mol of the olefin 2-[(1E)-prop-1-en-1-yl]-1,3-dioxolane **1a** [9], 2-[(E)-2-phenylvinyl]-1,3-dioxolane **1b** [12], 2-isopropyl-4,7-dihydro-1,3-dioxepin **1c** [13], diethyl-(2-methylpropylidene)-malonate **3a** [13], diethylbenzylidene malonate **3b** [14], 30 mL of chloroform, 32 g of 50% sodium hydroxide solution and 1% by weight of triethylbenzylammonium chloride was stirred under MWR conditions at a given temperature. The progress of the reaction was monitored by gas–liquid chromatography. At the end of the reaction the reaction mixture was washed with water, extracted with chloroform (Russia), dried with calcium chloride (Russia) and evaporated. The target compounds were then isolated by means of vacuum distillation.

2-(2,2-Dichloro-3-methylcyclopropyl)-1,3-dioxolane (**2a**). Colorless liquid. Boiling point $T_{b.p.}$ = 98–99°C (5 mm Hg). 78% yield. Mass spectrum *m*/*z*, (I_{rel}, %): 195/197/199 $[M]^+$, (0.37/0.25/0.04), 123/125/127(2.44/1.98/0.31),109/111/113(1.33/0.75/0.15), 75/77 (5.95/1.65), 73 (100), 45 (45), 43 (5.6), 39 (11.44). The spectral characteristics are in accordance with [9].

2-(2,2-Dichloro-3-phenylcyclopropyl)-1,3-dioxolane (**2b**). 92% yield. Colorless liquid. $T_{b.p.}$ = 103–104°C (2 mm Hg). The spectral characteristics are in accordance with [15]. Mass spectrum *m*/*z*, (I_{rel}, %): 260 (1) $[M]^+$, 252 (2), 219 (4), 147 (12), 114 (20), 101 (8), 77 (10), 73 (96), 63 (5), 46 (30).

8,8-Dichloro-4-isopropyl-3,5-dioxabicyclooctane (**2c**). 98% yield. Colorless liquid. $T_{b.p.}$ = 103–104°C (2 mm Hg). The spectral characteristics are in accordance with [16]. Mass spectrum *m*/*z*, (I_{rel}, %): (188/190)/(20/7), (77/75)/(100/35), (109/111)/(45/17), (51/53)/(80/30).

Diethyl-2,2-dichloro-3-phenylcyclopropane-1,1-dicarboxylate (**4a**). 92% yield. Colorless liquid. $T_{b.p.}$ = 154–155°C (2 mm Hg). ^{1}H NMR spectrum, δ, ppm (*J*, Hz): 1.36 t (3H, CH_3, ^3J 7.0), 3.45 s (CH_3), 3.89 qu. (2H, CH_2, ^3J 6.9), 7.20–7.40 (Ph-). ^{13}C NMR, δ_C, ppm: 15.30 (CH_3), 43.34 (CH), 52.00 (C), 62.49 (CH_2), 74.12 (C), 127.16–131.61 (Ph-), 162.02 (C=O). The spectral characteristics are in accordance with [14].

Diethyl-2,2-dichloro-3-isopropylcyclopropane-1,1-dicarboxylate (**4b**). 92% yield. Colorless liquid. $T_{b.p.}$ = 154–155°C (2 mm Hg). ^{1}H NMR spectrum, δ, ppm (*J*, Hz): 1.32 t (3H, CH_3, ^3J 7.1), 3.45 s (1H, CH, ^3J 7.1), 3.48 s (3H, CH_3), 4.32 qu. (4H, CH_2, ^3J 7.2), 7.40–7.49 (Ph-). ^{13}C NMR, δ_C, ppm: 14.33 (CH_3), 46.73 (CH), 55.92 (C), 58.45 (CH_3), 65.48 (CH_2), 78.10 (C), 127.15–130.61 (Ph-), 201.08 (C=O). The spectral characteristics are in accordance with [14].

RESULTS AND DISCUSSION

Dichlorocarbenation of cyclic acetals of unsaturated aldehydes **1a**,**b** under microwave irradiation enabled *gem*-dichlorocyclopropanes **2a**,**b** to be obtained at room temperature (25°C) in 1–2 h in quantitative yield (Scheme 1).

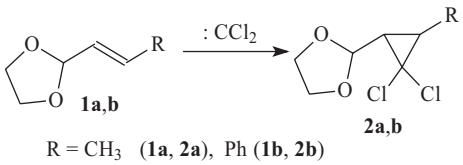

Scheme 1. Dichlorocarbenation of cyclic acetals of unsaturated aldehydes

It took 4–5 h to achieve similar results under thermal heating conditions (40°C) (Table 1). It should be noted that under the conditions being studied *trans*-**1a**,**b** form *trans-gem*-dichlorocyclopropanes **2a**,**b**.

The use of MBI for dichlorocarbenization of the endocyclic C=C bond in 2-isopropyl-4,7-dihydro-1,3-dioxepin **1c** was successful (Scheme 2).

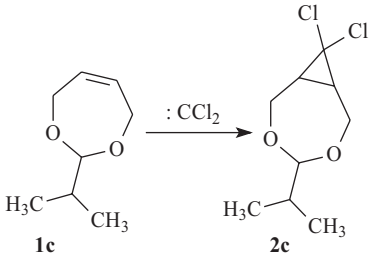

Scheme 2. Dichlorocarbenation of 2-isopropyl-4,7-dihydro-1,3-dioxepine

The corresponding bicyclic product **2c** was obtained at room temperature in 2 h in quantitative yield, whereas thermal heating (40°C) required 5 h (Table 1).

In dichlorocarbenation under MWR conditions, it was found that the endocyclic double C=C bond in 2-isopropyl-4,7-dihydro-1,3-dioxepin **1c** is 2 times more active than the exocyclic double C=C bond in 1,3-dioxolane **1a** (method of competitive reactions, conversion of initial olefins **1a**,**c** is not more than 30%).

1,1,2-Trisubstituted double C=C bonds in aryl- and alkylidenmalonates **3a**,**b** obtained according to the method [15] under thermal conditions show a low level of activity towards dichlorocarbenes (Scheme 3).

The yield of phenyl-substituted *gem*-dichlorocyclopropane **4a** using thermal heating (40°C) for 5 h is no more than ≤5%. With an increase in temperature the destruction of ether groups and intensive osmosis is observed. Using MWR at 25°C for 5 h the corresponding 1,1,2-trisubstituted *gem*-dichlorocyclopropane **4a** was obtained in 40% yield (Table 2).

Table 1. Synthesis conditions and yield of dichlorocarbenation products of compounds **2a-c**

No.	Initial compounds	Reaction conditions		Reaction products	Yield, %	Heating method
		T, °C	Reaction time, h			
1	**1a**	40	4	**2a**	35	Thermal heating
		40	5		40	
		25	1		55	MWR
		25	2		92	
2	**1b**	40	4	**2b**	70	Thermal heating
		40	5		90	
		25	1		70	MWR
		25	2		98	
3	**1c**	40	4	**2c**	70	Thermal heating
		40	5		93	
		25	1		60	MWR
		25	2		98	

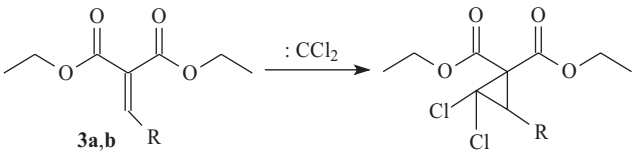

R = Ph (**3a**, **4a**), *i*-C_3H_7 (**3b, 4b**)

Scheme 3. Dichlorocarbenation of aryl- and alkylidenemalonates **3a**,**b**

Isopropylidene malonate **3b** was more active in the dichlorocarbenation reaction. Under thermal conditions (40°C, 5 h) the target product **4b** is formed in 30% yield. When using MWR (25°C, 2 h), there is quantitative formation of the product (Table 2).

Table 2. Synthesis conditions and yield of dichlorocarbenation products of compounds **4a**,**b**

No.	Initial compounds	Reaction conditions		Reaction products	Yield, %	Heating method
		T, °C	Reaction time, h			
1	**3a**	40	4	**4a**	≤1	Thermal heating
		40	5		≤3	
		25	1		28	MWR
		25	2		40	
2	**3b**	40	4	**4b**	25	Thermal heating
		40	5		30	
		25	1		70	MWR
		25	2		98	

CONCLUSIONS

Based on the results obtained, the use of MWR in the dichlorocarbenylation of double C=C bonds containing polar substituents allows the temperature and reaction time to be significantly reduced, and the yield of target *gem*-dichlorocyclopropanes to be increased.

Acknowledgments

The study was carried out under the Priority 2023 program.

Authors' contributions

Yu.G. Borisova—collecting and processing the material, writing the text of the article.

A.I. Musin—conducting research.

R.M. Sultanova—planning consultations.

S.S. Zlotskii—conceptualization of the research paper, critical revision with the introduction of valuable intellectual content.

The authors declare no conflict of interest.

REFERENCES

1. Kailania M.H., Al-Bakrib A.G., Saadeha H., Al-Hiari Y.M. Preparation and antimicrobial screening of novel 2, 2-dichloro-cyclopropane–*cis*-dicarbamates and comparison to their alkane and *cis*-alkene analogs. *Jordan J. Chem.* 2012;7(3):239–252.
2. Ziyat H., Ait Itto M.Y., Ait Ali M., Karim A., Riahi A., Daran J.C. Stereochemistry of two new polyfunctionalized *gem*-dihalocyclopropanes. *Acta Cryst.* 2002;C58(2):90–93. https://doi.org/10.1107/S0108270101019680
3. Fedorynski M. Syntheses of *gem*-dihalocyclopropanes and their use in organic synthesis. *Chem. Rev.* 2003;103(4):1099–1132. https://doi.org/10.1021/cr0100087
4. Kumar S., Neudecker T. The activation efficiency of mechanophores can be modulated by adjacent polymer composition. *RSC Advances*. 2021;11(13):7391–7396. http://doi.org/10.1039/D0RA09834E
5. Stanislawski P.C., Willis A.C., Banwell M.G. *Gem*-dihalocyclopropanes as building blocks in natural-product synthesis: enantioselective total syntheses of *ent*-erythramine and 3-*epi*-erythramine. *Chem. Asian J.* 2007;2(9):1127–1136. https://doi.org/10.1002/asia.200700155
6. Ouchi T., Bowser B.H., Kouznetsova T.B., Zheng X., Craig S.L. Strain-triggered acidification in a double-network hydrogel enabled by multi-functional transduction of molecular mechanochemistry. *Mater. Horiz*. 2023;10(2):585–593. https://doi.org/10.1039/D2MH01105K
7. Merrer D.C., Rablen P.R. Dichlorocarbene addition to cyclopropenes: a computational study. *J. Org. Chem*. 2005;70(5):1630–1635. https://doi.org/10.1021/jo048161z
8. Rablen P.R., Paiz A.A., Thuronyi B.W., Jones M. Computational investigation of the mechanism of addition of singlet carbenes to bicyclobutanes. *J. Org. Chem*. 2009;74(11):4252–4261. https://doi.org/10.1021/jo900485z
9. Mikhailova N.N., Giniyatullina E.Kh., Zlotskii S.S. Dihalocarbenation of 2-(1-propenyl)-1,3-dioxolane. *Izvestiya Vysshikh Uchebnykh Zavedenii, Khimiya i Khimicheskaya Tekhnologiya*. 2010;53(5):14–18 (in Russ.).
10. Thankachan A.P., Sindhu K.S., Krishnan K.K., Anilkumar G. Recent advances in the syntheses, transformations and applications of 1,1-dihalocyclopropanes. *Org. Biomol. Chem.* 2015;13(33):8780–8802. https://doi.org/10.1039/c5ob01088h
11. Musin A.I., Sultanova D.S., Borisova Yu.G., Mudrik T.P., Daminev R.R. Condensation of secondary amines with CH-acids and formaldehyde under the influence of microwave radiation. *Tonk. Khim. Tekhnol. = Fine Chem. Technol.* 2023;18(1):21–28 (Russ., Eng.). https://doi.org/10.32362/2410-6593-2023-18-1-21-28

СПИСОК ЛИТЕРАТУРЫ

1. Kailania M.H., Al-Bakrib A.G., Saadeha H., Al-Hiari Y.M. Preparation and antimicrobial screening of novel 2, 2-dichloro-cyclopropane–*cis*-dicarbamates and comparison to their alkane and *cis*-alkene analogs. *Jordan J. Chem.* 2012;7(3):239–252.
2. Ziyat H., Ait Itto M.Y., Ait Ali M., Karim A., Riahi A., Daran J.C. Stereochemistry of two new polyfunctionalized *gem*-dihalocyclopropanes. *Acta Cryst.* 2002;C58(2):90–93. https://doi.org/10.1107/S0108270101019680
3. Fedorynski M. Syntheses of *gem*-dihalocyclopropanes and their use in organic synthesis. *Chem. Rev.* 2003;103(4):1099–1132. https://doi.org/10.1021/cr0100087
4. Kumar S., Neudecker T. The activation efficiency of mechanophores can be modulated by adjacent polymer composition. *RSC Advances*. 2021;11(13):7391–7396. http://doi.org/10.1039/D0RA09834E
5. Stanislawski P.C., Willis A.C., Banwell M.G. *Gem*-dihalocyclopropanes as building blocks in natural-product synthesis: enantioselective total syntheses of *ent*-erythramine and 3-*epi*-erythramine. *Chem. Asian J.* 2007;2(9):1127–1136. https://doi.org/10.1002/asia.200700155
6. Ouchi T., Bowser B.H., Kouznetsova T.B., Zheng X., Craig S.L. Strain-triggered acidification in a double-network hydrogel enabled by multi-functional transduction of molecular mechanochemistry. *Mater. Horiz*. 2023;10(2):585–593. https://doi.org/10.1039/D2MH01105K
7. Merrer D.C., Rablen P.R. Dichlorocarbene addition to cyclopropenes: a computational study. *J. Org. Chem*. 2005;70(5):1630–1635. https://doi.org/10.1021/jo048161z
8. Rablen P.R., Paiz A.A., Thuronyi B.W., Jones M. Computational investigation of the mechanism of addition of singlet carbenes to bicyclobutanes. *J. Org. Chem*. 2009;74(11):4252–4261. https://doi.org/10.1021/jo900485z
9. Михайлова Н.Н., Гиниятуллина Э.Х., Злотский С.С. Дигалогенкарбенирование 2-(1-пропенил)-1,3-диоксолана. *Известия высших учебных заведений. Серия: Химия и химическая технология*. 2010;53(5):14–18.
10. Thankachan A.P., Sindhu K.S., Krishnan K.K., Anilkumar G. Recent advances in the syntheses, transformations and applications of 1,1-dihalocyclopropanes. *Org. Biomol. Chem.* 2015;13(33):8780–8802. https://doi.org/10.1039/c5ob01088h
11. Мусин А.И., Султанова Д.С., Борисова Ю.Г., Мудрик Т.П., Даминев Р.Р. Конденсация вторичных аминов с СН-кислотами и формальдегидом под действием микроволнового излучения. *Тонкие химические технологии*. 2023;18(1):21–28. https://doi.org/10.32362/2410-6593-2023-18-1-21-28

12. Sakhabutdinova G.N., Raskil'dina G.Z., Chanyshev R.R., Zlotskii S.S. Synthesis of derivatives of *gem*-dichlorocyclopropane containing 1,3-dioxolane fragments. *Bashkirskii khimicheskii zhurnal = Bashkir Chem. J.* 2020:27(1):22–26 (in Russ.).
13. Dzhumaev Sh.Sh., Borisova Yu.G., Raskil'dina G.Z., Zlotskii S.S. Synthesis and reactions of *cis*-2,3-disubstitutedgem-*gem*-dichlorocyclopropane. *Khimiya i tekhnologiya organicheskikh veshchestv = Chemistry and Technology of Organic Substances.* 2020;3(15):4–11(in Russ.).
14. Borisova Y.G., Raskil'dina G.Z., Zlotskii S.S. Synthesis of novel spirocyclopropylmalonates and barbiturates. *Dokl. Chem*. 2017;476(1):201–205. https://doi.org/10.1134/S0012500817090014
[Original Russian Text: Borisova Y.G., Raskil'dina G.Z., Zlotskii S.S. Synthesis of novel spirocyclopropylmalonates and barbiturates. *Doklady Akademii Nauk*. 2017;476(1):39–44 (in Russ.). https://doi.org/10.7868/S0869565217250090]
15. Raskil'dina G.Z., Sakhabutdinova G.N., Musin A.I., *et al*. Alkaline alcoholysis of *gem*-dichlorocyclopropane derivatives. *Russ. J. Gen. Chem.* 2021;91(4):596–601. https://doi.org/10.1134/S1070363221040034
[Original Russian Text: Raskil'dina G.Z., Sakhabutdinova G.N., Musin A.I., Zlotskii S.S. Alkaline alcoholysis of *gem*-dichlorocyclopropane derivatives. *Zhurnal Obshchei Khimii.* 2021;91(4):510–516 (in Russ.). https://doi.org/10.31857/S0044460X2104003X]
16. Baryshnikov R.N., Vafina R.M., Fedorenko V.Y., *et al*. Stereochemistry of seven-membered heterocycles: XLIII. Steric structure of diastereoisomeric 8,8-dichloro(dibromo)-4-R-3,5-dioxabicyclo[5.1.0]octanes. *Russ. J. Org. Chem.* 2003;39(7):1029–1033. https://doi.org/10.1023/B:RUJO.0000003198.64663.ac
[Original Russian Text: Baryshnikov R.N., Vafina R.M., Fedorenko V.Y., Shtyrlin Y.G., Klimovitskii E.N. Stereochemistry of seven-membered heterocycles: XLIII. Steric structure of diastereoisomeric 8,8-dichloro(dibromo)-4-R-3,5-dioxabicyclo[5.1.0]octanes. *Zhurnal Organicheskoi Khimii*. 2003;39(7):1092–1096 (in Russ.).]

12. Сахабутдинова Г.Н., Раскильдина Г.З., Чанышев Р.Р., Злотский С.С. Синтез производных *гем*-дихлорциклопропанов, содержащих 1,3-диоксолановые фрагменты. *Башкирский хим. журн.* 2020;27(1):22–26.
13. Джумаев Ш.Ш., Борисова Ю.Г., Раскильдина Г.З., Злотский С.С. Синтез и реакции *цис*-2,3-дизамещенных *гем*-дихлорциклопропанов. *Химия и технология органических веществ*. 2020;3(15):4–11.
14. Борисова Ю.Г., Раскильдина Г.З., Злотский С.С. Синтез новых спироциклопропилмалонатов и барбитуратов. *Доклады Академии наук.* 2017;476(1):39–44. https://doi.org/10.7868/S0869565217250090
15. Раскильдина Г.З., Сахабутдинова Г.Н., Мусин А.И., Злотский С.С. Щелочной алкоголиз производных *гем*-дихлорциклопропана. *Журн. общей химии.* 2021;91(4):510–516. https://doi.org/10.31857/S0044460X2104003X
16. Барышников Р.Н., Вафина Р.М., Федоренко В.Ю., Штырлин Ю.Г., Климовицкий Е.Н. Стереохимия семичленных гетероциклов. XLIII. Пространственная структура диастереомерных 8,8-дихлор(дибром)4-R-3,5-диоксабицикло[5.1.0]октанов. *Журн. орг. химии*. 2003;39(7):1092–1096.

About the authors

Yulianna G. Borisova, Cand. Sci. (Chem.), Teacher, Department of General, Analytical and Applied Chemistry, Ufa State Petroleum Technological University (1, Kosmonavtov ul., Ufa, 450064, Russia). E-mail: yulianna_borisova@mail.ru. Scopus Author ID 56526865000, Researcher ID P-9744-2017, RSCI SPIN-code 3777-0375, https://orcid.org/0000-0001-6452-9454

Airat I. Musin, Postgraduate Student, Department of General, Analytical and Applied Chemistry, Ufa State Petroleum Technological University (1, Kosmonavtov ul., Ufa, 450064, Russia). E-mail: musin_1995@list.ru. ResearcherID R-9142-2016, RSCI SPIN-code 9573-4624, https://orcid.org/0000-0002-8662-9680

Rimma M. Sultanova, Dr. Sci. (Chem.), Professor, Department of General, Analytical and Applied Chemistry, Ufa State Petroleum Technological University (1, Kosmonavtov ul., Ufa, 450064, Russia). E-mail: rimmams@yandex.ru. Scopus Author ID 6602738038, RSCI SPIN-code 8208-6060, https://orcid.org/0000-0001-6719-2359

Simon S. Zlotskii, Dr. Sci. (Chem.), Professor, Head of the Department of General, Analytical and Applied Chemistry, Ufa State Petroleum Technological University (1, Kosmonavtov ul., Ufa, 450064, Russia). E-mail: nocturne@mail.ru. Scopus Author ID 6701508202, ResearcherID W-6564-2018, RSCI SPIN-code 6529-3323, https://orcid.org/0000-0001-6365-5010

Об авторах

Борисова Юлианна Геннадьевна, к.х.н., преподаватель кафедры общей, аналитической и прикладной химии, ФГБОУ ВО «Уфимский государственный нефтяной технический университет» (450064, Россия, г. Уфа, ул. Космонавтов, д. 1). E-mail: yulianna_borisova@mail.ru. Scopus Author ID 56526865000, Researcher ID P-9744-2017, SPIN-код РИНЦ 3777-0375, https://orcid.org/0000-0001-6452-9454

Мусин Айрат Ильдарович, аспирант кафедры общей, аналитической и прикладной химии, ФГБОУ ВО «Уфимский государственный нефтяной технический университет» (450064, Россия, г. Уфа, ул. Космонавтов, д. 1). E-mail: musin_1995@list.ru. ResearcherID R-9142-2016, SPIN-код РИНЦ 9573-4624, https://orcid.org/0000-0002-8662-9680

Султанова Римма Марсельевна, д.х.н., профессор кафедры общей, аналитической и прикладной химии, ФГБОУ ВО «Уфимский государственный нефтяной технический университет» (450064, Россия, г. Уфа, ул. Космонавтов, д. 1). E-mail: rimmams@yandex.ru. Scopus Author ID 6602738038, SPIN-код РИНЦ 8208-6060, https://orcid.org/0000-0001-6719-2359

Злотский Семен Соломонович, д.х.н., заведующий кафедрой общей, аналитической и прикладной химии, ФГБОУ ВО «Уфимский государственный нефтяной технический университет» (450064, Россия, г. Уфа, ул. Космонавтов, д. 1). E-mail: nocturne@mail.ru. Scopus Author ID 6701508202, ResearcherID W-6564-2018, SPIN-код РИНЦ 6529-3323, https://orcid.org/0000-0001-6365-5010

Translated from Russian into English by H. Moshkov
Edited for English language and spelling by Dr. David Mossop

Tonkie Khimicheskie Tekhnologii = Fine Chemical Technologies.
2024;19(2):111–126 ISSN 2686-7575 (Online)

UDC 544.77.051:547.917:615.45
https://doi.org/10.32362/2410-6593-2024-19-2-111-126

RESEARCH ARTICLE

Obtaining chitosan sulfate nanoparticles in an aqueous medium and their colloidal protection with polysaccharides

Vadim S. Erasov✉, Yulia O. Maltseva

MIREA — Russian Technological University (M.V. Lomonosov Institute of Fine Chemical Technologies), Moscow, 119571 Russia

✉ *Corresponding author, e-mail: vadim.ersv@yandex.ru*

Abstract

Objectives. To develop a method to obtain a hydrosol of the salt of chitosan with sulfuric acid—chitosanium sulfate (ChS) hydrosol—and to study the effect of various water-soluble polysaccharides on its stability over time, as well as its resistance to indifferent and non-indifferent electrolytes.

Methods. κ-Carrageenan, sodium alginate (SA), and xanthan were used as polymers which perform the function of colloidal protection for ChS nanoparticles. Capillary viscometry was used to study the viscosity of polymer solutions, their molecular weight, and their adsorption on ChS. The stability of the sols over time and their resistance to indifferent and non-indifferent electrolytes were evaluated photometrically. The hydrosol particle size was determined by means of dynamic light scattering.

Results. On the surface of ChS, κ-carrageenan is adsorbed most strongly over a wide range of concentrations. The graphs of the dependencies of the relative change in the turbidity of sols with the addition of various polysaccharides on their weight concentration at a sol lifetime of 2 days have the shape of curves with a maximum. Sols with the addition of 0.0125% SA and κ-carrageenan in the range of 0.04% have the greatest stability over time. According to dynamic light scattering data, the average particle size of freshly prepared sols with the addition of the polymers to ensure their greatest stability over time are 10.8 nm and 14.6 nm, respectively. For freshly prepared sols without polysaccharides, this size is 24.8 nm. The hydrosol coagulation threshold with an indifferent electrolyte (NaCl) is 9.3 times higher than that with a non-indifferent electrolyte (Na_2SO_4). κ-Carrageenan and SA protect the hydrosol from coagulation with an indifferent electrolyte (NaCl) at all their used amounts. At the same polymer concentrations, no protection from coagulation with a non-indifferent electrolyte (Na_2SO_4) was observed.

Conclusions. A method was developed to obtain ChS hydrosol with a positive particle charge. The stability of ChS sols over time was studied both without and with the addition of SA, κ-carrageenan, and xanthan. Sol coagulation thresholds with indifferent and non-indifferent electrolytes, as well as the protective numbers for κ-carrageenan and SA against the coagulation of hydrosols with these electrolytes, were established. The mechanism of stability of sols at certain concentrations of water-soluble polysaccharides was explained using data on the adsorption of these polysaccharides on the surface of chitosan treated with a solution of sulfuric acid. Based on the results of the work, it can be concluded that SA and κ-carrageenan can be used for the efficient stabilization of ChS hydrosols over time and for the colloidal protection of ChS from coagulation with sodium chloride.

Keywords

colloid chemistry, nanoparticles, nanotechnology, sols, dispersed systems, polymers, carbohydrates, polysaccharides, chitosan, sodium alginate, carrageenans, xanthan, stability, coagulation

Submitted: 10.04.2023
Revised: 19.10.2023
Accepted: 04.03.2024

For citation

Erasov V.S., Maltseva Yu.O. Obtaining chitosan sulfate nanoparticles in an aqueous medium and their colloidal protection with polysaccharides. *Tonk. Khim. Tekhnol. = Fine Chem. Technol.* 2024;19(2):111–126. https://doi.org/10.32362/2410-6593-2024-19-2-111-126

НАУЧНАЯ СТАТЬЯ

Получение хитозан-сульфатных наночастиц в водной среде и их коллоидная защита полисахаридами

В.С. Ерасов✉, **Ю.О. Мальцева**

МИРЭА — Российский технологический университет (Институт тонких химических технологий им. М.В. Ломоносова), Москва, 119571 Россия

✉ *Автор для переписки, e-mail: vadim.ersv@yandex.ru*

Аннотация

Цели. Разработать методику получения гидрозоля сернокислой соли хитозана — сульфата хитозания (СХ), исследовать влияние различных водорастворимых полисахаридов на его устойчивость во времени и при добавлении индифферентного и неиндифферентного электролитов.

Методы. В качестве полимеров, выполняющих функцию коллоидной защиты наночастиц СХ, были использованы к-каррагинан, альгинат натрия (АН) и ксантан. Для определения вязкости растворов полимеров, их молекулярной массы и для исследования их адсорбции на СХ использовался метод капиллярной вискозиметрии. Оценка устойчивости золей во времени и при добавлении индифферентного и неиндифферентного электролитов проводилась фотометрически. Размер частиц гидрозоля определялся методом динамического светорассеяния.

Результаты. На поверхности СХ в широком диапазоне концентраций сильнее всего адсорбируется к-каррагинан. Графики зависимости относительного изменения мутности золей с добавками различных полисахаридов от их массовой концентрации при времени жизни золей 2 суток имеют вид кривых с максимумом. Наибольшей устойчивостью во времени обладают золи с добавками 0.0125% АН и к-каррагинана в диапазоне 0.04%. По данным динамического светорассеяния средний размер частиц свежеприготовленных золей с добавками полимеров, обеспечивших их наибольшую устойчивость во времени, составил соответственно 10.8 нм и 14.6 нм, тогда как для свежеприготовленных золей без полисахаридов — 24.8 нм. Порог коагуляции гидрозоля индифферентным электролитом (NaCl) в 9.3 раза выше порога коагуляции гидрозоля неиндифферентным электролитом (Na_2SO_4). к-Каррагинан и АН защищают гидрозоль от коагуляции индифферентным электролитом (NaCl) при всех их использованных количествах. В то же время, при тех же концентрациях полимера защиты от коагуляции неиндифферентным электролитом (Na_2SO_4) не наблюдалось.

Выводы. Разработана методика получения гидрозоля СХ с положительным зарядом частиц. Исследована устойчивость золей СХ во времени как без добавок, так и с добавками АН, к-каррагинана и ксантана во времени. Определены пороги коагуляции золей индифферентным и неиндифферентным электролитами, а также защитные числа от коагуляции гидрозоля этими электролитами для к-каррагинана и АН. Для объяснения механизма устойчивости золей при определенных концентрациях водорастворимых полисахаридов использованы полученные данные по адсорбции этих полисахаридов на поверхности хитозана, обработанного раствором серной кислоты. По результатам работы можно сделать вывод, что АН и к-каррагинан могут использоваться как эффективные стабилизаторы гидрозолей СХ во времени и для его коллоидной защиты от коагуляции хлоридом натрия.

Ключевые слова

коллоидная химия, наночастицы, нанотехнология, золи, дисперсные системы, полимеры, углеводы, полисахариды, хитозан, альгинат натрия, каррагинаны, ксантан, устойчивость, коагуляция

Поступила: 10.04.2023
Доработана: 19.10.2023
Принята в печать: 04.03.2024

Для цитирования

Ерасов В.С., Мальцева Ю.О. Получение хитозан-сульфатных наночастиц в водной среде и их коллоидная защита полисахаридами. *Тонкие химические технологии*. 2024;19(2):111–126. https://doi.org/10.32362/2410-6593-2024-19-2-111-126

INTRODUCTION

In medical and pharmaceutical nanotechnology, there is currently great interest in the polyaminosaccharide chitosan and its various derivatives. Chitosan and its derivatives are promising polymers for use in various fields of modern medicine. It can be used in the development of new drugs and drug delivery vehicles, wound dressings, suture materials, bone and dental implants, and embolization materials [1–20].

Chitosan is obtained by alkaline deacetylation of chitin: the second most abundant polysaccharide in nature after cellulose. The main natural sources of chitin and, accordingly, chitosan, are the outer integuments of arthropods, primarily crustaceans, as well as fungal cell walls. Due to features of the method for producing chitosan, unreacted chitin units always remain in it (Fig. 1a). Therefore, chitosan is characterized by the fraction of units containing amino groups, or by the degree of deacetylation (DD).

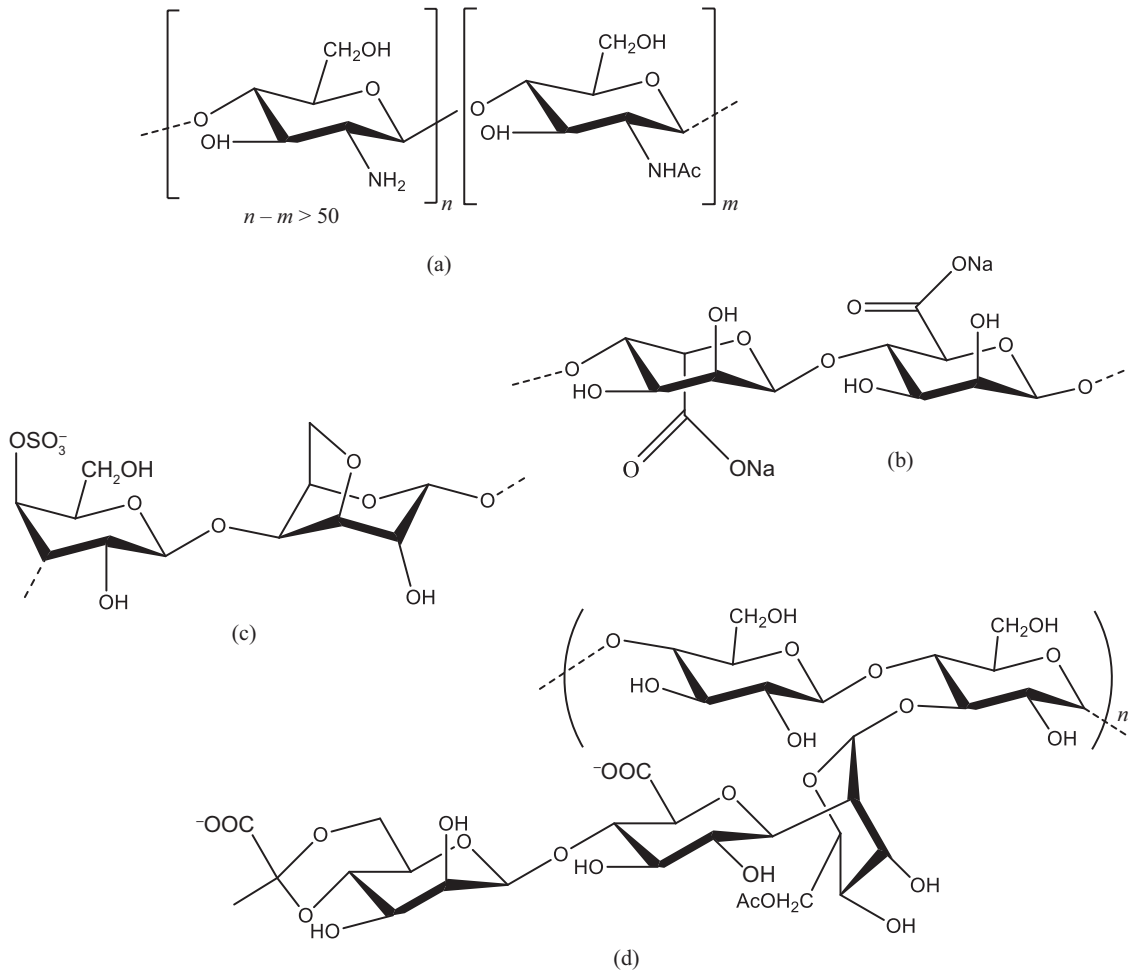

Fig. 1. Formulas of the polysaccharides used:
(a) chitosan,
(b) sodium alginate (SA),
(c) κ-carrageenan, and
(d) xanthan (xanthan gum)

An important advantage of micro- and nanoparticles of chitosan and its derivatives is that they can be prepared and loaded in an aqueous medium without using organic solvents. Chitosan is insoluble in water and organic solvents. Since chitosan is a weak base, in an acidic medium, its groups are protonated. At DD > 70%, it is soluble in an aqueous medium with pH < 6.5.

Salts of chitosan with various acids, e.g., its sulfate salt, chitosanium sulfate (ChS), are of interest for pharmacology and medicine. ChS is insoluble in water because of the cross-linking of chitosan macromolecules by sulfate anions by the interaction with their protonated amino groups (Fig. 2). This makes it possible to use ChS as a basis for nano- and microparticles. Since they possess biological activity themselves, they can also serve as delivery vehicles for other drugs [4, 21–25]. ChS nanoparticles can possibly also find application as fillers in polymer composite materials for bone and dental implants, as is the case with the use of chitosan [18].

In order to study the biological activity of nanoparticles and the possibilities of pharmaceutical use of chitosan and its derivatives, methods for their production and stabilization need to be developed. Furthermore, their stability under physiological conditions and during storage of drugs also need to be studied. The advantage of using biopolymers, including polysaccharides, in stabilizing dispersed systems is their biodegradability, environmental safety, availability, and, in many cases, biocompatibility [4].

The use of polysaccharides for the production and stabilization of various nanoparticles was considered previously (see, e.g., [26–29]). ChS sols were also studied [21–23], but without their stabilization by polymers.

In our study, ChS sols were stabilized by the anionic polysaccharides sodium alginate, κ-carrageenan, and xanthan (xanthan gum). Figures 1b–1d present their structural formulas.

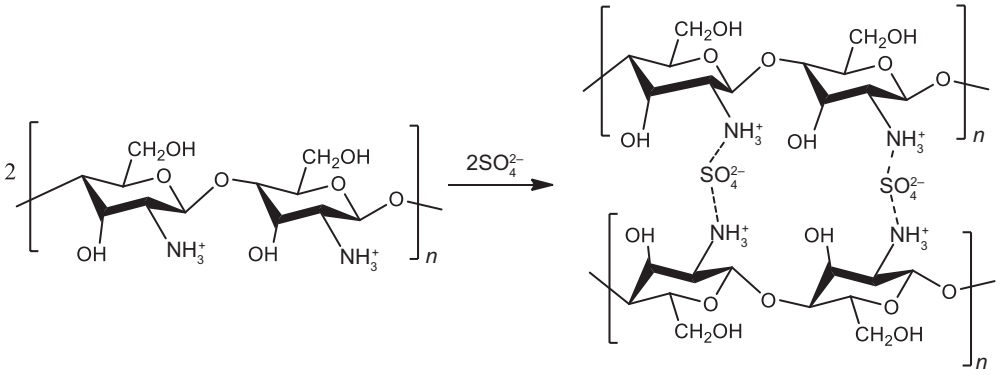

Fig. 2. Cross-linking of protonated chitosan (chitosanium polycations) with sulfate anions

EXPERIMENTAL

The main reagents were chitosan (*Slavyanskii Food Processing Plant*, Russia), sodium alginate (*Reaktivtorg*, Russia), BLK-1120 κ-carrageenan (*Shanghai Brilliant Gum*, China), and Kelzan xanthan (xanthan gum) (*CP Kelco*, Denmark). The other reagents (all of reagent grade, *Reaktivtorg*, Russia) were: sodium sulfate, sodium chloride, hydrochloric acid, sulfuric acid, sodium hydroxide, acetic acid, and sodium acetate.

The DD of chitosan was calculated based on experimental data of its titration with alkali according to the published procedure [30]. The molecular weights of chitosan, SA, κ-carrageenan, and xanthan were determined by capillary viscometry method with a VPZh-2 viscometer (*Ekros*, Russia) with a capillary diameter of 0.73 mm at 25°C using the Mark–Houwink equation.

In order to study the adsorption of SA, κ-carrageenan, and xanthan from their aqueous solutions on the surface of the ChS, a chitosan sample was first treated with a 2% sulfuric acid solution, filtered off, and dried at a temperature of about 70°C. Weighed specimens of the samples obtained were used to measure the viscosity of polysaccharide solutions of different concentrations after reaching adsorption equilibrium. In order to construct calibration graphs, solutions of polysaccharides were premixed with acidified water obtained after keeping the same specimens of a chitosan sample treated with a solution of sulfuric acid in distilled water. The pH of the medium (pH was 2.5–2.7) and ionic strength on the viscosity of the polysaccharide were taken into account. These determined by the presence of H^+ ions due to the dissociation of the surface of chitosan treated with a solution of sulfuric acid. The adsorption of water-soluble polysaccharide on chitosan treated with a solution of sulfuric acid (g adsorbate/g adsorbent) was found from the formula

$$A_{g/g} = \frac{\left(C_{in} - C_{eq}\right)V}{m}, \quad (1)$$

wherein C_{in} and C_{eq} are the viscometrically determined weight concentrations of water-soluble polysaccharides in the initial solution and upon reaching adsorption equilibrium, respectively; V is the volume of the system; and m is the weight of the sample of chitosan treated with a solution of sulfuric acid.

In order to obtain a ChS sol, chitosan was first converted into a soluble salt form by reacting it with hydrochloric acid. The ChS sol was produced by the metathesis reaction between the obtained chitosanium chloride and sodium sulfate:

$$2[Chit_n \cdot nH^+]Cl_n + nNa_2SO_4 = \\ = [Chit_{2n} \cdot 2nH^+](SO_4)_n + 2nNaCl, \quad (2)$$

wherein Chit is the deacetylated chitosan unit.

In order to obtain the sol, the reactants were taken in stoichiometric quantities (in the ratio ChS/Na_2SO_4 = 2/1).

In order to dissolve chitosan in a solution of hydrochloric acid, 0.41 g of chitosan and 0.093 g of hydrochloric acid were taken per 50 mL of water. This weight of chitosan, taking into account the DD, corresponds to an amount of 2 mmol (0.32 g) of deacetylated monomer units which enter into the reaction. Accordingly, the concentration of these units was 40 mM. The reaction mixture was heated in a water bath until the chitosan was completely dissolved. In order to obtain a sol, 50 mL of a 20 mM Na_2SO_4 solution (0.142 g Na_2SO_4) was added by drops into the cooled resulting solution of chitosan chloride with constant stirring using a submersible mixer. This sequence of mixing the solutions of reagents is necessary, in order to ensure a positive charge of the sol particles. The theoretical weight concentration of the obtained sol is 4.2 g/L.

To each of the obtained 100-mL portion of the initial sol, 25 mL of each of the solutions of polysaccharides were added so that the range of obtained polysaccharide concentrations in the sol was 0.0125–0.06 wt %. In order to maintain its concentration, 25 mL of distilled water was added to one of the portions of the sol instead of

a polysaccharide solution. After this, all sols were treated with ultrasound for 3 min. The pH values of the sols were about 2.5–2.7. The sols were prepared at a temperature of 25°C.

The studied ChS sols are colorless; therefore, only light scattering is observed for them, and absorption is virtually absent. The optical densities D of all studied sols were determined (wavelength 430 nm, cell thickness 1 cm) using a KFK-3KM single-beam spectrophotometer (*Uyniko-Sis*, Russia) (spectral wavelength range 325–1000 nm). The turbidity for freshly prepared sols and sols at certain time intervals was calculated from the optical density as $2.3D$, cm^{-1}. The error in measuring the optical density (turbidity) of the sols was 4.4%.

As a measure of the stability of sols at a certain time, the relative change in turbidity, τ_{rel}, as a percentage of the initial turbidity τ_0 was taken:

$$\tau_{rel} = \frac{100|\tau - \tau_0|}{\tau_0}. \quad (3)$$

A sol can be considered more stable, if its turbidity changes (in percentage) to a lesser extent in the given time, when compared with the turbidity of the sol immediately after synthesis.

In order to determine the coagulation threshold with electrolytes and to study the colloidal protection of sols with polymers, NaCl (3 M) was used as an indifferent electrolyte, while Na_2SO_4 (50 mM) was used as a non-indifferent electrolyte. The coagulation threshold was found from the turbidity of freshly prepared sols with the addition of gradually increasing volumes of polysaccharide solutions. The volume of the sol portion and the volume increment were 10 and 0.05 mL, respectively, for NaCl and 5 and 0.1 mL, respectively, for Na_2SO_4.

The sol coagulation threshold with electrolytes (mol/L) was calculated using the formula (4):

$$C_{coag} = \frac{c_{e0} V_e}{V_{sol}}, \quad (4)$$

wherein c_{e0} is the concentration of the electrolyte in the portion of its solution before addition to sol, V_e is the volume of the electrolyte solution in which coagulation occurs, and V_{sol} is the volume of the sol in the test tube.

The colloidal protection from each electrolyte by water-soluble polysaccharides was studied by means of the turbidity of portions of sols with the addition of gradually increasing volumes of polysaccharide solutions (in increments of 0.05 mL to protect the sol from NaCl and 0.1 mL to protect it from Na_2SO_4), and the subsequent addition of a portion of electrolyte the volume of which corresponds to a certain coagulation threshold.

The protective numbers (in weight percent) for water-soluble polysaccharides were calculated by the formula (5):

$$C_{prot} = \frac{c_{p0} V_p}{V_{sol}}, \quad (5)$$

wherein c_{p0} is the concentration of the polysaccharide in the added portion, wt %; V_p is the volume of the polysaccharide solution at which coagulation occurs; and V_{sol} is the volume of the sol in the test tube.

The size distribution of particles of sols was determined by dynamic light scattering using a Delsa Nano C A53878 automatic particle analyzer (*Beckman Coulter*, USA) in the measurement range from 0.6 nm to 30 μm.

RESULTS AND DISCUSSION

The potentiometric titration of chitosan converted into a soluble protonated form by reacting it with hydrochloric acid was performed according to the published procedure [30]. The result showed that the DD of chitosan is 77.28%. In the work of Wang *et al.* [31], the parameters of the Mark–Houwink equation for chitosan were shown to be dependent on its DD. The graphs of the dependencies of the constants k and α on DD were presented. According to the data of Wang *et al.* [31], the values of these constants at DD = 77.28% were found and used, in order to calculate the molecular weight of chitosan using the Mark–Houwink equation using capillary viscometry data.

Table 1 presents the results of determining the molecular weights of chitosan and water-soluble polysaccharides, the conditions for their viscometric determination, the corresponding values of the constants of the Mark–Houwink equation, and the determined values of the intrinsic viscosity of their solutions. According to the DD value, the macromolecule of the chitosan used contains 4968 deacetylated monomer units.

Figure 3 presents the adsorption isotherms (g/g) of water-soluble polysaccharides from their aqueous solutions on the surface of chitosan treated with a solution of sulfuric acid. The isotherms were obtained by processing capillary viscometry data, as shown in Fig. 3. At weight concentrations below 0.05%, the relative viscosity of solutions of the polysaccharides under study before adsorption is close to unity. After achieving adsorption equilibrium, it is unity. Therefore, at such low weight concentrations, the amount of polysaccharides remaining in the solution after reaching adsorption equilibrium for all three polysaccharides is insignificant for the use of viscometry data. In this case, it can also be assumed that almost all of their amount is adsorbed. At a concentration of 0.05% and higher, according to capillary viscometry data, differences in adsorption between different water-soluble polysaccharides are

Table 1. Values of molecular weights, intrinsic viscosity, parameters of the Mark–Hauwick equation, determination conditions, and references to relevant sources for chitosan and water-soluble polysaccharides

Polysaccharide	$k \cdot 10^5$, mL/g	α	Conditions	Reference	Intrinsic viscosity [μ], mL/g	Molecular weight *M*, kDa
Chitosan	50	1.02	0.2 M CH_3COOH/0.1 M CH_3COONa, $T = 30$°C	[31]	660	1001.3
SA	73	0.92	0.1 M NaCl, $T = 25$°C	[32]	300	103.5
κ-Carrageenan	10	0.9	Distilled water, $T = 25$°C	[33]	32	1308.7
Xanthan	2.49	1.2454	0.01 M NaCl, $T = 25$°C	[34]	785	771.4

already clearly visible. As can be seen, on the surface of chitosan treated with a solution of sulfuric acid, xanthan is least adsorbed throughout the concentration range studied here (Fig. 3, curve *3*). Up to a concentration of about 0.15%, κ-carrageenan is adsorbed best. The adsorption isotherm can be attributed to the Langmuir type (Fig. 3, curve *2*). SA is generally adsorbed worse than κ-carrageenan. However, at concentrations above 0.15%, its adsorption already begins to exceed that of κ-carrageenan. It is obvious that the adsorption of κ-carrageenan is facilitated not only by the electrostatic attraction of its polyanions to the positively charged surface, but also by the specific binding of sulfate groups of κ-carrageenan to the protonated amino groups of chitosan, as occurs in the case of SO_4^{2-} anions (Fig. 2).

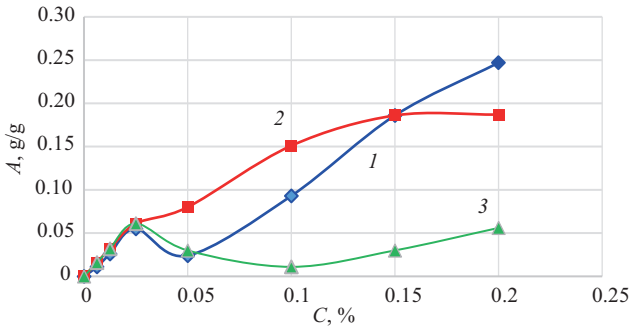

Fig. 3. Adsorption of polysaccharides on the surface of chitosan treated with a solution of sulfuric acid (containing ChS on the surface):
(*1*) SA,
(*2*) κ-carrageenan, and
(*3*) xanthan

Reaction (2) between chitosanium chloride and sodium sulfate gives insoluble ChS. It was shown [22] that the factor which most affects the rate of formation and characteristics of ChS is the molar ratio of the components of the mixture SO_4^{2-} and NH_3^+. With a decrease in the fraction of sulfate ions in the initial solution, the size of the resulting particles decreases. Their ξ-potential increases, helping to increase their stability.

The micelle of the ChS hydrosol, stabilized with chitosan chloride, with the positively charged surface can be represented by the general formula:

$$\{m\mathrm{Chit}_{2n}(\mathrm{SO}_4)_n\, k[\mathrm{Chit}_n\, n\mathrm{H}^+](k-x)n\mathrm{Cl}^-\}xn\mathrm{Cl}^-,$$

wherein Chit is the deacetylated chitosan unit (nondeacetylated fragments of chitosan are not taken into account).

The potential-determining groups are protonated groups of chitosan (chitosanium polycations), and the counterions are chloride anions.

For each of the water-soluble polysaccharides, graphs were constructed of the time dependencies of the turbidity of sols containing different weight concentrations of polysaccharides. Figure 4 presents examples of such graphs for the sol without the addition of a polysaccharide and for sols with polysaccharides at weight concentrations of 0.125 and 0.25%.

These graphs show that over time the turbidity in some cases can not only increase, but also decrease. According to Rayleigh's equation, $\tau \sim \nu V_p^2$, where ν is the number concentration of sol particles and V_p is the average particle volume. As a result of coagulation over time, the increase in the turbidity of the sol with an increase in the volume (size) of particles appears together with a decrease in turbidity and a decrease in the number concentration of the sol. On the one hand, the coagulation helps to reduce the number concentration of particles, thus decreasing the optical density (turbidity). On the other hand, the larger the particle aggregates, the more they scatter light, which contributes to an increase in optical density (turbidity). Thus, depending on the predominance of the former or latter trend, the turbidity either increases or decreases. For example, although the largest aggregates of particles scatter light more strongly, they are deposited to the bottom of the vessel, thereby leaving the bulk of the sol. Consequently, they are absent from the sol placed in the cell for measuring optical density. Thus, because of the ambiguity of assessing the stability of sols using the absolute values of optical density (turbidity), the stability of sols over time was characterized using not the absolute values of turbidity, but the relative change in percentage according

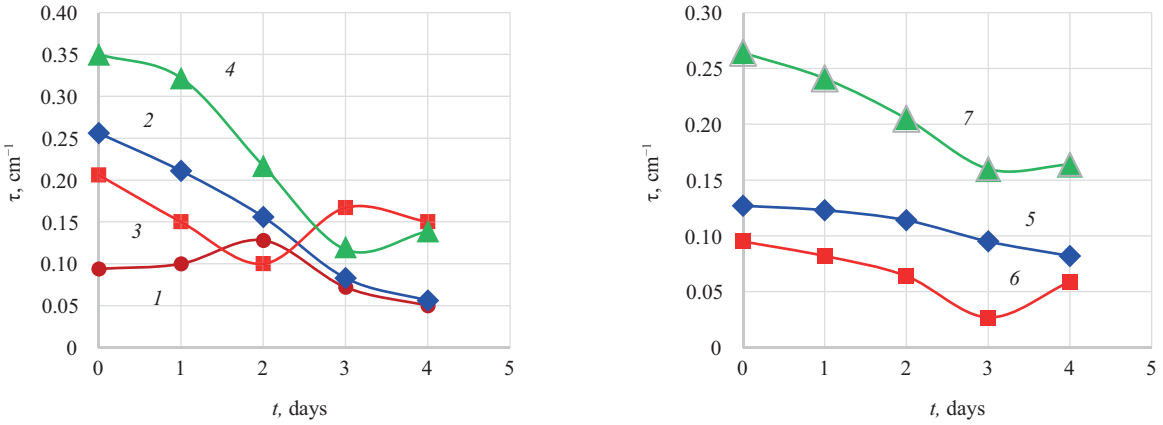

Fig. 4. Time dependencies of the turbidity of ChS sols
(*1*) without the addition of polysaccharides
and with the addition of (*2*) 0.025% SA,
(*3*) 0.025% κ-carrageenan,
(*4*) 0.025% xanthan,
(*5*) 0.0125% SA,
(*6*) 0.0125% κ-carrageenan, and
(*7*) 0.0125% xanthan

to formula (2). The more the turbidity of the sol changes, the less stable it can be considered. Figure 5 illustrates the relative change in the turbidity of sols after 2 days. The relative change in the turbidity of the sol without the addition of polymers for this time is 33%. Figure 5 shows that, at very low weight concentrations of polymers (less than 0.02%), the stability of the sols increases in comparison with the initial sol. The addition of each of all the three polysaccharides to a concentration of 0.0125% decreases the relative change in turbidity. These points of decrease in the relative change in turbidity at polysaccharide concentrations of 0.0125% can be conditionally considered points of minimum. However, a more accurate determination of the presence of a minimum and its value requires several more points in the concentration range less than 0.0125% to be examined. At concentrations above 0.0125%, the relative changes in turbidity for xanthan and SA increase, pass through a maximum, and decrease. In this case, the greatest decrease is observed for κ-carrageenan at its concentration of 0.04%. In this case, the turbidity changes only by 4.9%, which is close to the error in measuring the optical density (turbidity) of the sol.

Thus, polymers in certain weight concentration ranges contribute to a smaller change in the turbidity of the sol and, accordingly, to an increase in its aggregative stability. In this case, the curves of the relative change in turbidity over time for sols with the addition of different polymers have a similar shape to the curves with portions of decrease in relative change in turbidity and its maxima. At very low concentrations, the addition of polymer contributes to the stability of the sol. With increasing concentration, the stability of sol decreases, passing

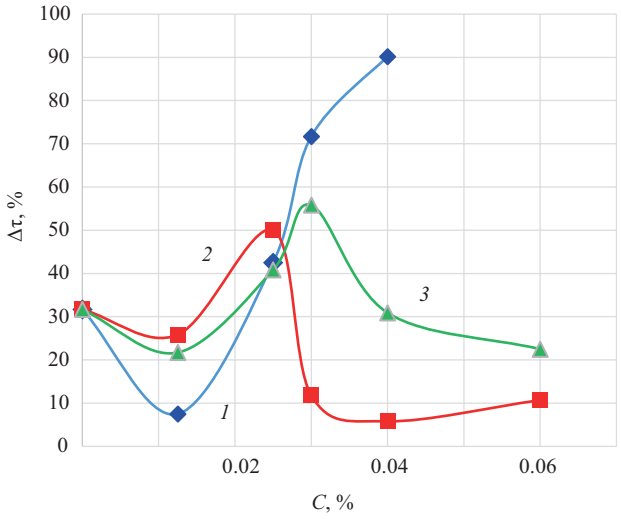

Fig. 5. Relative change in the turbidity of sols after two days in the presence of various weight concentrations of stabilizing polymers:
(*1*) SA,
(*2*) κ-carrageenan, and
(*3*) xanthan

through a minimum (which is also a maximum of the relative change in turbidity over time), and then increases again. The type of dependence of the relative change in turbidity on the concentration of polysaccharides shown in Fig. 5 can be explained by the relationship between the amount of adsorbed polysaccharide and its ability to induce particle flocculation. All the polysaccharides studied are polyelectrolytes which carry a charge opposite to the charge of the particle surface. Therefore, they contribute to a decrease in the thickness of the electric

double layer of micelles and, accordingly, to a decrease in the stability of the sol. At very low concentrations of water-soluble polysaccharides, the relative change in turbidity decreases. This indicates a stabilization of particles by polysaccharides at their given concentrations. In this case, the contribution of the stabilization of sols by polysaccharides exceeds their contribution to their destabilization. This is due to a decrease in the thickness of the electric double layer of micelles. The decrease in the relative change in turbidity with the subsequent increase can be explained as follows: due to the low degree of filling the surface of particles with polysaccharides, the macromolecules adsorbed by some of their ends on one particle can be adsorbed by other ends on the surface of another particle, connecting them by a bridging mechanism. Owing to this, the tendency of polysaccharides to cause flocculation of particles begins to increase, compensating for their stabilizing ability and then prevailing over it. Thus, after a certain decrease, the increase in the concentration of the polysaccharide enhances flocculation, and the relative change in turbidity increases. The value for the sol without the addition of polysaccharides begins to be exceeded, and thus the first maximum is reached. Then the relative change in turbidity decreases. This can be associated with the high degree of filling of the particle surface with adsorbed macromolecules. The surface of the particle is saturated with polymer macromolecules which begin to counteract the coagulation of particles. As a result, a stabilizing effect gradually begins to appear, reducing flocculation. Further, with increasing polysaccharide concentration, the relative change in turbidity gradually increases again. When the adsorption of polysaccharides on the surface is sufficiently high, their destabilizing effect on the sol due to a decrease in the thickness of the electric double layer of micelles begins to increase.

Initially, SA promotes flocculation less than the other two polysaccharides. This can be due to the fact that it has a significantly lower molecular weight (Table 1) and, consequently, a smaller macromolecule size. As a result, its ability to link sol particles with each other by a bridging mechanism is lower. This can explain the more pronounced decrease in stability at a concentration of 0.0125% in the case of the addition of SA.

The maxima on the curves in Fig. 5 for κ-carrageenan and xanthan are observed at their concentrations of 0.025 and 0.03%, respectively. This can be explained by the predominance of flocculation over the stabilizing effect of polymers at these concentrations. Moreover, in the case of κ-carrageenan, which has a higher molecular weight than xanthan (Table 1), this maximum occurs at a lower concentration. The degree of stabilization of the sol is greatest in the case of the addition of κ-carrageenan, which, as suggested by Fig. 3, in this concentration range, is adsorbed on the surface of ChS more strongly than the other two polymers and, moreover, has the highest molecular weight (Table 1). Consequently, in the concentration range where the stabilization begins to prevail over the flocculation, κ-carrageenan was found to be the most efficient stabilizer. This is due to its stronger adsorption resulting from the presence of specific interactions of its sulfate groups with the protonated amino groups of chitosan. For this reason, the adsorption of κ-carrageenan on the surface of sol particles creates a more voluminous and stronger structural-mechanical barrier. Therefore, in this concentration range, xanthan stabilizes sols over time much worse than κ-carrageenan. SA, which is adsorbed on ChS better than xanthan, exhibits an even lower stabilizing ability. This can be explained by the lower molecular weight of SA and, therefore, the less pronounced manifestation of the structural-mechanical stability factor. As can be seen from Fig. 5, the curve for SA obviously approaches a maximum only at concentrations above 0.04%. However, precipitation occurs at higher concentrations of the added SA (Fig. 5, curve *1*). As Fig. 3 shows, the adsorption of SA at this concentration is close to the adsorption of xanthan, but significantly lower than the adsorption of κ-carrageenan. This can be explained by the fact that the structural-mechanical barrier for SA is obviously less pronounced because of its lower molecular weight.

At higher concentrations, the stabilizing ability of water-soluble polysaccharides decreases again due to the increasing contribution of neutralization of the positive charge of the particle surface by polysaccharide polyions. At sufficiently high concentrations, polysaccharide anions cause rapid coagulation of positively charged ChS particles; something which is not considered in this work. Thus, although the water-soluble polysaccharides used in this study can cause coagulation of sol particles, there are certain concentration ranges in which they exhibit a stabilizing ability owing to the structural-mechanical stability factor. A mechanically strong protective shell is created around the ChS particle by the adsorption of polysaccharide macromolecules. This protective shell also carries negative charges, promoting the repulsion between polyanions adsorbed on different particles when these particles collide. Thus, despite the decrease in the electrostatic stability factor when polysaccharides are added to the sol, in the case of collision between two ChS particles with polyions adsorbed on them, the polyions can interfere with the coagulation for these reasons.

By means of dynamic light scattering with a Delsa Nano C particle size analyzer (*Beckman Coulter*, USA), the particle sizes measured in the sols demonstrated the highest stability over time and the sol without the addition of polymer. Table 2 presents the results for freshly prepared sols (time elapsed since preparation was about 1 h). In the histograms of the particle number size distribution for all sols, there is one peak with a fraction of 65–75%. The other peaks in the submicron and micron ranges are negligible (Fig. 6).

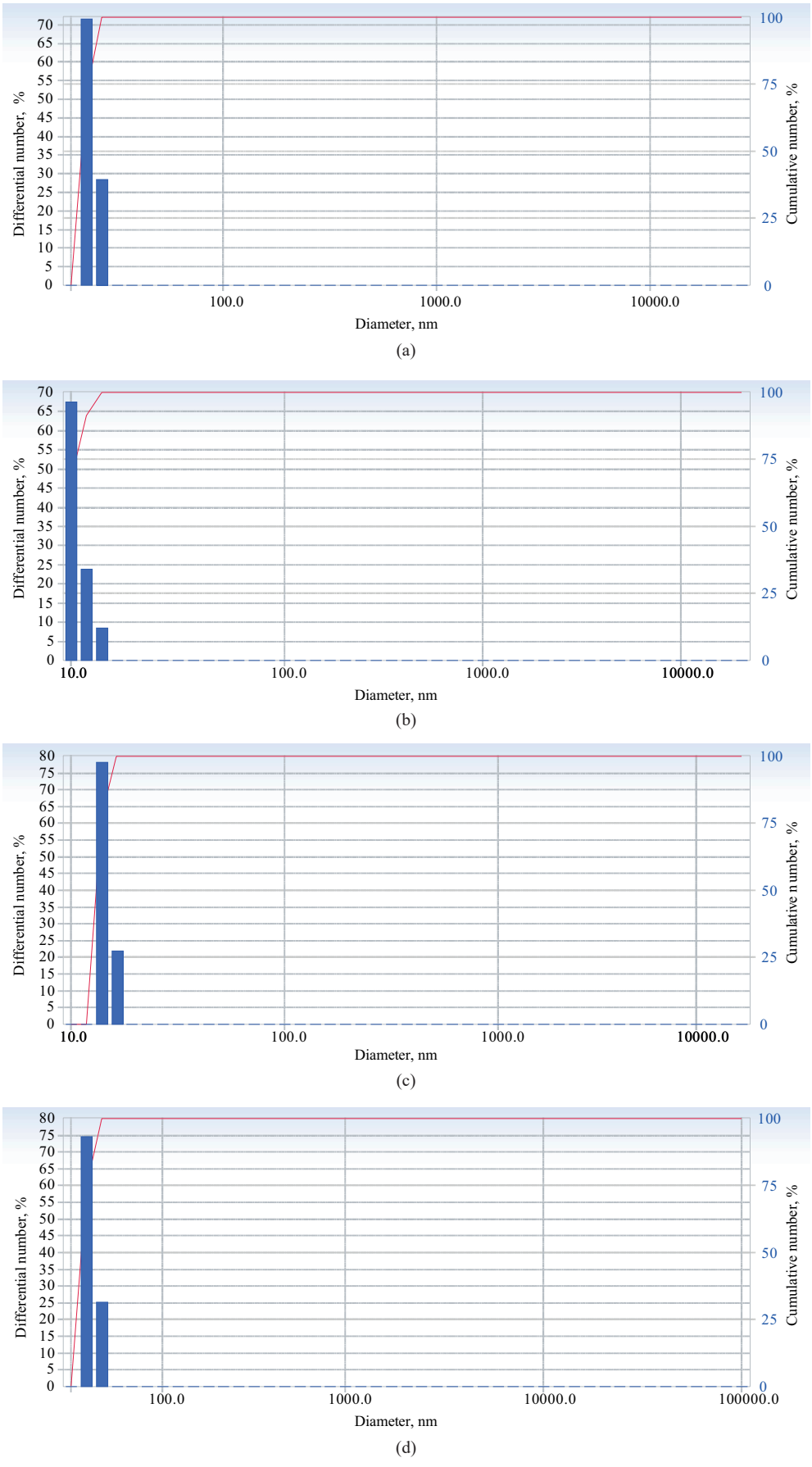

Fig. 6. Histograms of the particle number size distributions for ChS sols (a) without the addition of polysaccharide and with the addition of (b) 0.0125% SA, (b) 0.04% κ-carrageenan, and (d) 0.0125% xanthan

As can be seen, in the case of the addition of solutions of SA and κ-carrageenan to the sols to the indicated concentration, the average particle size decreases, while it increases in the case of addition of a xanthan solution. The decrease in the particle size in the sol can be related to the stabilizing effect of added polysaccharides at these concentrations. At the same time, the observed slight increase in the turbidity of freshly prepared sols in the case of the addition of κ-carrageenan and SA (in accordance with Fig. 4) can be explained by an increase in the number concentration of particles which are more protected from coagulation when polysaccharides are added.

At a concentration of 0.0125%, the smallest average particle size (smaller than the particle size without the addition of polysaccharides) is observed for SA, whereas that for xanthan is noticeably larger. This is consistent with the above considerations since at this concentration, SA contributes less to flocculation. Despite the fact that when xanthan is added, the particles become almost twice as large, sols with the addition of xanthan retain their particle size longer than without it (Fig. 5). This can be explained by the fact that the tendency for xanthan to stabilize particles over time begins to prevail over the tendency to promote flocculation. At a κ-carrageenan concentration of 0.04%, the particle size is smaller than that without the addition of polysaccharides. It is close to that with the addition of 0.0125% SA.

Figures 7 and 8 show the graphs of the dependencies of the turbidity of solutions on the amount of added electrolytes. Sodium chloride is an indifferent electrolyte in relation to ChS. Therefore, it does not affect the charge and electrical potential of the particle surface, but only compresses the electric double layer, promoting concentration coagulation. Coagulation begins when 0.1 mL of 3M sodium chloride solution is added to 5 mL of sol.

Sodium sulfate is a non-indifferent electrolyte in relation to ChS, since it can bind potential-determining chitosanium polycations, thereby changing the surface charge. When Na_2SO_4 is started to be added, the surface charge decreases because of the interaction of sulfate anions with potential-determining chitosanium

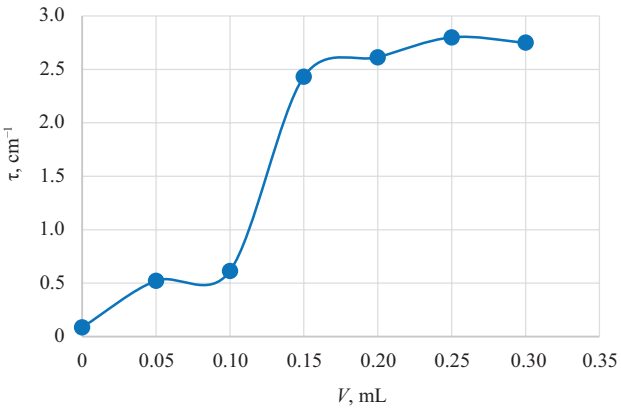

Fig. 7. Dependence of the turbidity of the ChS sol on the volume of the added NaCl solution

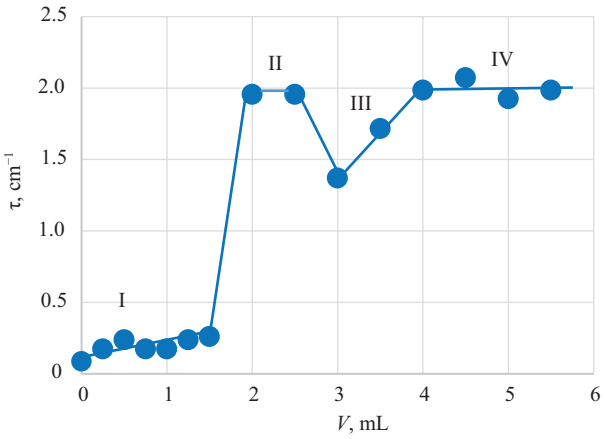

Fig. 8. Dependence of the turbidity of the ChS sol on the volume of the added Na_2SO_4 solution

polycations. When 1.75 mL of 0.5 M sodium sulfate is added to 10 mL of sol, the turbidity sharply increases, indicating that the coagulation threshold has been reached. In region II in Fig. 8, the sol is rapidly coagulated. When 3 mL of the electrolyte is added, the turbidity decreases and a new region of sol stability appears (Fig. 8, region III). This can be explained by the attainment of the equivalence point. This is the point where the electrolyte recharges the surface of the micelle, making it negatively

Table 2. Average particle sizes of sols with the addition of various polysaccharides

Sol composition	Average particle size, nm	Coefficient of variation, %
Without addition of water-soluble polymers	25	17
With addition of 0.0125% SA	11	23
With addition of 0.04% κ-carrageenan	15	30
With addition of 0.0125% xanthan	55	8

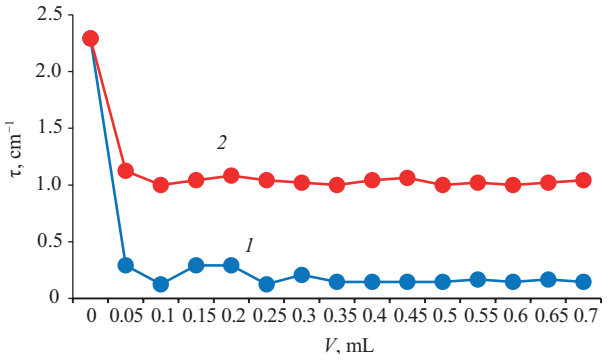

Fig. 9. Dependence of the turbidity of the ChS sol on the volume of added solution of (*1*) SA and (*2*) κ-carrageenan in the presence of NaCl sufficient for coagulation

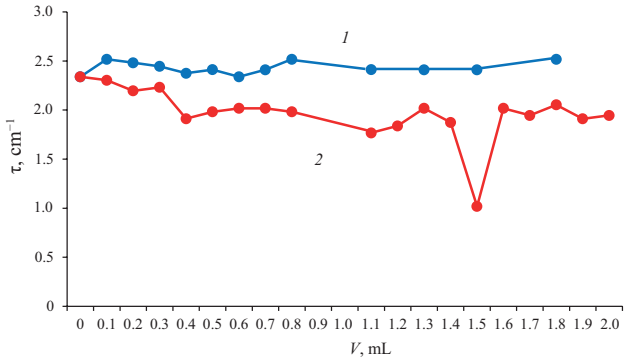

Fig. 10. Dependence of the turbidity of the ChS sol on the volume of added solution of (*1*) SA and (*2*) κ-carrageenan in the presence of Na_2SO_4 sufficient for coagulation

charged, thereby exerting a stabilizing effect. Then, when sodium sulfate is added, the turbidity of the sol begins to increase again and a new region of coagulation appears (Fig. 8, region IV). This is due to a decrease in the thickness of the electric double layer with an increase in the concentration of counterions which are now sodium ions. This type of dependence of turbidity on the volume of added electrolyte is typical of the case where a sol is supplemented with a non-indifferent electrolyte carrying non-indifferent ions charged opposite to the potential-determining ions. This proves that the surface of the resulting sols is positively charged.

For colloidal protection of the ChS sol from coagulation with electrolytes, SA and κ-carrageenan were taken as polymers which showed themselves to be the most optimal stabilizers.

These polysaccharides protect the sol from coagulation under the action of sodium chloride (Fig. 9), although inefficient against the action of sodium sulfate (Fig. 10). The decrease in turbidity by approximately half at one of the points in curve *2* (Fig. 10) is likely to be caused by the fact that κ-carrageenan, the molecules of which have a greater electrical charge, recharges the surface when taken in the given amount. However, this stabilizing effect is insufficient to prevent coagulation.

The sol coagulation thresholds with electrolytes were calculated using formula (4), while the protective numbers for polysaccharides were calculated using formula (5) (Table 3). The coagulation threshold with an indifferent electrolyte is 9.3 times higher than that with a non-indifferent electrolyte. The protective number against the coagulation with an indifferent electrolyte is 4.8 times lower for SA than for κ-carrageenan. The protective numbers for both of these polysaccharides are significantly lower than the concentrations at which, in accordance with Fig. 5, the relative changes in the turbidity of the sols over time (their maximum stability over time) are minimum. Therefore, at these concentrations of SA and κ-carrageenan, their efficient protection against the coagulation with sodium chloride is also ensured.

CONCLUSIONS

A method was developed to obtain ChS hydrosol with a positive particle charge. It was shown that the addition of polysaccharides to certain concentrations improves the stability of sols. The mechanisms of the stabilization of sols by polysaccharides are explained using experimental capillary viscometry data on the adsorption of these polysaccharides on the surface of ChS. In this case, in the widest concentration range, κ-carrageenan

Table 3. Coagulation thresholds of ChS sols with sodium chloride and sodium sulfate, and the protective numbers of polysaccharides against the coagulation of ChS sols with these electrolytes

Electrolyte causing coagulation	Coagulation threshold, mM	Stabilizer	Protective number, %
NaCl	73	SA	$6.1 \cdot 10^{-5}$
NaCl		κ-Carrageenan	$2.9 \cdot 10^{-4}$
Na_2SO_4	7.88	SA	Does not protect
Na_2SO_4		κ-Carrageenan	Does not protect

is adsorbed most strongly, whereas xanthan is adsorbed least of all. The stronger adsorption of κ-carrageenan can be attributed to the specific binding of sulfate groups to the ChS surface.

Based on experimental data on the relative change in turbidity over time, which has complex behavior with extrema, the polysaccharides studied herein predominantly either stabilize or destabilize the sol according to the degree of filling the surface of the particles with polysaccharide macromolecules, depending on their concentration. The stabilization of sols by polysaccharides is ensured by the structural-mechanical stability factor.

The most stable over time are the sols with the addition of 0.0125% SA and κ-carrageenan in the range of 0.04%. In the former case, this can be explained by the lower molecular weight of SA, which is less conducive to the flocculation of sol particles at lower polysaccharide concentrations. In the latter case, at a higher polysaccharide concentration, this may be a consequence of better adsorption of κ-carrageenan, as well as its higher molecular weight. This makes a greater contribution to the structural-mechanical stability factor.

κ-Carrageenan and SA protect the sol against coagulation with an indifferent electrolyte (NaCl) at all amounts of polysaccharides used. At the same time, at the same amounts of polysaccharides, no protection against the coagulation by a non-indifferent electrolyte (Na_2SO_4) was observed. The protective number against the coagulation with sodium chloride is lower for SA than for κ-carrageenan.

Based on the results of the work, it can be concluded that SA and κ-carrageenan can be used as efficient stabilizers of ChS hydrosols over time and to protect them against the flocculation with sodium chloride.

Acknowledgments

The work was carried out within the framework of the State Task of the Russian Federation No. FSFZ-2023-0003. The authors thank Doctor of Chemical Sciences, Professor N.A. Yashtulov, Head of the S.S. Voyutsky Department of Nanoscale Systems and Surface Phenomena at the MIREA—Russian Technological University.

Authors' contributions

V.S. Erasov—idea of the study, acquisition and processing of experimental data, analysis of results, and writing the text of the article.

Yu.O. Maltseva—obtaining and processing experimental data.

The authors declare no conflict of interest.

REFERENCES

1. Varlamov V.P., Il'ina A.V., Shagdarova B.T., *et al.* Chitin/chitosan and its derivatives: Fundamental problems and practical approaches. *Biochemistry Moscow*. 2020; 85(Suppl. 1):154–176. https://doi.org/10.1134/S0006297920140084 [Original Russian Text: Varlamov V.P., Il'ina A.V., Shagdarova B.Ts., Lun'kov A.P., Mysyakina I.S. Chitin/chitosan and its derivatives: Fundamental problems and practical approaches. *Uspekhi Biologicheskoi Khimii*. 2020;60:317–368 (in Russ.).]
2. Skryabin K.G., Mihajlov S.N., Varlamov V.P. (Eds.). *Khitozan* (*Chitosan*). Moscow: Bioinzheneriya; 2013. 591 p. (in Russ.). ISBN 978-5-4253-0596-1
3. Samujlenko A.Ya. (Ed.). *Biologicheski aktivnye veshchestva* (*khitozan i ego proizvodnye*) (*Biologically active substances (Chitosan and its derivatives)*). Krasnodar: KubGAU; 2018. 329 p. (in Russ.). ISBN 978-5-00097-319-6
4. Khvostov M.V., Tolstikova T.G., Borisov S.A., Dushkin A.V. Application of natural polysaccharides in pharmaceutics. *Russ. J. Bioorg. Chem.* 2019; 45(6):438–450. https://doi.org/10.1134/S1068162019060219 [Original Russian Text: Khvostov M.V., Tolstikova T.G., Borisov S.A., Dushkin A.V. Application of natural polysaccharides in pharmaceutics. *Bioorganicheskaya Khimiya.* 2019;45(6): 563–575 (in Russ.). https://doi.org/10.1134/S0132342319060241]
5. Garg U., Chauhan S., Nagaich U., Jain N. Current advances in chitosan nanoparticles based drug delivery and targeting. *Adv. Pharm. Bull*. 2019;9(2):195–204. https://doi.org/10.15171/apb.2019.023

СПИСОК ЛИТЕРАТУРЫ

1. Варламов В.П., Ильина А.В., Шагдарова Б.Ц., Луньков А.П., Мысякина И.С. Хитин/хитозан и его производные: фундаментальные и прикладные аспекты. *Успехи биологической химии*. 2020;60:317–368.
2. Скрябин К.Г., Михайлов С.Н., Варламов В.П. (ред.). *Хитозан*. М.: Центр «Биоинженерия» РАН; 2013. 591 с. ISBN 978-5-4253-0596-1
3. Самуйленко А.Я. (ред.). *Биологически активные вещества* (*хитозан и его производные*). Краснодар: КубГАУ; 2018. 329 с. ISBN 978-5-00097-319-6
4. Хвостов М.В., Толстикова Т.Г., Борисов С.А., Душкин А.В. Применение природных полисахаридов в фармацевтике. *Биоорганическая химия*. 2019;45(6):563–575. https://doi.org/10.1134/S0132342319060241
5. Garg U., Chauhan S., Nagaich U., Jain N. Current advances in chitosan nanoparticles based drug delivery and targeting. *Adv. Pharm. Bull*. 2019;9(2):195–204. https://doi.org/10.15171/apb.2019.023
6. Li J., Cai Ch., Li J., Li J., Li J., Sun T., Wang L., Wu H., Yu G. Chitosan-based nanomaterials for drug delivery. *Molecules.* 2018;23(10):2661. https://doi.org/10.3390/molecules23102661
7. Bernkop-Schnürch A., Dünnhaupt S. Chitosan-based drug delivery systems. *Europ. J. Pharm. Biopharm*. 2012;81(3): 463–469. https://doi.org/10.1016/j.ejpb.2012.04.007
8. Hasnain M.S., Sarwar B., Nayak A.K. (Eds.). *Chitosan in drug delivery*. USA: Academic Press (Elsevier); 2021. 556 p. ISBN 978 0128-1933-65

6. Li J., Cai Ch., Li J., Li J., Li J., Sun T., Wang L., Wu H., Yu G. Chitosan-Based Nanomaterials for Drug Delivery. *Molecules.* 2018;23(10):2661. https://doi.org/10.3390/molecules23102661
7. Bernkop-Schnürch A., Dünnhaupt S. Chitosan-based drug delivery systems. *Europ. J. Pharm. Biopharm*. 2012;81(3): 463–469. https://doi.org/10.1016/j.ejpb.2012.04.007
8. Hasnain M.S., Sarwar B., Nayak A.K. (Eds.). *Chitosan in Drug Delivery*. USA: Academic Press (Elsevier); 2021. 556 p. ISBN 978 0128-1933-65
9. Parhi R. Drug delivery applications of chitin and chitosan: a review. *Environ. Chem. Lett.* 2020;18(2):577–594. https://doi.org/10.1007/s10311-020-00963-5
10. Mikušová V., Mikuš P. Advances in chitosan-based nanoparticles for drug delivery. *Int. J. Mol. Sci.* 2021;22(17):9652. https://doi.org/10.3390/ijms22179652
11. Ghosh R., Mondal S., Mukherjee D., Adhikari A., Saleh A.A., Alsantali I., Khder A.S., Altass H.M., Moussa Z., Das R., Bhattacharyya M., Pal S.K. Oral drug delivery using a polymeric nanocarrier: chitosan nanoparticles in the delivery of rifampicin. *Mater. Adv.* 2022;3(11):4622–4628. https://doi.org/10.1039/D2MA00295G
12. Radha D., Lal J.S., Devaky K.S. Chitosan-based films in drug delivery applications. *Starch-Starke.* 2022;74(7–8):2100237. https://doi.org/10.1002/star.202100237
13. Herdiana Y., Wathoni N., Shamsuddin Sh., Muchtaridi M. Drug release study of the chitosan-based nanoparticles. *Heliyon*. 2022;8(1):e08674. https://doi.org/10.1016/j.heliyon.2021.e08674
14. Lau A. K.-T., Hussain F., Dafdie H. (Eds.). *Nano- i biokompozity* (*Nano- and Biocomposites*): transl. from Engl. Moscow: BINOM. Laboratoriya znanii; 2020. 390 p. (in Russ.). ISBN 978-00101-727-1 [Lau A.K.-T., Hussain F., Dafdie H. (Eds.). *Nano- and Biocomposites.* Boca Raton: CRC Press; 2010. 408 p.]
15. Munawar A.M., Syeda J.T.M., Wasan K.M., Wasan E.K. An overview of chitosan nanoparticles and its application in non-parenteral drug delivery. *Pharmaceutichs*. 2017;9(4):53. https://doi.org/10.3390/pharmaceutics9040053
16. Azimov Zh.T., Oksengendler B.L., Turaeva N.N., *et al*. Effect of the structure of the biopolymer chitosan on its bactericidal activity. *Polym. Sci. Ser. A.* 2013;55(2):98–101. https://doi.org/10.1134/S0965545X13020028
[Original Russian Text: Azimov Zh.T., Oksengendler B.L., Turaeva N.N., Rashidova S.Sh. Effect of the structure of the biopolymer chitosan on its bactericidal activity. *Vysokomolekulyarnye Soedineniya. Ser. A.* 2013;55(2):165–101 (in Russ.). https://doi.org/10.7868/S0507547513020025]
17. Kritchenkov A.S., Andranovitšc S., Skorik Yu.A. Chitosan and its derivatives: vectors in gene therapy. *Russ. Chem. Rev*. 2017;86(3):231–239. https://doi.org/10.1070/rcr4636
[Original Russian Text: Kritchenkov A.S., Andranovitšc S., Skorik Yu.A. Chitosan and its derivatives: vectors in gene therapy. *Uspekhi Khimii*. 2017;86(3):231–239 (in Russ.).]
18. Povernov P.A., Shibryaeva L.S., Lusova L.R., Popov A.A. Modern polymer composite materials for bone surgery: Problems and prospects. *Tonk. Khim. Tekhnol. = Fine Chem. Technol.* 2022;17(6):514–536 (Russ., Eng.). https://doi.org/10.32362/2410-6593-2022-17-6-514-536
19. Lykoshin D.D., Zaitsev V.V., Kostromina M.A., Esipov R.S. New-generation osteoplastic materials based on biological and synthetic matrices. *Tonk. Khim. Tekhnol. = Fine Chem. Technol.* 2021;16(1):36–54 (Russ., Eng.). https://doi.org/10.32362/2410-6593-2021-16-1-36-54
20. Ignatieva P.E., Zhavoronok E.S., Legonkova O.A., Kedik S.A. Compositions based on aqueous solutions of chitosan and glutar aldehyde for embolization of blood vessels. *Tonk. Khim. Tekhnol. = Fine Chem. Technol.* 2019;14(1):25–31 (Russ., Eng.). https://doi.org/10.32362/2410-6593-2019-14-1-25-31
9. Parhi R. Drug delivery applications of chitin and chitosan: a review. *Environ. Chem. Lett.* 2020;18(2):577–594. https://doi.org/10.1007/s10311-020-00963-5
10. Mikušová V., Mikuš P. Advances in chitosan-based nanoparticles for drug delivery. *Int. J. Mol. Sci.* 2021;22(17):9652. https://doi.org/10.3390/ijms22179652
11. Ghosh R., Mondal S., Mukherjee D., Adhikari A., Saleh A.A., Alsantali I., Khder A.S., Altass H.M., Moussa Z., Das R., Bhattacharyya M., Pal S.K. Oral drug delivery using a polymeric nanocarrier: chitosan nanoparticles in the delivery of rifampicin. *Mater. Adv.* 2022;3(11):4622–4628. https://doi.org/10.1039/D2MA00295G
12. Radha D., Lal J.S., Devaky K.S. Chitosan-based films in drug delivery applications. *Starch-Starke.* 2022;74(7–8):2100237. https://doi.org/10.1002/star.202100237
13. Herdiana Y., Wathoni N., Shamsuddin Sh., Muchtaridi M. Drug release study of the chitosan-based nanoparticles. *Heliyon*. 2022;8(1):e08674. https://doi.org/10.1016/j.heliyon.2021.e08674
14. Лау А.К.-Т., Хуссейн Ф., Дафди Х. (ред.). *Нано- и биокомпозиты*: пер. с англ. М.: БИНОМ. Лаборатория знаний; 2020. 390 с. ISBN 978 00101-727-1
15. Munawar A.M., Syeda J.T.M., Wasan K.M., Wasan E.K. An overview of chitosan nanoparticles and its application in non-parenteral drug delivery. *Pharmaceutichs*. 2017;9(4):53. https://doi.org/10.3390/pharmaceutics9040053
16. Азимов Ж.Т., Оксенгендлер Б.Л., Тураева Н.Н., Рашидова С.Ш. Влияние строения биополимера хитозана на его бактерицидную активность. *Высокомол. соединения. Сер. А.* 2013;55(2);165–169. https://doi.org/10.7868/S0507547513020025
17. Критченков А.С.., Andranovitš S., Скорик Ю.А. Хитозан и его производные: векторы в генной терапии. *Успехи химии.* 2017.86(3):231–239.
18. Повернов П.А., Шибряева Л.С., Люсова Л.Р., Попов А.А. Современные полимерные композиционные материалы для костной хирургии: проблемы и перспективы. *Тонкие химические технологии.* 2022;17(6):514–536. https://doi.org/10.32362/2410-6593-2022-17-6-514-536
19. Лыкошин Д.Д., Зайцев В.В., Костромина М.А., Есипов Р.С. Остеопластические материалы нового поколения на основе биологических и синтетических матриксов. *Тонкие химические технологии.* 2021;16(1):36–54. https://doi.org/10.32362/2410-6593-2021-16-1-36-54
20. Игнатьева П.Е., Жаворонок Е.С., Легонькова О.А., Кедик С.А. Композиции на основе водных растворов хитозана и глутарового альдегида для эмболизации кровеносных сосудов. *Тонкие химические технологии*. 2019;14(1):25–31. https://doi.org/10.32362/2410-6593-2019-14-1-25-31
21. Al-Remawi M.M. Properties of chitosan nanoparticles formed using sulfate anions as crosslinking bridges. *Am. J. Applied Sci.* 2012;9(7):1091–1100. https://doi.org/10.3844/AJASSP.2012.1091.1100
22. Мезина Е.А., Липатова И.М. Исследование процесса образования дисперсной фазы в смешанных растворах хитозана и сульфата магния. *Журнал прикладной химии*. 2014;87(6): 821–827.
23. Мезина Е.А., Липатова И.М. Влияние пероксидной деполимеризации хитозана на свойства получаемых из него хитозан-сульфатных наночастиц. *Журнал прикладной химии*. 2015;88(10):1390–1395.
24. Гордиенко М.Г., Сомов Т.Н., Юсупова Ю.С., Чупикова Н.И., Меньшуткина Н.В. Получение микрочастиц из биодеградируемых природных и синтетических полимеров для применения их в области регенеративной медицины. *Тонкие химические технологии.* 2015;10(5):66–76.

21. Al-Remawi M.M. Properties of Chitosan Nanoparticles Formed Using Sulfate Anions as Crosslinking Bridges. *Am. J. Applied Sci.* 2012;9(7):1091–1100. https://doi.org/10.3844/AJASSP.2012.1091.1100
22. Mezina E.A., Lipatova I.M. Formation of the dispersed phase in mixed solutions of chitosan and magnesium sulfate. *Russ. J. Appl. Chem.* 2014;87(6):830–835. https://doi.org/10.1134/S1070427214060275
[Original Russian Text: Mezina E.A., Lipatova I.M. Formation of the dispersed phase in mixed solutions of chitosan and magnesium sulfate. *Zhurnal Prikladnoi Khimii.* 2014;87(6):821–827 (in Russ.).]
23. Mezina E.A., Lipatova I.M. Effect of peroxide depolymerization of chitosan on properties of chitosan sulfate particles produced from this substance. *Russ. J. Appl. Chem*. 2015;88(10):1576–1581. https://doi.org/10.1134/S1070427215100031
[Original Russian Text: Mezina E.A., Lipatova I.M. Effect of peroxide depolymerization of chitosan on properties of chitosan sulfate particles produced from this substance. *Zhurnal Prikladnoi Khimii.* 2015;88(10):1390–1395 (in Russ.).]
24. Gordienko M.G., Somov T.N., Yusupova Y.S., Chupikova N.I., Menshutina N.V. Preparation of spherical microparticles from biodegradable natural and synthetic polymers for their application in regenerative medicine. *Fine Chem. Technol*. 2015;10(5):66–76 (in Russ.).
25. Zhang C., Zhang H., Li R., Xing Y. Morphology and adsorption properties of chitosan sulfate salt microspheres prepared by a microwave-assisted method. *RSC Adv.* 2017;7(76):48189–48198. https://doi.org/10.1039/C7RA09867G
26. Apryatina K.V., Mochalova A.E., Gracheva T.A., *et al*. Influence of the molecular mass of chitosan on the dimensional characteristics of silver nanoparticles. *Polymer Sci. Ser. B.* 2015;57(2):145–149. https://doi.org/10.1134/S1560090415020013
[Original Russian Text: Apryatina K.V., Mochalova A.E., Gracheva T.A., Kuz'micheva T.A., Smirnova L.A., Smirnova O.N. Influence of the molecular mass of chitosan on the dimensional characteristics of silver nanoparticles. *Vysokomolekulyarnye Soedineniya. Ser. B.* 2015;57(2):154–1158 (in Russ.). https://doi.org/10.7868/S2308113915020011]
27. Tyukova I.S., Safronov A.P., Kotel'nikova A.P., *et al*. Electrostatic and steric mechanisms of iron oxide nanoparticle sol stabilization by chitosan. *Polymer Sci. Ser. A.* 2014;56(4):498–504. https://doi.org/10.1134/S0965545X14040178
[Original Russian Text: Tyukova I.S., Safronov A.P., Kotel'nikova A.P., Agalakova D.Yu. Electrostatic and steric mechanisms of iron oxide nanoparticle sol stabilization by chitosan. *Vysokomolekulyarnye Soedineniya. Ser. A.* 2014;56(4):419–426 (in Russ.). https://doi.org/10.7868/S2308112014040178]
28. Bochek A.M., Vokhidova N., Saprykina N.N., *et al*. The properties of chitosan-cobalt nanoparticle solutions and related composite films. *Polymer Sci. Ser. A.* 2015;57(4):460–466. https://doi.org/10.1134/S0965545X15040033
[Original Russian Text: Bochek A.M., Vokhidova N., Saprykina N.N., Ashurov N.S., Yugai S.M., Rashidova S.S. The properties of chitosan-cobalt nanoparticle solutions and related composite films. *Vysokomolekulyarnye Soedineniya. Ser. A.* 2015;57(4):354–360 (in Russ.). https://doi.org/10.7868/S2308112015040033]
29. Wilson B.K., Prud'homme R.K. Processing Chitosan for Preparing Chitosan-Functionalized Nanoparticles by Polyelectrolyte Adsorption. *Langmuir.* 2021;37(28):8517–8524. https://doi.org/10.1021/acs.langmuir.1c00990
30. Czechowska-Biskup R., Jarosińska D., Rokita B., *et al.* Determination of degree of deacetylation of chitosan – Comparison of methods. *Progress on Chemistry and Application of Chitin and its Derivatives.* 2012;17:5–20.
25. Zhang C., Zhang H., Li R., Xing Y. Morphology and adsorption properties of chitosan sulfate salt microspheres prepared by a microwave-assisted method. *RSC Adv.* 2017;7(76):48189–48198. https://doi.org/10.1039/C7RA09867G
26. Апрятина К.В., Мочалова А.Е., Грачева Т.А., Кузьмичева Т.А., Смирнова О.Н., Смирнова Л.А. Влияние молекулярной массы хитозана на размерные характеристики наночастиц серебра. *Высокомол. соединения. Сер. Б.* 2015;57(2):154–158. https://doi.org/10.7868/S2308113915020011
27. Тюкова И.С., Сафронов А.П., Котельникова А.П., Аглакова Д.Ю. Роль электростатического и стерического механизмов стабилизации хитозаном золей наночастиц оксида железа. *Высокомол. соединения. Сер. А.* 2014;56(4):419–426. https://doi.org/10.7868/S2308112014040178
28. Бочек А.М., Вохидова Н.Р., Сапрыкина Н.Н., Ашуров Н.Ш., Югай С.М., Рашидова С.Ш. Свойства растворов смесей хитозана с наночастицами кобальта и композитных пленок на их основе. *Высокомол. соединения. Сер. А.* 2015;57(4):354–360. https://doi.org/10.7868/S2308112015040033
29. Wilson B.K., Prud'homme R.K. Processing chitosan for preparing chitosan-functionalized nanoparticles by polyelectrolyte adsorption. *Langmuir.* 2021;37(28):8517–8524. https://doi.org/10.1021/acs.langmuir.1c00990
30. Czechowska-Biskup R., Jarosińska D., Rokita B., *et al.* Determination of degree of deacetylation of chitosan – Comparison of methods. *Progress on Chemistry and Application of Chitin and its Derivatives.* 2012;17:5–20.
31. Wang W., Bo Sh., Li S., Qin W. Detrmination of the Mark–Houwink equation for chitosans with different degrees of deacetylation. *Int. J. Biol. Macromol.* 1991;13(5):281–285. https://doi.org/10.1016/0141-8130(91)90027-R
32. Belalia F., Djelali N.-E. Rheological properties of sodium alginate solutions. *Revue Roumaine de Chimie*. 2014;59(2):135–145.
33. Distantina S., Wiratni, Fahrurrozi M., Rochmadi. Carrageenan properties extracted from *Eucheuma cottonii*, Indonesia. *Int. J. Chem. Mol. Eng.* 2011;5(6):501–505.
34. Masuelli M.A. Mark–Houwink parameters for aqueous-soluble polymers and biopolymers at various temperatures. *J. Polymer Biopolymer Phys. Chem.* 2014;2(2):37–43. https://doi.org/10.12691/jpbpc-2-2-2

31. Wang W., Bo Sh., Li S., Qin W. Detrmination of the Mark–Houwink equation for chitosans with different degrees of deacetylation. *Int. J. Biol. Macromol.* 1991;13(5):281–285. https://doi.org/10.1016/0141-8130(91)90027-R
32. Belalia F., Djelali N.-E. Rheological properties of sodium alginate solutions. *Revue Roumaine de Chimie*. 2014;59(2):135–145.
33. Distantina S., Wiratni, Fahrurrozi M., Rochmadi. Carrageenan properties extracted from *Eucheuma cottonii*, Indonesia. *Int. J. Chem. Mol. Eng.* 2011;5(6):501–505.
34. Masuelli M.A. Mark–Houwink parameters for aqueous-soluble polymers and biopolymers at various temperatures. *J. Polymer Biopolymer Phys. Chem.* 2014;2(2):37–43. https://doi.org/10.12691/jpbpc-2-2-2

About the authors

Vadim S. Erasov, Cand. Sci. (Eng.), Senior Lecturer, S.S. Voyutsky Department of Nanoscale Systems and Surface Phenomena, M.V. Lomonosov Institute of Fine Chemical Technologies, MIREA – Russian Technological University (86, Vernadskogo pr., Moscow, 119571, Russia). E-mail: vadim.ersv@yandex.ru. Scopus Author ID 57484351900, RSCI SPIN-code 1268-2737, https://orcid.org/0000-0003-2501-759X

Yuliya O. Mal'tseva, Student, M.V. Lomonosov Institute of Fine Chemical Technologies, MIREA – Russian Technological University (86, Vernadskogo pr., Moscow, 119571, Russia). E-mail: uliaxmaltseva@mail.ru

Об авторах

Ерасов Вадим Сергеевич, к.х.н., старший преподаватель, кафедра наноразмерных систем и поверхностных явлений им. С.С. Воюцкого, Институт тонких химических технологий им. М.В. Ломоносова, ФГБОУ ВО «МИРЭА – Российский технологический университет» (119571, Россия, Москва, пр-т Вернадского, д. 86). E-mail: vadim.ersv@yandex.ru. Scopus Author ID 57484351900, SPIN-код РИНЦ 1268-2737, https://orcid.org/0000-0003-2501-759X

Мальцева Юлия Олеговна, студент, Институт тонких химических технологий им. М.В. Ломоносова, ФГБОУ ВО «МИРЭА – Российский технологический университет» (119571, Россия, Москва, пр-т Вернадского, д. 86). E-mail: uliaxmaltseva@mail.ru

Translated from Russian into English by V. Glyanchenko
Edited for English language and spelling by Dr. David Mossop

Tonkie Khimicheskie Tekhnologii = Fine Chemical Technologies.
2024;19(2):127–138 ISSN 2686-7575 (Online)

Chemistry and technology of medicinal compounds
and biologically active substances

Химия и технология лекарственных препаратов
и биологически активных соединений

UDC 547.466:543.544
https://doi.org/10.32362/2410-6593-2024-19-2-127-138

RESEARCH ARTICLE

One-pot determination of amino acids in drugs by pre-column derivatization with phenyl isothiocyanate

Pavel A. Kalmykov[1], Tatyana P. Kustova[2,✉], Stanislav O. Kustov[1,2], Polina S. Shestakovskaya[1,2], Timur R. Azmetov[1], Alyona A. Kalmykova[1]

[1] *GENERIUM, Volginskiy, Vladimir oblast, 601125 Russia*

[2] *Ivanovo State University, Ivanovo, 153025 Russia*

✉ *Corresponding author, e-mail: kustovatp@ivanovo.ac.ru*

Abstract

Objectives. To develop a new method to determine amino acids in drugs by means of reverse-phase high-performance chromatography (RP HPLC) with pre-column derivatization using phenyl isothiocyanate (PITC) and *one-pot* sample preparation.

Methods. The initial standard solutions of amino acids were prepared by weighing, followed by dissolution in water. Working solutions were then prepared: standard, test, and blank, by dilution in 20 mM hydrochloric acid. Further sample preparation was carried out in Safe-lock polypropylene tubes (*Eppendorf*) in a reaction buffer containing mobile phase A, acetonitrile, and triethylamine in a ratio of 85 : 10 : 5, labeled with a 5% PITC solution in acetonitrile. After thorough mixing for 3–5 min on a vortex, the tubes were kept in a solid-state thermostat with a thermally insulating lid for 2 h. The samples were then cooled for 10 min, centrifuged for 1 min at 13000 rpm, the supernatant was transferred into vials, and the mixture of amino acids was separated by RP HPLC using hydrophobic silica gel with grafted C18 groups as a stationary phase. The quantitative determination of amino acid derivatives was carried out using a diode array detector.

Results. A new method for the separation and determination of amino acids in medicinal preparations was developed and validated. Simple *one-pot* sample preparation using available reagents and equipment enabled studies to be carried out without using commercial kits, for example, the AccQ·Tag Ultra Derivatization Kit, USA. Using the analysis of mixtures of histidine and glycine as an example, it was shown that when using two mobile phases, an acceptable separation of amino acid derivatives in a gradient mode can be achieved for 20 min at a flow rate of 1.0 mL/min. The samples prepared according to the new method demonstrated a high level of stability in use and storage. A composition of mobile phases A and B consisting of 10 mM acetate buffer pH 3.5 and 80% acetonitrile solution was proposed. Validation of the method hereby developed in the analysis of the drug Innonafactor®, containing glycine and histidine as excipients, demonstrated high convergence of the results of the quantitative determination of these amino acids.

Conclusions. The new method to determine amino acids in medicinal preparations by RP HPLC with PITC pre-column derivatization has a wide range of applications, has a number of advantages when compared to imported commercial kits for the determination of amino acids. These include: lower cost of reagents and materials, high accuracy and repeatability. Thus, it can be recommended for use in quality control laboratories of pharmaceutical enterprises.

Keywords

amino acids, glycine, histidine, RP HPLC, pre-column derivatization, PITC (phenyl isothiocyanate), quality control of medicines

Submitted: 29.08.2023
Revised: 07.11.2023
Accepted: 06.03.2024

For citation

Kalmykov P.A., Kustova T.P., Kustov S.O., Shestakovskaya P.S., Azmetov T.R., Kalmykova A.A. *One-pot* determination of amino acids in drugs by pre-column derivatization with phenyl isothiocyanate. *Tonk. Khim. Tekhnol. = Fine Chem. Technol.* 2024;19(2):127–138. https://doi.org/10.32362/2410-6593-2024-19-2-127-138

НАУЧНАЯ СТАТЬЯ

One-pot определение аминокислот в лекарственных препаратах методом предколоночной дериватизации с фенилизотиоцианатом

П.А. Калмыков[1], Т.П. Кустова[2,✉], С.О. Кустов[1,2], П.С. Шестаковская[1,2], Т.Р. Азметов[1], А.А. Калмыкова[1]

[1] *Генериум, пос. Вольгинский, Владимирская область, 601125 Россия*

[2] *Ивановский государственный университет, Иваново, 153025 Россия*

✉ *Автор для переписки, e-mail: kustovatp@ivanovo.ac.ru*

Аннотация

Цели. Разработать новую методику определения аминокислот в лекарственных препаратах методом обращенно-фазовой высокоэффективной жидкостной хроматографии (ОФ ВЭЖХ) с предколоночной дериватизацией фенилизотиоцианатом (ФИТЦ) с применением *one-pot* пробоподготовки.

Методы. Исходные стандартные растворы аминокислот готовили методом навесок с последующим растворением в воде, после чего готовили рабочие растворы: стандартный, испытуемый и холостой, путем разведения в 20 мМ соляной кислоте. Дальнейшая пробоподготовка осуществлялась в полипропиленовых пробирках Safe-lock (*Eppendorf*) в реакционном буфере, содержащем подвижную фазу А, ацетонитрил и триэтиламин в соотношении 85 : 10 : 5 с окрашиванием 5% раствором ФИТЦ в ацетонитриле. После тщательного перемешивания в течение 3–5 мин на вортексе пробирки выдерживали в твердотельном термостате с термоизоляционной крышкой в течение 2 ч. Далее пробы охлаждали в течение 10 мин, центрифугировали в течение 1 мин при 13000 об/мин. Надосадочную жидкость переносили в виалы и проводили разделение смеси аминокислот методом ОФ ВЭЖХ с использованием в качестве неподвижной фазы гидрофобного силикагеля с привитыми группами С18. Количественное определение дериватов аминокислот проводили с применением диодно-матричного детектора.

Результаты. Разработана и валидирована новая методика разделения и определения аминокислот в лекарственных препаратах, позволяющая на основе простой *one-pot* пробоподготовки с использованием доступных реактивов и оборудования проводить исследования без использования коммерческих наборов, например AccQ×Tag Ultra Derivatization Kit, США. На примере анализа смесей гистидина и глицина показано, что при использовании двух подвижных фаз удается достичь приемлемого разделения дериватов аминокислот в градиентном режиме в течение 20 мин со скоростью потока 1.0 мл/мин. Приготовленные по новой методике пробы продемонстрировали высокую стабильность в применении и хранении. Предложен состав подвижных фаз А и Б, состоящий из 10 мМ ацетатного буфера с pH 3.5 и 80% раствора ацетонитрила. Валидация разработанной методики при анализе лекарственного препарата Иннонафактор®, содержащего в качестве вспомогательных веществ глицин и гистидин, продемонстрировала высокую сходимость результатов количественного определения данных аминокислот.

Выводы. Новая методика определения аминокислот в лекарственных препаратах методом ОФ ВЭЖХ с предколоночной дериватизацией ФИТЦ обладает широким диапазоном применения, имеет ряд преимуществ по сравнению с импортными коммерческими наборами для определения аминокислот: низкую стоимость реактивов и материалов, высокую точность и повторяемость, в связи с чем она может быть рекомендована к использованию в лабораториях контроля качества фармацевтических предприятий.

Ключевые слова

аминокислоты, глицин, гистидин, ОФ ВЭЖХ, предколоночная дериватизация, ФИТЦ (фенилизотиоцианат), контроль качества лекарственных средств

Поступила: 29.08.2023
Доработана: 07.11.2023
Принята в печать: 06.03.2024

Для цитирования

Калмыков П.А., Кустова Т.П., Кустов С.О., Шестаковская П.С., Азметов Т.Р., Калмыкова А.А. *One-pot* определение аминокислот в лекарственных препаратах методом предколоночной дериватизации с фенилизотиоцианатом. *Тонкие химические технологии*. 2024;19(2):127–138. https://doi.org/10.32362/2410-6593-2024-19-2-127-138

INTRODUCTION

In the second half of 2022, a number of foreign pharmaceutical companies announced their suspension of investments in the Russian market. They ceased clinical trials in the country which are required for registration of new drugs. Certain drugs are in short supply due to problems with logistics of finished dosage forms or pharmaceutical substances. Problems with the availability of innovative foreign drugs are most acute in the therapy of orphan (rare) diseases. It should also be noted that certain Russian pharmaceutical companies produce such drugs independently. For example, *Generium*[1] produces drugs for the treatment of hemophilia, cystic fibrosis and Gaucher disease [1]. This is important, since in 2023 Russia introduced expanded neonatal screening of newborns for 36 congenital diseases, including inherited diseases of amino acid, organic acid, and fatty acid metabolism.

Analysis of the Russian pharmaceutical market for 2022[2] showed that the production of pharmaceuticals in the country increased by 8.6% when compared to 2021. According to the Strategy for the Development of the Pharmaceutical Industry until 2030, adopted by the Government of the Russian Federation in June 2023, the share of Russian full-cycle drugs in the market of the Russian Federation is due to increase to almost 70%, while the volume of drug production in monetary terms is expected to double to RUR 1.4 trn.[3]

Drugs containing amino acids and proteins are widely used in medical practice for the treatment of metabolic disorders, cardiovascular, infectious and dermatologic diseases, cancer, gastrointestinal, kidney and central nervous system diseases, as well as pain syndromes [1]. The segment of the pharmaceutical market related to the production of peptide drugs is steadily growing. Therefore, pharmaceutical manufacturers urgently need to improve amino acid analysis for quality control of such drugs. When queried for "amino acid analysis," the *sciencedirect.com* platform currently produces more than 64000 results, 2700 of which are in the last 5 years [2–5].

The Pharmacopoeia of the Eurasian Economic Union (EEU)[4] recommends 12 methods of amino acid analysis. Seven of these methods involve pre-column derivatization of amino acids. Derivatization of amino acids is necessary due to the absence of chromophore groups in the structure of most of their molecules. This does not allow for the use of optical detectors for analysis. In this regard, the professional community is focusing on the functionalization of amino acids, primarily by the *N*-terminal amino group [6–8]. One of the most reliable and well-established methods for amino acid determination is reversed-phase high-performance liquid chromatography (RP-HPLC) with precolumn derivatization with phenyl isothiocyanate (PITC). In amino acid analysis, the HPLC method is used much more often than other methods, since peptides are complex organic compounds which are thermolabile (degrade when heated). This method is characterized by a high level of sensitivity and selectivity. Derivatives with PITC at the *N*-terminal amino group form all amino acids. The reaction proceeds rapidly and quantitatively with the formation of stable amino acid derivatives. No other compounds are formed which interfere with the determination of amino acids. Thus, [9] proposed a method for the quantitative determination of a number of free amino acids (glutamic and asparagic, serine, glycine, histidine, proline, alanine, etc.) in samples of veal meat, laying hens and dried extract of cow brain by SP HPLC with pre-column PITC derivatization. The authors used 3 mobile phases: 2 acetate buffers with pH 4.05 and pH 5.5 and a 1% solution of isopropyl alcohol in acetonitrile. The sample preparation took on average about 20 h. It included acid hydrolysis of proteins, ethanol extraction of free amino acids, selection and drying of aliquots, addition of sodium hydroxide solution, labeling solution (PITC), re-drying and dissolution of the dry residue in bi-distilled water. During amino acid analysis, some analyte loss is known to occur during prolonged sample preparation. Therefore, it is important to limit the number of sample manipulations, since this will increase the analyte detection value and reduce the labor input of the staff.

The objective of this study was the development and validation of a new method using *one-pot* sample preparation with available reagents and equipment without the use of commercial kits of foreign production for the determination of amino acids in drugs by RP-HPLC with pre-column derivatization with PITC. Innonafactor®, a drug belonging to the "Coagulants (including blood coagulation factors), hemostatics" pharmaceutical group was chosen as a model system for the development of the methodology [10]. Recombinant blood coagulation

[1] https://www.generium.ru/products/#. Accessed August 02, 2023.

[2] The pharmaceutical market of Russia for 2022. Analytical review of DSM GROUP. https://dsm.ru/docs/analytics/Annual_report_2023_rus.pdf. Accessed August 02, 2023.

[3] Decree of the Government of the Russian Federation dated June 7, 2023, No. 1495-r "Strategy for the Development of the Pharmaceutical Industry until 2030." http://government.ru/docs/48801/. Accessed August 02, 2023.

[4] https://eec.eaeunion.org/comission/department/deptexreg/formirovanie-obshchikh-rynkov/pharmacopoeia/pharmacopoeia_utv.php. Accessed August 02, 2023.

factor IX, a single-chain glycoprotein with a molecular mass of about 55 kDa, consists of 415 amino acid residues[5]. In order to stabilize the glycoprotein in the preparation, a mixture of amino acids is used in sufficient excess (29-fold for glycine, 2.3-fold for histidine)[6]. Determination of the quantitative content of these amino acids is regulated and must be controlled during release control. In this regard, there is an urgent need for analytical methods to be developed to determine amino acids, which will give reproducible results with simple sample preparation in minimal time.

EXPERIMENTAL

All the reagents and solvents used in the work were considered chemically pure: histidine (*PanReac AppliChem*, Spain, Cat. No. A1341), glycine (*PanReac AppliChem*, Spain, Cat. No. 143040), sodium acetate (*Sigma-Aldrich*, USA, Cat. No. S2889), concentrated acetic acid (*PanReac AppliChem*, Spain, Cat. No. 141008), hydrochloric acid (*Pallav*, India, Cat. No. 1379B), PITC (*Sigma-Aldrich*, USA, Cat. No. 78780), sodium hydroxide (*PanReac AppliChem*, Spain, Cat. No. 141687), sodium chloride (*Nouryan*, Denmark, Cat. No. 8004337), polysorbate 80 (*PanReac AppliChem*, Spain, Cat. No. 142050), triethylamine (*Sigma-Aldrich*, USA, Cat. No. 471283), acetonitrile (*PanReac AppliChem*, Spain, Cat. No. 221881). Ultrapure water (type I) (Milli-Q, *Merck Millipore*, USA) was used to prepare working solutions.

The labeling solution was prepared in a 2-mL Safe-lock polypropylene tube (*Eppendorf*, Germany) by mixing 950 μL of acetonitrile and 50 μL of PITC.

In order to prepare the mobile phase A (MP A), 0.82 g of sodium acetate was added to a 1-L beaker, and about 800 mL of water was added. Then the pH of the solution was adjusted with acetic acid to 3.5 ± 0.1 using a pH meter (Seven Easy S20, *Mettler Toledo*, Switzerland). The resulting solution was transferred to a 1-L volumetric flask, brought to the mark with water, stirred, filtered through a membrane filter with a pore diameter of 0.45 μm and then degassed using a vacuum pump.

For the preparation of the mobile phase B (MP B), 800 mL of acetonitrile was placed in a chemical beaker with a capacity of 1 L, and 200 mL of water was added. This was then stirred, and filtered through a membrane filter with a pore diameter of 0.45 μm and degassed.

The reaction buffer was prepared in a 15 mL test tube. 8.5 mL of MP A, 1 mL of acetonitrile and 500 μL of triethylamine in the ratio 85 : 10 : 5 were added to the test tube, and the contents were stirred.

The initial test solution of Innonafactor® 500 IU was prepared as follows: 5.0 mL of water for injections was added to the vial with the lyophilizate. It was gently mixed avoiding foaming according to the drug instructions. At such dilution the content of histidine is about 1.55 mg/mL (7.76 mg/flask), and glycine—about 19.52 mg/mL (97.6 mg/flask) which corresponds to the middle of the range specified in the drug instructions.

The initial standard solutions of amino acids were prepared by the method of suspensions with subsequent dissolution in water: the concentration of histidine was 1.55 mg/mL, and glycine—19.52 mg/mL. Then working solutions were then prepared. The initial test solution, initial standard solution, and placebo solution (without histidine and glycine) of 100 μL each were placed in 1.5 mL polypropylene tubes. Then 400 μL of 20 mM hydrochloric acid solution were added and mixed.

Further sample preparation was carried out in 1.5 mL polypropylene tubes in a reaction buffer with staining using labeling solution. After thorough mixing for 3–5 min, the tubes were held in a solid-state thermostat with a Gnome thermo-insulating lid (*DNA-Technology*, Moscow, Russia) for 2 h at 65°C. Then the samples were cooled in a refrigerator for 10 min, and centrifuged for 1 min at 13000 rpm. The supernatant was transferred to vials and the amino acid mixture was separated in a high-pressure liquid chromatograph (Waters e2695 with an Alliance separation module with Waters 2998 PDA detector, USA). Hydrophobic silica gel[7] with grafted C18 groups was used as the stationary phase.

Before commencing amino acid determination, the chromatographic column was equilibrated with a mixture of mobile phases in the ratio 97 : 3 until a stable base line was formed. Then conditioning in gradient mode was carried out at least 2 times.

Chromatographic conditions:

- Diaspher-110-C18 stainless steel column, 4.6 × 250 mm (particle size 5 μm) (*BioChemMak ST*, Russia);
- 2 mobile phases: MP A and MP B;
- MP flow rate: 1.0 mL/min;
- column thermostat temperature: 45°C;
- sample temperature: 5 ± 3°C;
- diode array detector (λ = 254.0 ± 4.8 nm);
- injection volume: 5 μL for glycine estimation, 50 μL for histidine estimation;
- chromatogram recording time: 20 min;
- sample injection order: blank solution (1 injection, 5 μL), standard solution (for glycine estimation,

[5] Register of medicines of Russia: *Nonacogum alfa*. https://www.rlsnet.ru/active-substance/nonakog-alfa-2595. Accessed August 02, 2023.

[6] Instructions for the medical use of the drug Innonafaktor®. https://www.generium.ru/upload/preparations/manual/Instruktsiya-Innonafaktor.pdf. Accessed August 02, 2023.

[7] https://bcmst.ru/kolonki/diaspher/. Accessed August 02, 2023.

3–5 injections, 5 μL), test solution (1–3 injections, 5 μL), standard solution (for histidine estimation, 3–5 injections, 50 μL), test solution (1–3 injections, 50 μL).

Elution was carried out in gradient mode. The samples were chromatographed according to the order of sample input. The peaks of the blank solution were not taken into account when processing the chromatograms.

The chromatographic system was considered suitable, if the following acceptance criteria were met:

- the relative standard deviation of retention time and peak area of the derivative no more than 2.0%;
- derivative peak asymmetry factor between 0.8 and 1.5;
- the efficiency of the chromatographic column for the derivative peak at least 50000 theoretical plates.

Amino acid content (X) in mg/flask was calculated according to the following formula:

$$X = \frac{S_{test}}{S_{st}} \times C \times 5,$$

wherein S_{test} is the peak area of histidine/glycine derivatives on the chromatogram of the test solution; S_{st} is the peak area of histidine/glycine derivatives on the chromatogram of standard solution; C is the histidine/glycine content in standard solution, mg/mL; 5 is the volume of water added to the vial of the test drug solution during reconstitution of the lyophilizate, mL.

RESULTS AND DISCUSSION

Specificity. The specificity of the method was evaluated by means of visually comparing chromatograms of blank solution, standard and test solutions. On the chromatogram of the blank solution, there are no peaks with retention times of histidine derivatives (about 8.6 min), or glycine derivatives (about 10.8 min) present on the chromatograms of standard and test solutions (Fig. 1). Thus, the specificity of the technique was proven in relation to the matrix of the test solution (protein, placebo auxiliary components).

Four peaks were found in the retention time domain of amino acid derivatives. One is present on the chromatogram of the blank solution and belongs to the placebo solution. In order to identify the other peaks, the method of single amino acid standards was used. This method showed that the peak with retention time about 10.8 min belongs to the glycine derivative. The peaks with retention times of about 8.6 min and 10.4 min belong to the histidine derivative. According to the data available in literature [2] derivatives of amino acids with several nitrogen atoms in the structure are unstable and may undergo degradation. In order to evaluate these peaks and determine their nature, the absorption spectra of the derivatives in the wavelength range of 200–400 nm were studied using a diode array

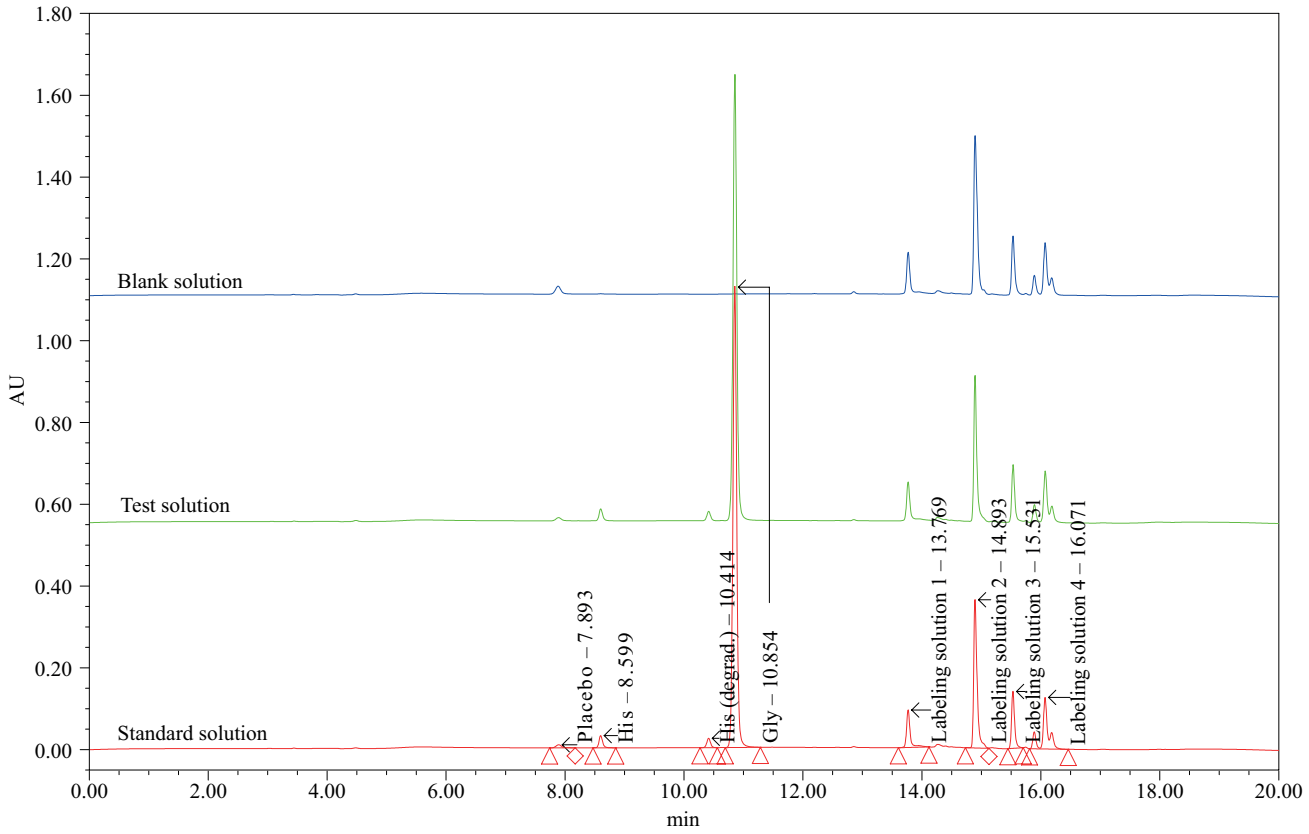

Fig. 1. Chromatograms of blank, test, and standard solutions

detector. A slice of peaks in the range of 6–11 min on the 3D spectrum of the chromatogram was established for the standard solution (Fig. 2).

According to the data obtained, the peak of glycine derivative has a spectrum with absorption maximum around 250 nm (Fig. 2d). This is in agreement with the data available in literature (254 nm). A similar spectrum is observed for the peak with retention time of around 8.6 min (Fig. 2b). The peaks with retention times of around 7.9 min and 10.4 min have no absorption maximum around 250 nm. Thus, it can be concluded that the peak of histidine derivative is selected for estimation of quantitative histidine content.

Peaks with a retention time of more than 12 min belong to the PITC dye peaks and system peaks (gradient region of column rewashing).

Linearity, correctness and analytical range of the method. In order to evaluate the linearity, correctness and analytical range of the technique, the method of calibration solutions was used. For this purpose, model solutions (MS) of amino acids in the range of 40–140% of the nominal concentration (the middle of the range of Innonafactor® content) were prepared. The preparation of MS for linearity evaluation is described in Table 1.

Sample preparation was performed according to the method described above; each MR in three repetitions. The results of the linearity evaluation of the methodology on the peak of glycine derivative are summarized in Table 2, and histidine derivative in Table 3 and Fig. 3.

The method is show to have linearity in the selected range with a correlation coefficient of more than 0.98. The technique also shows an acceptable level of correctness in the confidence interval 95–105% for glycine, 90–110% for histidine. This can be associated with a fairly low concentration of histidine in the working test solution.

Table 1. Preparation of model solutions (MS) for evaluation of linearity and analytical area

MS No.	1	2	3	4	5	6
Glycine/histidine content, %	40	60	80	100	120	140
Glycine content, mg/mL	7.81	11.71	15.62	19.52	23.42	27.33
Histidine content, mg/mL	0.62	0.93	1.24	1.55	1.86	2.17
Initial standard solution, μL	40	60	80	100	120	140
20 mM hydrochloric solution acids, μL	460	440	420	400	380	360

Table 2. Evaluation of the linearity of the method and the analytical area of the method for determining the content of glycine

MS No.	1	2	3	4	5	6
Calculated concentration, mg/mL	7.81	11.71	15.62	19.52	23.42	27.33
Practical concentration, mg/mL	7.53	11.36	16.41	20.32	23.31	26.88
Detection percent	96.4	97.0	105.0	104.0	99.5	98.4

Table 3. Evaluation of the linearity of the method and the analytical area of the method for determining the content of histidine

MS No.	1	2	3	4	5	6
Calculated concentration, mg/mL	0.62	0.93	1.24	1.55	1.86	2.17
Practical concentration, mg/mL	0.58	0.88	1.34	1.63	1.85	2.10
Detection percent	93.5	94.6	108.0	105.2	99.5	96.8

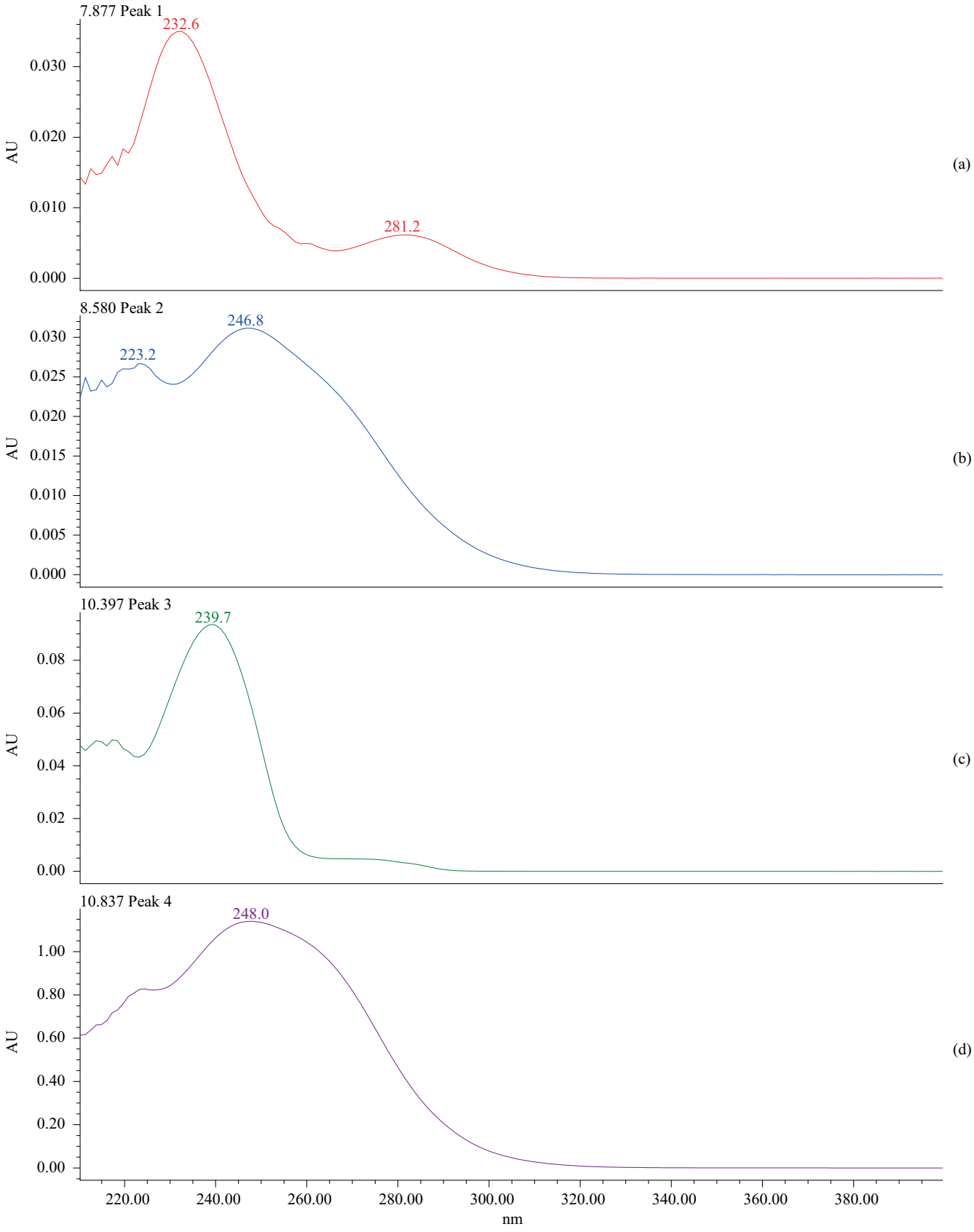

Fig. 2. Absorption spectra of peaks on the standard solution chromatogram with a retention time of
(a) 7.9;
(b) 8.6;
(c) 10.4;
(d) 10.8 min

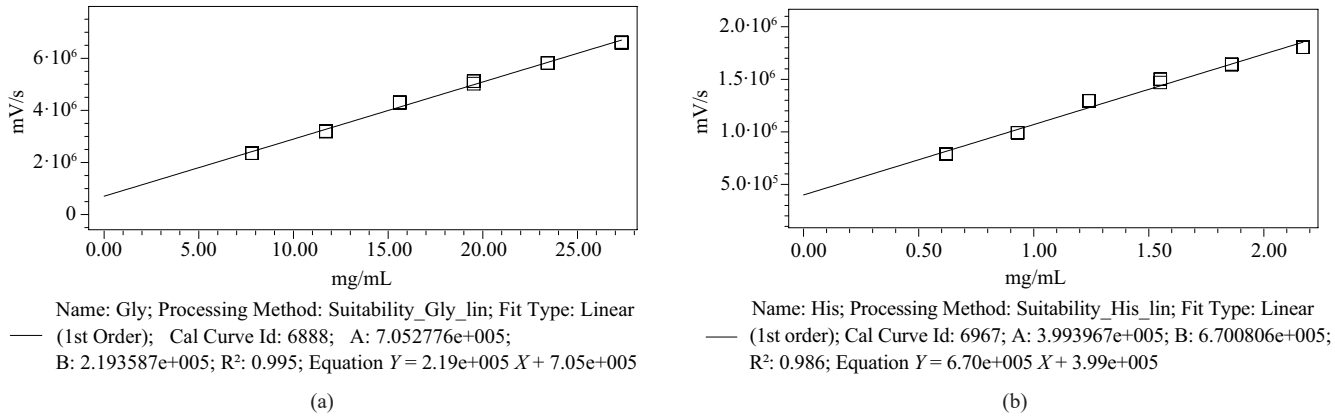

Fig. 3. Calibration plots for determining the linearity and analytical area of the method:
(a) glycine content estimate;
(b) histidine content estimate

The analytical technique has an acceptable level of linearity and correctness in the concentration range of 40–140% of nominal or 0.62–2.17 mg/mL for histidine and 7.81–27.33 mg/mL for glycine. Therefore, this concentration range is the analytical domain of the technique.

***Limit of quantification* (*LOQ*).** Based on the test results, the limit of quantification was determined by the calculation method according to the following formula:

$$\mathrm{LOQ} = \frac{X \times 10}{S / n},$$

where X is the concentration of histidine/glycine in the standard solution, mg/mL; S/n is the signal-to-noise ratio for the histidine/glycine derivative peak in

Table 4. Assessment of the repeatability of the analytical method

Injection No.	Amino acid content, mg/flask			
	Histidine		Glycine	
	(1)	(2)	(1)	(2)
1	7.89	7.73	96.93	96.39
2	7.89	7.73	96.67	96.16
3	7.87	7.72	96.30	95.84
4	7.87	7.72	95.71	95.34
5	7.70	7.60	95.94	95.54
6	7.70	7.60	95.21	94.91
7	7.72	7.61	94.84	94.60
8	7.72	7.62	95.03	94.77
9	8.16	7.93	95.03	94.76
10	8.15	7.92	98.27	97.53
11	8.17	7.93	98.43	97.66
12	8.17	7.93	98.52	97.74
Average	7.9	7.8	96.6	96.1
SD*	0.2	0.1	1.4	1.2
RSD**, %	2.5	1.8	1.5	1.3

* SD—standard deviation.

** RSD—relative standard deviation.

the chromatogram of the standard solution; 10 is the limit of the signal-to-noise ratio for the estimation of LOQ.

The evaluation was performed for 6 consecutive injections of standard solution. The system acceptance criteria were fulfilled.

According to the data obtained, the analytical technique has high sensitivity. The initial concentration of amino acids in the initial test solution for histidine was about 0.01 mg/mL, for glycine about 0.024 mg/mL, corresponding to the limit of quantification.

Repeatability. In order to assess the repeatability of the methodology, tests were conducted to evaluate the quantitative content of histidine and glycine in Innonafactor®. The test solution was prepared in 6 repetitions and each solution was injected twice. The test results are presented in Table 4. The results were calculated using two methods: (1) by linearity calibration plot and (2) by 6 consecutive injections of standard solution to evaluate the suitability of the system.

According to the data obtained, the technique has a high level of repeatability characteristic of HPLC techniques. Thus, for 6 sample preparations, the relative standard deviation of amino acid determination was about 2–3%. The data obtained for the two methods of calculation of amino acid content coincide. They are in the range of ±10% of the nominal content, according to the preparation instructions. Thus, calculation method (2) can be considered a sufficient condition for the suitability of the system for estimating the amino acid content.

Stability of standard and test solutions. The stability of the analytical methodology within the framework of shelf-life evaluation of the standard and test solutions was performed for freshly prepared solutions (A) and after 1 day of storage in a thermostat at 2 to 8°C (B). The results of amino acid content estimation are presented in Tables 5 and 6.

Table 5. Evaluation of the stability of the tested solutions

Injection No.	Amino acid content, mg/flask			
	Histidine		Glycine	
	(A)	(B)	(A)	(B)
1	7.73	7.82	96.39	96.92
2	7.73	7.82	96.16	97.43
3	7.72	7.77	95.84	96.98
4	7.72	7.77	95.34	96.77
5	7.60	7.65	95.54	96.77
6	7.60	7.65	94.91	95.42
7	7.61	7.66	94.60	95.84
8	7.62	7.66	94.77	95.78
9	7.93	7.96	94.76	96.11
10	7.92	7.96	97.53	98.38
11	7.93	7.96	97.66	98.64
12	7.93	7.96	97.74	99.01
Average	7.8	7.8	96.1	97.1
SD	0.1	0.1	1.2	1.2
RSD, %	1.8	1.7	1.3	1.2
Average	7.8		96.5	
SD	0.1		1.3	
RSD, %	1.7		1.3	

Table 6. Evaluation of the stability of the standard solution

Injection No.	Amino acid derivative peak area, μV/s			
	Histidine		Glycine	
	(A)	(B)	(A)	(B)
1	1457768	1467593	5075402	5112246
2	1460085	1470084	5064962	5098915
3	1460186	1470991	4999555	5121785
4	1460216	1475217	4994879	5140767
5	1460957	1474622	4994327	5139811
6	1461680	1476159	4991779	5138833
Average	1460149	1472444	5020151	5125393
SD	1317	3390	38975	17389
RSD, %	0.1	0.2	0.8	0.3
Average	1466297		5072772	
SD	6873		62037	
RSD, %	0.5		1.2	

The stability of the standard and test solutions was confirmed within 1 day of storage in the thermostat at 2 to 8°C. This can be considered an advantage over similar methods for amino acid determination, such as derivatives with ortho-phthalic aldehyde which have a shelf life of about 2–3 min [11]. The relative standard deviation was less than 2%.

CONCLUSIONS

The new technique thus developed for the separation and determination of amino acids in pharmaceuticals on the basis of simple *one-pot* sample preparation using available reagents and equipment meets all the required criteria for HPLC quantification methods according to the EEU Pharmacopoeia and the State Pharmacopoeia of the Russian Federation. It can therefore be recommended for use in the laboratories of pharmaceutical companies. The technique is more economical compared to imported commercial kits for amino acid determination in terms of cost of reagents and materials. It also possesses a high level of accuracy and repeatability. Furthermore, the method is universal and has a wide range of application, since the formation of derivatives of amino acids with PITC at the *N*-terminal amino group is characteristic of all amino acids. In the present study, the range of application of this technique was confirmed for the quantification of histidine 0.62–2.17 mg/mL and glycine 7.81–27.33 mg/mL in the initial test solution. The limit of quantification was about 0.01 mg/mL for histidine and about 0.024 mg/mL for glycine. The proposed technique has a high level of repeatability, typical for HPLC techniques which is within the range of 2.0%.

Authors' contributions

P.A. Kalmykov—idea of a new method, concept of the study, analysis and interpretation of experimental data, and writing of the text of the article.

T.P. Kustova—concept of the study, analysis of literature on the research topic, analysis and interpretation of experimental data, and writing of the text of the article.

S.O. Kustov—experimental studies, and participation in writing of the text of the article.

P.S. Shestakovskaya—experimental studies and participation in writing of the text of the article.

T.R. Azmetov—experimental studies and participation in writing of the text of the article.

A.A. Kalmykova—experimental studies and participation in writing of the text of the article.

The authors declare no conflicts of interest.

REFERENCES

1. Slominsky P.A., Shadrina M.I. Peptide Pharmaceuticals: Opportunities, Prospects and Limitations. *Mol. Genet., Microbiol. Virol.* 2018;33(1):8–14. https://doi.org/10.3103/S0891416818010123
[Original Russian Text: Slominsky P.A., Shadrina M.I. Peptide Pharmaceuticals: Opportunities, Prospects and Limitations. *Molekulyarnaya Genetika, Mikrobiologiya i Virusologiya.* 2018;36(1):8–14 (in Russ.). https://doi.org/10.18821/0208-0613-2018-36-1-8-14]
2. Wahl O., Holzgrabe U. Amino acid analysis for pharmacopoeial purposes. *Talanta*. 2016;154:150–163. https://doi.org/10.1016/j.talanta.2016.03.071
3. Nwachukwu I.D., Aluko R.E. A systematic evaluation of various methods for quantifying food protein hydrolysate peptides. *Food Chem*. 2019;270:25–31. https://doi.org/10.1016/j.foodchem.2018.07.054
4. Lamp A., Kaltschmitt M., Lüdtke O. Improved HPLC-method for estimation and correction of amino acid losses during hydrolysis of unknown samples. *Anal. Biochem.* 2018;543;140–145. https://doi.org/10.1016/j.ab.2017.12.009
5. Polunin K.E., Fedotkina O.S., Polunina I.A., *et al.* Modeling the chromatographic behavior of antibacterial peptides under conditions of RP HPLS. *Russ. J. Phys. Chem. A*. 2022;96(6):1314–1321. https://doi.org/10.1134/S0036024422060188
[Original Russian Text: Polunin K.E., Fedotkina O.S., Polunina I.A., Buryak A.K. Modeling the chromatographic behavior of antibacterial peptides under conditions of RP HPLS. *Zhurnal Fizicheskoi Khimii.* 2022;96(6):895–903 (in Russ.). https://doi.org/10.31857/S004445372206019X]
6. Kochetova L.B., Kustova T.P., Kuritsyn L.V. Reactivity of α-amino acids in the reaction with esters in aqueous–1,4-dioxane media. *Russ. J. Gen. Chem.* 2018;88(1):80–85. https://doi.org/10.1134/S1070363218010127
[Original Russian Text: Kochetova L.B., Kustova T.P., Kuritsyn L.V. Reactivity of α-amino acids in the reaction with esters in aqueous–1,4-dioxane media. *Zhurnal Obshchei Khimii.* 2018;88(1):84–89 (in Russ.).]
7. Kustova T.P., Kochetova L.B. Kinetics and mechanism of sulfonylation of α-amino acids and dipeptides. *Russ. Chem. Bull.* 2019;68(4):809–816. https://doi.org/10.1007/s11172-019-2489-0
[Original Russian Text: Kustova T.P., Kochetova L.B. Kinetics and mechanism of sulfonylation of α-amino acids and dipeptides. *Izvestiya Akademii Nauk. Seriya khimicheskaya.* 2019;4:809–816 (in Russ.).]
8. Kustova T.P., Kochetova L.B., Khachatryan D.S. Comparison of the reactivities of tyrosine–proline-based dipeptides toward acylation with nitrophenyl benzoates. *Russ. J. Org. Chem.* 2022;58(4):512–517. https://doi.org/10.1134/S1070428022040078
[Original Russian Text: Kustova T.P., Kochetova L.B., Khachatryan D.S. Comparison of the reactivities of tyrosine–proline-based dipeptides toward acylation with nitrophenyl benzoates. *Zhurnal Organicheskoi Khimii.* 2022;58(4):422–429 (in Russ.). https://doi.org/10.31857/S0514749222040073]
9. Zakharova A.M., Grinshteyn I.L., Kartsova L.A. Determination of amino acids in dry extract of cow brain, meat samples of cow and chicken. *Sorbtsionnye i khromatograficheskie protsessy = Sorption and Chromatography Processes.* 2012;12(6):845–853 (in Russ.).

СПИСОК ЛИТЕРАТУРЫ

1. Сломинский П.А., Шадрина М.И. Пептидные лекарственные средства: возможности, перспективы и ограничения. *Молекулярная генетика, микробиология и вирусология.* 2018;36(1):8–14. https://doi.org/10.18821/0208-0613-2018-36-1-8-14
2. Wahl O., Holzgrabe U. Amino acid analysis for pharmacopoeial purposes. *Talanta*. 2016;154:150–163. https://doi.org/10.1016/j.talanta.2016.03.071
3. Nwachukwu I.D., Aluko R.E. A systematic evaluation of various methods for quantifying food protein hydrolysate peptides. *Food Chem*. 2019;270:25–31. https://doi.org/10.1016/j.foodchem.2018.07.054
4. Lamp A., Kaltschmitt M., Lüdtke O. Improved HPLC-method for estimation and correction of amino acid losses during hydrolysis of unknown samples. *Anal. Biochem.* 2018;543;140–145. https://doi.org/10.1016/j.ab.2017.12.009
5. Полунин К.Е., Федоткина О.С., Полунина И.А., Буряк А.К. Моделирование хроматографического поведения антибактериальных пептидов в условиях ОФ ВЭЖХ. *Журн. физ. химии*. 2022;96(6):895–903. https://doi.org/10.31857/S004445372206019X
6. Кочетова Л.Б., Кустова Т.П., Курицын Л.В. Реакционная способность α-аминокислот при взаимодействии со сложными эфирами в системе вода – 1,4-диоксан. *Журн. общей химии.* 2018;88(1):84–89.
7. Кустова Т.П., Кочетова Л.Б. Кинетика и механизм сульфонилирования α-аминокислот и дипептидов. *Известия Академии наук. Серия химическая.* 2019;4:809–816.
8. Кустова Т.П., Кочетова Л.Б., Хачатрян Д.С. Сравнительная реакционная способность в ацилировании дипептидов на основе тирозина и пролина. *Журн. орг. химии.* 2022;58(4):422–429. https://doi.org/10.31857/S0514749222040073
9. Захарова А.М., Гринштейн И.Л., Карцова Л.А. Определение аминокислот в сухом экстракте мозга коров, пробах мяса телят и кур методом высокоэффективной жидкостной хроматографии. *Сорбционные и хроматографические процессы*. 2012;12(6):845–853.
10. Тарасова И.С. Иннонафактор – первый отечественный рекомбинантный фактор свертывания крови IX. *Вопросы гематологии/онкологии и иммунопатологии в педиатрии*. 2015;14(5):70–75. https://doi.org/10.24287/1726-1708-2015-14-3-70-75
11. Тутельян В.А., Эллер К.И. (ред.). *Методы анализа минорных биологически активных веществ пищи*. М.: Династия; 2010. 180 с. ISBN 978-5-98125-073-6

10. Tarasova I.S. Innonafactor: The first Russian recombinant factor IX. *Voprosy gematologii/onkologii i immunopatologii v pediatrii = Pediatric Hematology/Oncology and Immunopathology.* 2015;14(5):70–75 (in Russ.). https://doi.org/10.24287/1726-1708-2015-14-3-70-75
11. Tutel'yan V.A., Eller K.I. (Eds.). *Metody analiza minornykh biologicheski aktivnykh veshchestv pishchi* (*Methods for Analyzing Minor Biologically Active Substances in Food*). Moscow: Dinastiya; 2010. 180 p. (in Russ.). ISBN 978-5-98125-073-6

About the authors

Pavel A. Kalmykov, Cand. Sci. (Chem.), Leading Specialist, Group for Transfer and Validation of Analytical Methods, Generium (14, Vladimirskaya ul., Volginskii, Vladimir oblast, 601125, Russia). E-mail: p.kalmykov@generium.ru. Scopus Author ID 55502543100, ReseacherID M-8148-2014, https://orcid.org/0000-0003-1358-0334

Tatyana P. Kustova, Dr. Sci. (Chem.), Professor, Director of the Institute of Mathematics, Information Technologies and Natural Sciences; Head of the Department of Fundamental and Applied Chemistry, Ivanovo State University (39, Yermaka ul., Ivanovo, 153025, Russia). E-mail: kustovatp@ivanovo.ac.ru. Scopus Author ID 6603679916, ReseacherID F-9318-2013, RSCI SPIN-code 1331-5782, https://orcid.org/0000-0001-5683-6470

Stanislav O. Kustov, Student, Ivanovo State University (39, Yermaka ul., Ivanovo, 153025, Russia); Intern, Group for Transfer and Validation of Analytical Methods, Generium (14, Vladimirskaya ul., Volginskii, Vladimir oblast, 601125, Russia). E-mail: stanislaskustov@yandex.ru. https://orcid.org/0009-0008-8698-3429

Polina S. Shestakovskaya, Student, Ivanovo State University (39, Yermaka ul., Ivanovo, 153025, Russia); Documentation Specialist, Group for Transfer and Validation of Analytical Methods, Generium (14, Vladimirskaya ul., Volginskii, Vladimir oblast, 601125, Russia). E-mail: p.shestakovskaya@generium.ru. https://orcid.org/0009-0008-0453-6335

Timur R. Azmetov, Chemist, Group for Transfer and Validation of Analytical Methods, Generium (14, Vladimirskaya ul., Volginskii, Vladimir oblast, 601125, Russia). E-mail: t.azmetov@generium.ru. https://orcid.org/0009-0002-7666-9870

Alyona A. Kalmykova, Senior Biochemist, Group for Transfer and Validation of Analytical Methods, Generium (14, Vladimirskaya ul., Volginskii, Vladimir oblast, 601125, Russia). E-mail: a.kalmykova@generium.ru. https://orcid.org/0000-0002-9452-7879

Об авторах

Калмыков Павел Алексеевич, к.х.н., ведущий специалист группы переноса и валидации аналитических методик, АО «Генериум» (601125, Россия, Владимирская обл., Петушинский район, пос. Вольгинский, ул. Владимирская, д. 14). E-mail: p.kalmykov@generium.ru. Scopus Author ID 55502543100, ReseacherID M-8148-2014, https://orcid.org/0000-0003-1358-0334

Кустова Татьяна Петровна, д.х.н., профессор, директор Института математики, информационных технологий и естественных наук; заведующий кафедрой фундаментальной и прикладной химии, ФГБОУ ВО «Ивановский государственный университет» (153025, Россия, г. Иваново, ул. Ермака, д. 39). E-mail: kustovatp@ivanovo.ac.ru. Scopus Author ID 6603679916, ReseacherID F-9318-2013, SPIN-код РИНЦ 1331-5782, https://orcid.org/0000-0001-5683-6470

Кустов Станислав Олегович, студент, ФГБОУ ВО «Ивановский государственный университет» (153025, Россия, г. Иваново, ул. Ермака, д. 39); стажер группы переноса и валидации аналитических методик, АО «Генериум» (601125, Россия, Владимирская обл., Петушинский район, пос. Вольгинский, ул. Владимирская, д. 14). E-mail: stanislaskustov@yandex.ru. https://orcid.org/0009-0008-8698-3429

Шестаковская Полина Сергеевна, студент, ФГБОУ ВО «Ивановский государственный университет» (153025, Россия, г. Иваново, ул. Ермака, д. 39); специалист по документации группы переноса и валидации аналитических методик, АО «Генериум» (601125, Россия, Владимирская обл., Петушинский район, пос. Вольгинский, ул. Владимирская, д. 14). E-mail: p.shestakovskaya@generium.ru. https://orcid.org/0009-0008-0453-6335

Азметов Тимур Рустемович, химик группы переноса и валидации аналитических методик, АО «Генериум» (601125, Россия, Владимирская обл., Петушинский район, пос. Вольгинский, ул. Владимирская, д. 14). E-mail: t.azmetov@generium.ru. https://orcid.org/0009-0002-7666-9870

Калмыкова Алёна Александровна, старший биохимик группы переноса и валидации аналитических методик, АО «Генериум» (601125, Россия, Владимирская обл., Петушинский район, пос. Вольгинский, ул. Владимирская, д. 14). E-mail: a.kalmykova@generium.ru. https://orcid.org/0000-0002-9452-7879

Translated from Russian into English by H. Moshkov
Edited for English language and spelling by Dr. David Mossop

Tonkie Khimicheskie Tekhnologii = Fine Chemical Technologies.
2024;19(2):139–148 ISSN 2686-7575 (Online)

Synthesis and processing of polymers and polymeric composites

Синтез и переработка полимеров и композитов на их основе

UDC 678.4-1:678.7-1
https://doi.org/10.32362/2410-6593-2024-19-2-139-148

RESEARCH ARTICLE

Natural and synthetic isoprene rubbers obtained using Ziegler–Natta catalysts

Anton A. Zuev[1,✉], Valentin L. Zolotarev[2], Igor P. Levenberg[2], Lyudmila A. Kovaleva[1], Ildus Sh. Nasyrov[3]

[1] *MIREA — Russian Technological University (M.V. Lomonosov Institute of Fine Chemical Technologies), Moscow, 119571 Russia*

[2] *Macrochem-R, Moscow, 123610 Russia*

[3] *Sintez-Kauchuk, Sterlitamak, 453110 Russia*

✉ *Corresponding author, e-mail: zuev_aa@mirea.ru*

Abstract

Objectives. To compare the properties of rubber compounds and rubbers based on natural rubber RSS1 and synthetic isoprene rubbers obtained using Ti, Nd, Gd catalysts, both when used individually in the formulation of rubber compounds and when synthetic analogues partially replace natural rubber.

Methods. Rubber compounds were prepared using a laboratory roll and a 100 cm^3 rubber mixer. For rubber compounds, the following factors were determined: Mooney viscosity, cohesive strength, and vulcanization characteristics. For rubbers, the following factors were determined: physical and mechanical parameters, Shore A hardness, rebound resilience, and volume loss upon abrasion.

Results. Based on the results of the rubber compound tests, the study showed that compounds based on all the synthetic polyisoprenes studied are significantly inferior to compounds based on natural rubber in terms of cohesive strength. The partial replacement of natural rubber with synthetic rubber (regardless of the type of catalytic system) leads to a significant decrease in the cohesive strength of the blends. Despite the differences observed in the properties of the rubber compounds, the results of the rubbers based on individual rubbers do not manifest significant differences.

Conclusions. The study demonstrated the influence of defects (oligomers, gel, low molecular weight fractions, branches, and 3,4-units) in the structure of synthetic polyisoprenes on the cohesive strength index of rubber compounds based on them, in which the number of 3,4-units plays a decisive role. The study also showed the potential of studying synthetic polyisoprenes as analogues of natural rubber in formulations of rubber compounds in the aims of resolving the problem of import substitution in the tire and rubber goods industry.

Keywords

natural rubber, synthetic isoprene rubber, carbon black, rubber compound, Mooney viscosity, cohesive strength, rubber

Submitted: 09.12.2022
Revised: 18.09.2023
Accepted: 05.03.2024

For citation

Zuev A.A., Zolotarev V.L., Levenberg I.P., Kovaleva L.A., Nasyrov I.Sh. Natural and synthetic isoprene rubbers obtained using Ziegler–Natta catalysts. *Tonk. Khim. Tekhnol. = Fine Chem. Technol.* 2024;19(2):139–148. https://doi.org/10.32362/2410-6593-2024-19-2-139-148

НАУЧНАЯ СТАТЬЯ

Натуральный и синтетические изопреновые каучуки, полученные с использованием катализаторов Циглера–Натта

А.А. Зуев[1], В.Л. Золотарев[2], И.П. Левенберг[2], Л.А. Ковалева[1], И.Ш. Насыров[3]

[1] *МИРЭА — Российский технологический университет (Институт тонких химических технологий им. М.В. Ломоносова), Москва, 119571 Россия*

[2] *Макрохем-Р, Москва, 123610 Россия*

[3] *Синтез-Каучук, Стерлитамак, 453110 Россия*

✉ *Автор для переписки, e-mail: zuev_aa@mirea.ru*

Аннотация

Цели. Сравнение свойств резиновых смесей и резин на основе натурального каучука RSS1 и синтетических изопреновых каучуков, полученных с использованием Ti, Nd, Gd катализаторов, как при индивидуальном использовании в рецептуре резиновых смесей, так и при частичной замене натурального каучука синтетическими аналогами.

Методы. Резиновые смеси изготавливали с использованием лабораторных вальцев и резиносмесителя объемом 100 см^3. Для резиновых смесей определяли вязкость по Муни, когезионную прочность и вулканизационные характеристики, для резин — физико-механические показатели, твердость по Шору А, эластичность по упругому отскоку и потерю объема при истирании.

Результаты. На основании результатов испытаний резиновых смесей показано, что смеси на основе всех исследованных синтетических полиизопренов значительно уступают по когезионной прочности смеси на основе натурального каучука, при этом частичная замена натурального каучука синтетическим (независимо от типа каталитической системы) приводит к существенному снижению когезионной прочности смесей. Несмотря на выявленные различия в свойствах резиновых смесей, показатели резин на основе индивидуальных каучуков не имеют значительных различий.

Выводы. Показано влияние «дефектов» структуры (олигомеры, гель, низкомолекулярные фракции, разветвления, 3,4-звенья) синтетических полиизопренов на показатель когезионной прочности резиновых смесей на их основе, из которых решающую роль играет количество 3,4-звеньев. Показана перспективность исследования синтетических полиизопренов в качестве аналога натурального каучука в рецептурах резиновых смесей для решения проблемы импортозамещения в промышленности шин и резинотехнических изделий.

Ключевые слова

натуральный каучук, синтетический изопреновый каучук, технический углерод, резиновая смесь, вязкость по Муни, когезионная прочность, резина

Поступила: 09.12.2022
Доработана: 18.09.2023
Принята в печать: 05.03.2024

Для цитирования

Зуев А.А., Золотарев В.Л., Левенберг И.П., Ковалева Л.А., Насыров И.Ш. Натуральный и синтетические изопреновые каучуки, полученные с использованием катализаторов Циглера–Натта. *Тонкие химические технологии*. 2024;19(2):139–148. https://doi.org/10.32362/2410-6593-2024-19-2-139-148

INTRODUCTION

In 2020, the Moscow Institute of High Chemical Technologies marked the 120th anniversary of its foundation [1]. In 2022, another anniversary was marked: one of the oldest departments of this Institute—the F.F. Koshelev Chemistry and Technology of Elastomer Processing—celebrated its 90th anniversary. The study of the "synthesis of rubbers–structure–properties–application" chain in rubbers has always been one of the traditional directions of scientific research of the department. An invaluable contribution to this field was made by the works of such outstanding staff members as F.F. Koshelev, A.E. Kornev, I.T. Gridunov, and A.M. Bukanov. The department is currently continuing its work on the study of rubbers of both general [2–6] and special purpose [7–11].

One of the main rubbers in the production of tires and rubber products is polyisoprene. Due to the features of its structure [12], synthetic isoprene rubber (IR) is significantly inferior to natural rubber (NR) in a number of properties. This is especially important for the tire industry since rubber compounds based on it have low cohesive strength, and rubbers are characterized by a higher level of hysteresis losses and low tear

resistance [13]. The molecular colloidal structure of polyisoprene has a decisive influence on its ability to crystallize. Detailed study has shown that even a small proportion of structural inhomogeneities significantly reduces the ability of rubber to crystallize. The half-life of polyisoprene crystallization increases by almost an order of magnitude as the content of *cis*-1,4 units decreases from 98 to 95% [14].

Another significant element is the location of the raw material base. NR is a scarce imported product, and synthetic polyisoprene is produced by factories located in Russia: *Nizhnekamskneftekhim*, *Tolyattikauchuk*, and *Syntez-Kauchuk*. The pricing of natural and synthetic polyisoprenes substitutes is characterized by cross demand, raising the important question of creating a full-fledged synthetic analog of NR.

Over the past 60 years, several ways have been identified to resolve this problem: the search for alternative raw materials in the production of NR [15], the introduction of protein components into synthetic polyisoprene [16, 17], the chemical modification of IR at the stages of rubber synthesis [18], or the introduction of active functional compounds in the production of rubber compounds. All of these methods have their advantages and disadvantages. However, so far none of them have been implemented on an industrial scale, with the exception of the industrial production of titanium IR (Ti–IR) (with a capacity of up to 60000 t) modified with *para*-nitrosodiphenylamine, in the 1970s at the *Kuibyshev Synthetic Rubber Plant* [13, 19].

The development of synthetic polyisoprene production technology should not be forgotten. The search for new catalytic systems and improved synthesis of IRs have always been aimed at reproducing the properties of standard NR due to its unique characteristics: the highest possible content of *cis*-1,4 bonds, the presence of solid phase branching, high linearity of the chains, absence of side groups and branching.

The production of stereoregular synthetic IR commenced in 1964. It was based on a titanium catalytic system at the *Kuibyshev Synthetic Rubber Plant* (Tolyatti) and at the *Volga Synthetic Rubber Plant* [13, 20], then at the *Sterlitamak Synthetic Rubber Plant*, *Nizhnekamskneftekhim*, and *Yaroslavl Synthetic Rubber Plant*. Almost 60 years have passed, during which time a lot of work has been carried out aimed at eliminating the disadvantages of Ti–IR and bringing its properties closer to NR. A large number of studies have been conducted at these industrial production facilities, resulting in the transition to a low-temperature catalyst (*Nizhnekamskneftekhim*), the introduction of modified (three-component) catalytic systems, catalytic complexes. These studies also led to an increase in the quality of rubber, uniformity, stereoregularity, and a decrease in the content of gel and oligomers.

Since 2000, there has been a decrease in the production of Ti–IR in the world due to the establishment of production facilities for synthetic polyisoprene using catalytic systems based on rare earth metals. Neodymium (Nd) IR has a number of undoubted advantages: the absence of gel, oligomers, and a slightly higher molecular weight [21].

Although Russia is a pioneer in the field of research and implementation of new catalytic systems in the production of synthetic rubbers (the work of the Research Institute of Synthetic Rubber devoted to the study of lanthanide catalytic systems dates back to the 1970s and 1980s), there is a low level of Nd–IR production. However, in China, three-quarters of the IR produced is based on the Nd catalyst. This difference is quite understandable given that China is currently the main producer and importer of Nd oxide in the world—the main component in the production of a catalyst.

Among the currently known catalysts based on rare earth elements, the synthesis of polyisoprene on gadolinium (Gd) catalysts appears to be most attractive due to its lower cost relative to the Nd catalyst, low costs for the implementation of the process, and the high quality of the rubber obtained [22].

MATERIALS AND METHODS

Gd–IR and Nd–IR (*Sintez-Kauchuk*, Sterlitamak, Russia) obtained using rare-earth catalysts were selected as the objects of research (Table 1). Comparison objects were RSS1 NR (*PT. Pinago Utama Tbk*, Indonesia) and Ti–IR (*Sintez-Kauchuk*, Sterlitamak, Russia).

The rubber mixtures used to establish cohesive strength and Mooney viscosity contained only elastomeric base and carbon black. The study also examined not only rubber compounds based on individual rubbers, but also blended combinations of RSS1 with other investigated polyisoprenes, the content of which was varied from 10 to 90 pts. wt. in 10 pts. wt. increments.

Before mixing, all rubbers were decrystallized in the SNOL 60/300 drying cabinet (*SNOL-TERM*, Tver, Russia) at a temperature of 70°C for 1 h. Rubber plasticization was carried out on an LB 250 100/100 laboratory roll (*L.B. Krasin Kostroma Plant of Polymer Engineering*, Kostroma, Russia) at a temperature of 100°C for 2 min. After plasticization, the rubber was loaded into a Benbury-type rubber mixer (*Rubber Industry Research Institute*, Sergiev Posad, Russia) with a chamber volume of 100 cm^3. Carbon black N330 (*YATU named after V.Yu. Orlov,* Yaroslavl, Russia) (35 pts. wt. per 100 pts. wt. of rubber) was then added and mixed at 100°C. The rubber mixture was discharged after 2.5 min and then homogenized on the LB 250 100/100 roll.

The Mooney viscosity of rubber compounds was determined in accordance with DIN 53523 (Parts 2, 3, and 4) using a MV 3000 Basic Mooney viscometer

Table 1. Specifications of polyisoprenes *Sintez-Kauchuk*

Parameters	Gd–IR	Nd–IR	Ti–IR
Mooney viscosity ML 1+4 (100°C)	73.0	75.0	71.0
Loss on drying, %	0.13	0.27	0.39
Content of 3,4-units, %	1.0	2.1	0.8
Glass transition temperature, °C	−56.6	−56.8	−59.4
Molecular weight characteristics			
Number average molecular weight $M_n \cdot 10^{-3}$	361	327	288
Weight average molecular weight $M_w \cdot 10^{-3}$	1603	1592	1125
Average molecular weight $M_z \cdot 10^{-3}$	3635	2540	2539
Polydispersity coefficient M_w/M_n	4.4	4.9	3.9
Branching factor g_f	0.947	0.945	0.954
Fractional composition			
>1000000	48.5	49.0	38.5
500000–1000000	20.5	20.0	22.5
100000–500000	24.0	24.0	31.0
<100000	7.0	7.0	8.0

(*MonTech*, Buchen, Germany). The cohesive strength was determined according to the ASTM D 6746-15 "Standard Method for determining the cohesive Strength and Stress Relaxation of Crude Rubber or Non-vulcanized Rubber Compounds" using a AI-3000-U universal testing machine (*GOTECH Testing Machines Inc*. and *UGNLAB Testing Equipment,* Taichung, Taiwan).

In order to determine the physical, mechanical, and operational properties of rubbers based on individual rubbers, rubber mixtures of the following composition (per 100.0 pts. wt. of rubber) were made: stearic acid (*VitaHim*, Dzerzhinsk, Russia)—2.0 pts. wt., zinc oxide (*Empils-zinc*, Rostov-on-Don, Russia)—5.0 pts. wt., zinc oxide (*Empils-zinc*, Rostov-on-Don, Russia)—5.0 pts. wt., Sulfenamide C (*VitaHim*, Dzerzhinsk, Russia)—0.7 pts. wt., carbon black N330 (*YATU named after V.Yu. Orlov*, Yaroslavl, Russia)—35.0 pts. wt., sulfur (*VitaHim*, Dzerzhinsk, Russia)—2.25 pts. wt.

The procedure of decrystallization of rubbers prior to mixing was similar to that previously described. The plasticization of rubber and the manufacture of rubber mixtures were carried out on the LB 320 160/160 roll (*Metallist*, Russia) according to ASTM D3184-11—for NR, and according to GOST 14925-79[1]—for synthetic polyisoprenes.

The vulcanization characteristics of rubber compounds were determined at 150°C using an MDR3000 rotor-free rheometer (*MonTech*, Buchen, Germany) according to ISO 6502 (ASTM D 5289, DIN 53529).

The rubber samples were vulcanized in a hydraulic vulcanization press with electric heating of the plates at a temperature of 150°C during the optimal vulcanization time.

[1] GOST 14925-79. State Standard of the USSR. Synthetic *cis*-isoprene rubber. Technical conditions. Moscow: Izdatel'stvo standartov; 1988.

The physico-mechanical properties of rubbers were determined on the AI-3000-U universal testing machine according to GOST 270-75[2]. The elasticity by elastic rebound was established using the GT-7042-RDA (*GOTECH Testing Machines Inc*. and *UGNLAB Testing Equipment*, Taichung, Taiwan) apparatus according to DIN 53512 (ISO 4662). Shore A hardness was determined using the HT3000 device (*MonTech*, Buchen, Germany) according to ASTM D 2240 (DIN 53505). Rubber abrasion resistance when sliding on a renewable surface was established using the ABR3000 device (*MonTech*, Buchen, Germany) according to DIN 53516 (ISO 4649:2002 (E)).

RESULTS AND DISCUSSION

Figure 1 shows the test results of rubber compounds based on individual rubbers.

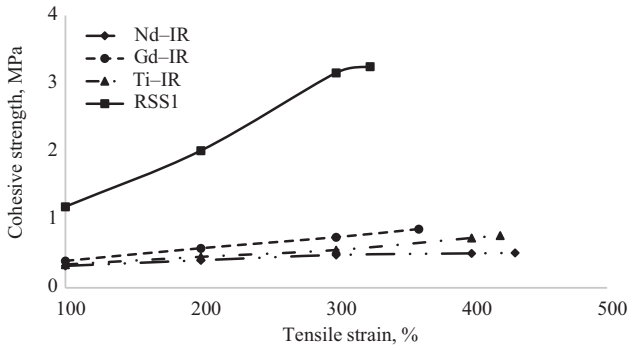

Fig. 1. Cohesive strength of rubber compounds based on RSS1 and synthetic polyisoprenes

The results obtained correlate well with the data available in literature. The significant tendency of NR to crystallization explains the high cohesive strength of the RSS1-based rubber compound. This significantly exceeds the values of this indicator for mixtures based on all the considered synthetic polyisoprenes. It should also be noted that there are practically no differences in the indicators of cohesive strength between rubbers obtained on the basis of Ti and Nd catalysts. The slightly higher values for Gd–IR can generally be attributed to the measurement error of the device.

Due to their frequent use in real rubber formulations, mixed compositions of synthetic polyisoprenes with RSS1 NR were also considered. The graphical dependencies of cohesive strength and Mooney viscosity are shown in Figs. 2–4.

A significant variation in both the Mooney viscosity and cohesive strength is most probably related to the method of manufacturing mixtures. The rolling process has a significant effect on the molecular weight of rubbers.

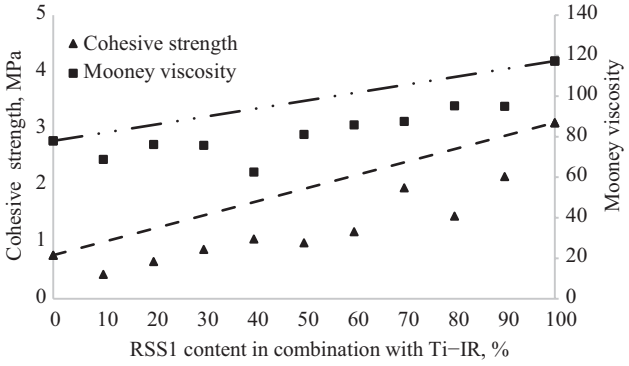

Fig. 2. Dependence of cohesive strength and Mooney viscosity of rubber mixtures based on combination of Ti–IR and RSS1 rubbers on RSS1 content

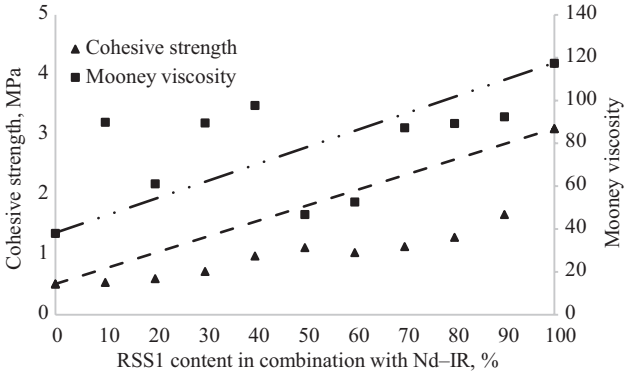

Fig. 3. Dependence of cohesive strength and Mooney viscosity of rubber mixtures based on combination of Nd–IR and RSS1 rubbers on RSS1 content

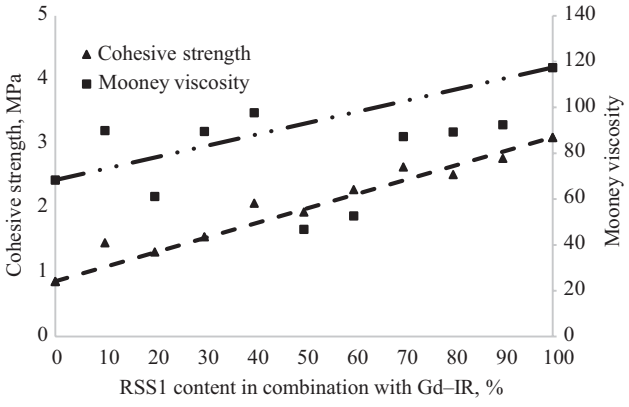

Fig. 4. Dependence of cohesive strength and Mooney viscosity of rubber mixtures based on combination of Gd–IR and RSS1 rubbers on RSS1 content

[2] GOST 270-75. Interstate Standard. Rubber. Method for determining elastic-strength properties under tension. Moscow: Standartinform; 2008.

This weight decreases due to the predominant process of mechanical destruction. A decrease in molecular weight leads to a decrease in the considered indicators [23]. It is also important to note the significant deviation of the experimental values of the indicators from the straight line, based on the principle of additivity for mixed compositions. The replacement of even 10% NR results in a significant decrease in cohesive strength. A slightly different picture is observed in mixtures with Gd–IR. In this case the deviations from the straight line, built on the principle of additivity, as significantly smaller.

For both individual rubbers and mixed compositions, a decrease in the cohesive strength of rubber compounds is associated with defects in the structure of synthetic polyisoprenes (oligomers, gel, low molecular weight fractions, branching, 3,4-links). The use of Nd-catalytic systems in comparison with Ti-catalysts has made it possible to completely remove gel, *trans*-1,4-links, and head-to-head and tail-to-tail type connections from rubber. However, the content of 3,4-links increased. Synthetic polyisoprene, obtained on the basis of the Gd-catalytic system, does not contain gel, and the content of 3,4-links is lower when compared to Nd-rubber. The results obtained confirm that the content of 3,4-links plays an important role in reducing the tendency of IRs to crystallization.

In order to study the effect of the type of rubber on the properties of rubbers, we selected standard formulations of rubber mixtures. The vulcanization characteristics are shown in Fig. 5 and in Table 2.

In practice, the results obtained do not differ from each other for all polyisoprenes. The slightly higher vulcanization rate of Ti–IR is probably due to the presence of oligomers and gel in the rubber.

The results of the physico-mechanical and certain operational properties of rubbers also indicate the absence of any significant differences between the rubbers under consideration (Fig. 6 and 7).

The values of these indicators are decisively influenced by the presence of an active filler in the formulation of rubber compounds.

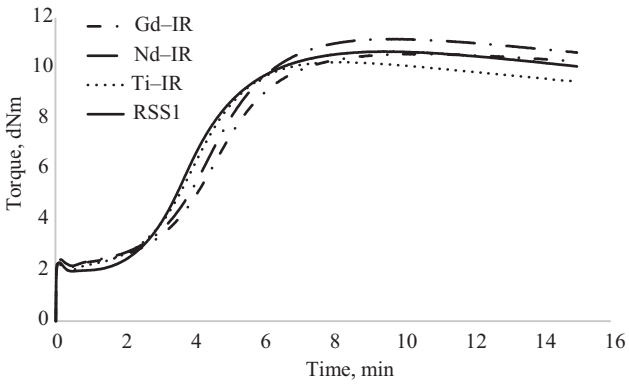

Fig. 5. Vulcanization properties of rubber compounds based on various polyisoprenes

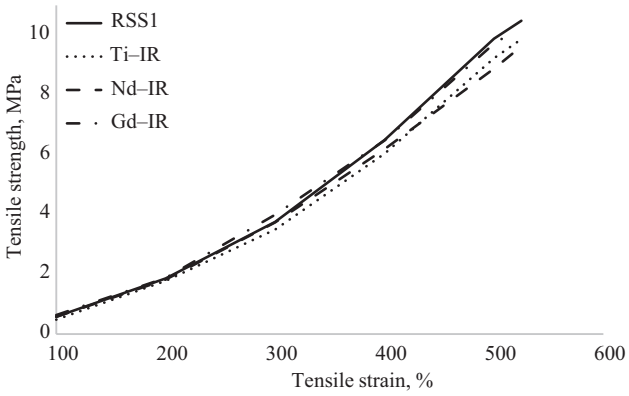

Fig. 6. Dependence of conditional stress on the relative elongation of rubber

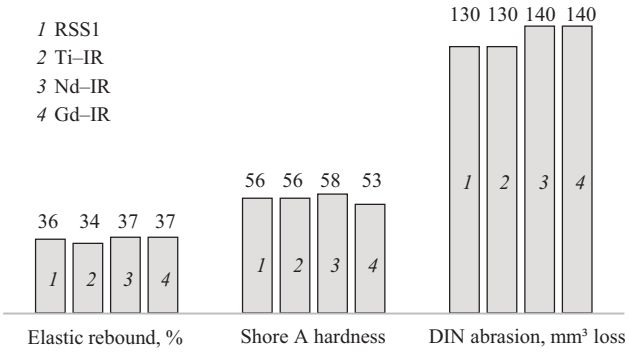

Fig. 7. Performance properties of rubbers based on various polyisoprenes

Table 2. Vulcanization characteristics of rubber compounds (test temperature 150°C)

Mixture	S'_{min}	S'_{max}	$S'_{max} - S'_{min}$	Scorch time	t_{C90}
RSS1	1.97	10.66	8.69	2.51	6.11
Ti–IR	1.99	10.24	8.25	2.4	5.69
Nd–IR	2.18	11.15	8.97	2.66	6.56
Gd–IR	2.13	10.57	8.44	2.76	6.71

Note: S'_{min} is the minimum torque, S'_{max} is the maximum torque, $S'_{max} - S'_{min}$ is the difference between the maximum and minimum torques, and t_{C90} is the optimal vulcanization time.

CONCLUSIONS

Unfortunately, due to the lack of dynamic test results, the work performed on comparing polyisoprenes is incomplete. Thus is does not allow us to draw comprehensive conclusions about the effect of the type of catalyst used in the synthesis of synthetic polyisoprene on the properties of rubber compounds and rubbers.

However, the study suggests the possible potential of using gadolinium in the production of IR both from an economic point of view, and also from the point of view of creating a more perfect microstructure. This is because the low tendency to crystallization and the high hysteresis losses of synthetic rubbers currently produced by the industry, in comparison with NRs, significantly limit their use in the tire industry. The volume of experimental data so far obtained forms the basis for further research in this area. This is especially important in the current situation, which requires methods of import substitution of expensive and often inaccessible foreign raw materials to be developed.

Acknowledgments

The work was financially supported by the contract for the performance of research work (A-107 dated March 25, 2021).

Authors' contributions

A.A. Zuev—analyzing the literature on the research topic, performing experimental studies, discussing the results obtained, and writing the text of the article.

V.L. Zolotarev—initiation of the research and development of its concept, scientific advising, and making valuable scientific comments in the text of the article.

I.P. Levenberg—formulation of the problem and formulation of the research task, discussion of the results obtained.

L.A. Kovaleva—search and classification of literary sources, performance of experimental studies, design of the article in accordance with the requirements of the publishing house, and discussion of the obtained results.

I.Sh. Nasyrov—synthesis of polyisoprene prototypes, discussion of the results obtained.

The authors declare no conflicts of interest.

REFERENCES

1. Frolkova A.K. To the true benefit and glory of the Fatherland. *Fine Chem. Technol*. 2020;15(6):7–8 (in Russ.). https://doi.org/10.32362/2410-6593-2020-15-6-7-8
2. Zolotaryov V.L., Levenberg I.P., Kovaleva L.A. Long-benchmenal branches of macromolecules 1,4-*cis*-polybutadiene. *Promyshlennoe proizvodstvo i ispol'zovanie elastomerov = Industrial Production and Use of Elastomers*. 2018;2:19–22 (in Russ.). https://doi.org/10.24411/2071-8268-2018-10203
3. Zolotaryov V.L., Levenberg I.P., Kovaleva L.A., Zuev A.A., Lyusova L.R. *Cis*-1,4-polybutadiene and frost resistance of rubber based on it. *Promyshlennoe proizvodstvo i ispol'zovanie elastomerov = Industrial Production and Use of Elastomers*. 2020;3–4:3–7 (in Russ.). https://doi.org/10.24412/2071-8268-2020-3-4-3-7
4. Zolotaryov V.L., Levenberg I.P., Zuev A.A., Kovaleva L.A., Lyusova L.R., Lipatova A.A. Once again about *cis*-1.4-polyisoprene rubber. *Promyshlennoe proizvodstvo i ispol'zovanie elastomerov = Industrial Production and Use of Elastomers*. 2021;2:3–9 (in Russ.). https://doi.org/10.24412/2071-8268-2021-2-03-09
5. Lyusova L.R., Chernyshov S.V. Study of the possibility of modifying synthetic polyisoprene by combining it with a highly cohesive polymer. *Promyshlennoe proizvodstvo i ispol'zovanie elastomerov = Industrial Production and Use of Elastomers*. 2022;1:40–44 (in Russ.). https://doi.org/10.24412/2071-8268-2022-1-40-44
6. Chernyshov S.V., Lyusova L.R., Makhmudova S.R., Zolotaryov V.L. The effect of 1,2-polybutadiene on the properties of elastomeric materials made of synthetic polyisoprene. *Kauchuk i rezina*. 2023;82(2):66–70 (in Russ.). https://doi.org/10.47664/0022-9466-2023-82-2-66-70

СПИСОК ЛИТЕРАТУРЫ

1. Фролкова А.К. К истинной пользе и славе Отечества. *Тонкие химические технологии*. 2020;15(6):7–8. https://doi.org/10.32362/2410-6593-2020-15-6-7-8
2. Золотарев В.Л., Левенберг И.П., Ковалева Л.А. Длинноцепочечные разветвления макромолекул 1,4-*цис*-полибутадиена. *Промышленное производство и использование эластомеров*. 2018;2:19–22. https://doi.org/10.24411/2071-8268-2018-10203
3. Золотарев В.Л., Левенберг И.П., Ковалева Л.А., Зуев А.А., Люсова Л.Р. *Цис*-1,4-полибутадиен и морозостойкость резин на его основе. *Промышленное производство и использование эластомеров*. 2020;3–4:3–7. https://doi.org/10.24412/2071-8268-2020-3-4-3-7
4. Золотарев В.Л., Левенберг И.П., Зуев А.А., Ковалева Л.А., Люсова Л.Р., Липатова А.А. Еще раз о 1,4-*цис*-полиизопренах. *Промышленное производство и использование эластомеров*. 2021;2:3–9. https://doi.org/10.24412/2071-8268-2021-2-03-09
5. Люсова Л.Р., Чернышов С.В. Изучение возможности модификации синтетического полиизопрена путем совмещения с высококогезионным полимером. *Промышленное производство и использование эластомеров*. 2022;1:40–44. https://doi.org/10.24412/2071-8268-2022-1-40-44
6. Чернышов С.В., Люсова Л.Р., Махмудова С.Р., Золотарев В.Л. Влияние 1,2-полибутадиена на свойства эластомерных материалов из синтетического полиизопрена. *Каучук и резина*. 2023;82(2):66–70. https://doi.org/10.47664/0022-9466-2023-82-2-66-70
7. Боброва И.И., Котова С.В., Наумова Ю.А. Исследование влияния стеарата кальция на свойства резиновых смесей и их вулканизатов на основе бутадиен-нитрильных каучуков. *Промышленное производства и использование эластомеров*. 2021;4:3–7. https://doi.org/10.24412/2071-8268-2021-4-3-7

7. Bobrova I.I.., Kotova S.V., Naumova Yu.A. Investigation of the calcium stearate influence on the rubber mixtures and their vulcanizates based on nitrile butadiene rubbers properties. *Promyshlennoe proizvodstvo i ispol'zovanie elastomerov = Industrial Production and Use of Elastomers*. 2021;4:3–7 (in Russ.). https://doi.org/10.24412/2071-8268-2021-4-3-7
8. Dulina O.A., Eskova E.V., Tarasenko A.D., Kotova S.V. Influence of various factors on surface properties of elastomeric materials based on nitrile butadiene rubbers. *Tonk. Khim. Tekhnol. = Fine Chem. Technol*. 2022;17(2):152–163 (Russ., Eng.). https://doi.org/10.32362/2410-6593-2022-17-2-152-163
9. Bobrova I.I., Sinelnikova L.N., Kotova S.V., Gamlitsky Yu.A. Adhesive properties of vulcanizates based on various butadiene-nitrile rubber grades investigation. *Kauchuk i rezina*. 2022;81(6):292–297 (in Russ.). https://doi.org/10.47664/0022-9466-2022-81-6-292-297
10. Bobrova I.I., Kotova S.V., Lyusova L.R., Zabuga N.N. Study of adhesion modifiers for rubbers based on nitrile butadiene rubber. *Promyshlennoe proizvodstvo i ispol'zovanie elastomerov = Industrial Production and Use of Elastomers*. 2022;2:18–23 (in Russ.). https://doi.org/10.24412/2071-8268-2022-2-18-23
11. Volkov A.O., Naumova Yu.A., Kozlova A.O., Konovalova K.D., Kovaleva L.A., Dorokhov A.V. The effect of aluminum-doped zinc oxide on the properties of an elastomeric composition based on nitrile rubber. *Izvestiya Kabardino-Balkarskogo gosudarstvennogo universiteta = Proceedings of the Kabardino-Balkarian State University*. 2022;XII(5):49–53 (in Russ.).
12. Tanaka Y., Kawahara S., Tangpakdee J. Structural characterization of natural rubber. *Kautschuk Gummi Kunststoffe*. 1997;50(1):6–11.
13. Zolotaryov V.L. "Titanic" IR. *Promyshlennoe proizvodstvo i ispol'zovanie elastomerov = Industrial Production and Use of Elastomers*. 2009;6:8–12 (in Russ.).
14. Vasil'ev V.A., Nasyrov I.Sh. *Otechestvennye promyshlennye stereoregulyarnye kauchuki. Issledovaniya i razrabotki* (*Domestic Industrial Stereoregular Rubbers. Research and Development*). Ufa: Gilem; 2018. 288 p. (in Russ.). ISBN 978-5-88185-426-3
15. Zolotaryov V.L. Once again about BR sodium butadiene rubber. *Promyshlennoe proizvodstvo i ispol'zovanie elastomerov = Industrial Production and Use of Elastomers*. 2010;4:3–6 (in Russ.).
16. Potapov E.E., Goncharova Yu.E., Imnadze E.G., Lonina N.I. Chemical modification of elastomers as a method for obtaining a synthetic analogue of NK. *Kauchuk i rezina*. 2004;1:48–57 (in Russ.).
17. Rakhmatullina A.P., Chan Kh.T., Potapov E.E. Effect of the amount of protein-lipid complexes acting as a modifier on the characteristics of synthetic polyisoprene vulcanisates. *Kauchuk i rezina*. 2019;78(6):350–355 (in Russ.).
18. Vasil'ev V.A., Khvostik G.M., Smirnov V.P., Morozov Yu.V., Nasyrov I.Sh., Bazhenov Yu.P., Slanevskii A.A. Modification of Isoprene rubber with maleic acid monoesters. *Kauchuk i rezina*. 2010;6:2–6 (in Russ.).
19. Boreyko N.P., Papkov V.N., Komarov E.V. Prerequisites for the development of a state_program to create an artificial analogue of natural rubber. *Kauchuk i rezina*. 2019;78(6):380–383 (in Russ.).
20. Masagutova L.V. Once more on polyisoprene. (Historical aspect). *Kauchuk i rezina*. 2015;2:44–47 (in Russ.).
21. Smirnova L.A., Kovalev N.F., Tsypkina I.M., Kormer V.A. Influence of the molecular characteristics of polyisoprene on the quality of mixing with carbon black and the properties of rubber compounds. *Kauchuk i rezina*. 1991;4:5–7 (in Russ.).
8. Дулина О.А., Еськова Е.В., Тарасенко А.Д., Котова С.В. Влияние различных факторов на поверхностные свойства эластомерных материалов на основе бутадиен-нитрильных каучуков. *Тонкие химические технологии*. 2022;17(2):152–163. https://doi.org/10.32362/2410-6593-2022-17-2-152-163
9. Боброва И.И., Синельникова Л.Н., Котова С.В., Гамлицкий Ю.А. Исследование адгезионных свойств резин на основе различных марок бутадиен-нитрильных каучуков. *Каучук и резина*. 2022;81(6):292–297. https://doi.org/10.47664/0022-9466-2022-81-6-292-297
10. Боброва И.И., Котова С.В., Люсова Л.Р., Забуга Н.Н. Исследование модификаторов адгезии для резин на основе бутадиен-нитрильного каучука. *Промышленное производство и использование эластомеров*. 2022;2:18–23. https://doi.org/10.24412/2071-8268-2022-2-18-23
11. Волков А.О., Наумова Ю.А., Козлова А.О., Коновалова К.Д., Ковалева Л.А., Дорохов А.В. Влияние оксида цинка, легированного алюминием, на свойства эластомерной композиции на основе бутадиен-нитрильного каучука. *Известия Кабардино-Балкарского государственного университета*. 2022;XII(5):49–53.
12. Tanaka Y., Kawahara S., Tangpakdee J. Structural characterization of natural rubber. *Kautschuk Gummi Kunststoffe*. 1997;50(1):6–11.
13. Золотарев В.Л. Российскому «титановому» СКИ – 45 лет. *Промышленное производство и использование эластомеров*. 2009;6:8–12.
14. Васильев В.А., Насыров И.Ш. *Отечественные промышленные стереорегулярные каучуки. Исследования и разработки*. Уфа: Гилем; 2018. 288 с. ISBN 978-5-88185-426-3
15. Золотарев В.Л. Еще раз о натрийбутадиеновом каучуке СКБ. *Промышленное производство и использование эластомеров*. 2010;4:3–6.
16. Потапов Е.Э., Гончарова Ю.Э., Имнадзе Е.Г., Лонина Н.И. Химическая модификация эластомеров как способ получения синтетического аналога НК. *Каучук и резина*. 2004;1:48–57.
17. Рахматтулина А.П. Чан Х.Т., Потапов Е.Э. Влияние количества белково-липидных комплексов, действующих в качестве модификатора, на характеристики резин на основе синтетического полиизопрена. *Каучук и резина*. 2019;78(6):350–355.
18. Васильев В.А., Хвостик Г.М., Смирнов В.П., Морозов Ю.В., Насыров И.Ш., Баженов Ю.П., Сланевский А.А. Модификация изопренового каучука моноэфирами малеиновой кислоты. *Каучук и резина*. 2010;6:2–6.
19. Борейко Н.П., Папков В.Н., Комаров Е.В. Предпосылки для разработки государственной программы создания искусственного аналога натурального каучука. *Каучук и резина*. 2019;78(6):380–383.
20. Масагутова Л.В. Еще раз о полиизопрене. (Исторический аспект). *Каучук и резина*. 2015;2:44–47.
21. Смирнова Л.А., Ковалев Н.Ф., Цыпкина И.М., Кормер В.А. Влияние молекулярных характеристик полиизопрена на качество смешения с техническим углеродом и свойства резиновых смесей. *Каучук и резина*. 1991;4:5–7.
22. Насыров И.Ш., Фаизова В.Ю., Жаворонков Д.А., Шурупов О.К., Васильев В.А. Натуральный и синтетический *цис*-полиизопрены. Часть 2. Свойства СКИ мировых производителей и российских торговых марок производства ОАО «Синтез-Каучук». *Промышленное производство и использование эластомеров*. 2020;3–4:45–55.
23. Куперман Ф.Е. *Новые каучуки для шин: приоритетные требования, методы оценки*. М.: Научно-технический центр «НИИШП»; 2005. 329 с. ISBN 5-98746-005-0

22. Nasyrov I.Sh., Faizova V.Yu., Zhavoronkov D.A., Shurupov O.K., Vasiliev V.A. Natural rubber and synthetic *cis*-polyisoprene. Part 2. Properties of polyisoprenes of global manufacturers and Russian brands production of *Sintez-Kauchuk*. *Promyshlennoe proizvodstvo i ispol'vanie elastomerov = Industrial Production and Use of Elastomers*. 2020;3–4:45–55 (in Russ.).
23. Kuperman F.Ye. *Novye kauchuki dlya shin: prioritetnye trebovaniya, metody otsenki* (*New Rubbers for Tires: Priority Requirements, Evaluation Methods*). Moscow: NIIShP; 2005. 329 p. (in Russ.). ISBN 5-98746-005-0

About the authors

Anton A. Zuev, Cand. Sci. (Eng.), Associate Professor, F.F. Koshelev Department of Chemistry and Technology of Elastomer Processing, M.V. Lomonosov Institute of Fine Chemical Technologies, MIREA – Russian Technological University (86, Vernadskogo pr., Moscow, 119571, Russia). E-mail: zuev_aa@mirea.ru. Scopus Author ID 57525558100, RSCI SPIN-code 1068-1663, https://orcid.org/0000-0003-0507-9427

Valentin L. Zolotarev, Cand. Sci. (Chem.), Advisor to the General Director, Macrochem-R (12, Krasnopresnenskaya nab., Moscow, 123610, Russia). E-mail: zolotarev.valentin@yandex.ru. RSCI SPIN-code 7821-8813

Igor P. Levenberg, Founder of Macrochem-R (12, Krasnopresnenskaya nab., Moscow, 123610, Russia). E-mail: Igor.Levenberg@makrochem.com

Lyudmila A. Kovaleva, Cand. Sci. (Eng.), Associate Professor, F.F. Koshelev Department of Chemistry and Technology of Elastomer Processing, M.V. Lomonosov Institute of Fine Chemical Technologies, MIREA – Russian Technological University (86, Vernadskogo pr., Moscow, 119571, Russia). E-mail: kovaleva_l@mirea.ru. Scopus Author ID 56055705000, RSCI SPIN-code 2833-5264, https://orcid.org/0000-0002-9949-8464

Ildus Sh. Nasyrov, Cand. Sci. (Chem), Deputy General Director for Development (for Science), Sintez-Kauchuk (14, Technicheskaya ul., Sterlitamak, The Republic of Bashkortostan, 453100, Russia). E-mail: nasyrovish@mail.ru. Scopus Author ID 6603373003, https://orcid.org/0000-0001-8273-3651

Об авторах

Зуев Антон Алексеевич, к.т.н., доцент кафедры химии и технологии переработки эластомеров им. Ф.Ф. Кошелева, Институт тонких химических технологий им. М.В. Ломоносова, ФГБОУ ВО «МИРЭА – Российский технологический университет» (119571, Россия, Москва, пр-т Вернадского, д. 86). E-mail: zuev_aa@mirea.ru. Scopus Author ID 57525558100, SPIN-код РИНЦ 1068-1663, https://orcid.org/0000-0003-0507-9427

Золотарев Валентин Лукьянович, к.х.н., советник генерального директора, ООО «Макрохем-Р» (123610, Россия, Москва, Краснопресненская набережная, д. 12). E-mail: zolotarev.valentin@yandex.ru. SPIN-код РИНЦ 7821-8813

Левенберг Игорь Павлович, учредитель ООО «Макрохем-Р» (123610, Россия, Москва, Краснопресненская набережная, д. 12). E-mail: Igor.Levenberg@makrochem.com

Ковалева Людмила Александровна, к.т.н., доцент кафедры химии и технологии переработки эластомеров им. Ф.Ф. Кошелева, Института тонких химических технологий им. М.В. Ломоносова, ФГБОУ ВО «МИРЭА – Российский технологический университет» (119571, Россия, Москва, пр-т Вернадского, д. 86). E-mail: kovaleva_l@mirea.ru. Scopus Author ID 56055705000, SPIN-код РИНЦ 2833-5264, https://orcid.org/0000-0002-9949-8464

Насыров Ильдус Шайхитдинович, к.х.н., заместитель генерального директора по развитию (по науке), АО «Синтез-Каучук» (453110, Россия, Республика Башкортостан, Стерлитамак, ул. Техническая, д. 14). E-mail: nasyrovish@mail.ru. Scopus Author ID 6603373003, https://orcid.org/0000-0001-8273-3651

Translated from Russian into English by N. Isaeva
Edited for English language and spelling by Dr. David Mossop

Tonkie Khimicheskie Tekhnologii = Fine Chemical Technologies.
2024;19(2):149–162
ISSN 2686-7575 (Online)

UDC 621.039.7
https://doi.org/10.32362/2410-6593-2024-19-2-149-162

RESEARCH ARTICLE

A study of the mechanical and thermophysical properties of crystal matrices for the immobilization of high-level wastes

Ivan V. Kuznetsov[1], ✉, Anna Yu. Zobkova[1], Maya Yu. Kalenova[1], Andrey S. Shchepin[1], Oleg N. Budin[1], Vladimir A. Stepanov[2], Irina M. Melnikova[1], Olga I. Stefanovskaya[3], Kirill V. Klemazov[2]

[1] *B.N. Laskorin Leading Research Institute, Moscow, 115524 Russia*

[2] *Obninsk Institute of Atomic Energy, National Research Nuclear University MEPhI, Obninsk, Kaluga oblast, 249039 Russia*

[3] *A.N. Frumkin Institute of Physical Chemistry and Electrochemistry, Russian Academy of Sciences, Moscow, 119071 Russia*

✉ *Corresponding author, e-mail: ivan7501966@mail.ru*

Abstract

Objectives. The aim of the study was to confirm the compliance of the mechanical and thermophysical properties of titanate-zirconate mineral-like matrices intended for immobilization of the rare-earth-actinide fraction of high-level waste (HLW) with pyrochlore structures (Nd_2ZrTiO_7) and orthorhombic titanate of rare earth elements ($Nd_4Ti_9O_{24}$+TiO_2) with the Russian requirements for the final forms of radioactive waste sent for disposal. With regard to fractionated radioactive waste, this type of matrix is preferable when compared with conservative aluminophosphate and borosilicate glasses. This is due to larger capacity, and a better level of chemical, thermal, and radiation resistance.

Methods. The synthesis of mineral-like matrices was carried out by remelting a granular precursor consisting of mineral-forming metal oxides and a solution imitating the rare earth-actinide fraction of HLW in an induction furnace with a cold crucible. The thermal diffusivity was determined by the laser flash method. The heat capacity of the matrix samples was measured by differential scanning calorimetry. Ultimate flexural and compressive strengths were determined using universal test machines. The elastic moduli (Young's) were measured by the acoustic method. The temperature coefficients of linear expansion were determined using a high-temperature dilatometer.

Results. The ultimate strength of the matrices (Nd_2ZrTiO_7) and ($Nd_4Ti_9O_{24}$+TiO_2) was found to be 150–179 and 20.6–57.8 MPa in compression and bending respectively. Young's moduli vary from $3.7 \cdot 10^7$ to $2.15 \cdot 10^8$ kN/m^2. With an increase in temperature from 50 to 500°C, the values of thermal conductivity have a pronounced tendency to decrease from 1.71 to 0.91 W/(m·K). The temperature coefficients of linear expansion increase from $6.96 \cdot 10^{-6}$ to $1.01 \cdot 10^{-5}$ K^{-1} in the same temperature range.

Conclusions. Comprehensive studies of titanate-zirconate mineral-like matrices show that their mechanical and thermal properties in certain cases significantly exceed the minimum requirements of regulatory documentation for the final forms of HLW.

Keywords

high-level waste, pyrochlore, orthorhombic titanate, strength, thermal conductivity

Submitted: 28.04.2023
Revised: 29.05.2023
Accepted: 11.03.2024

For citation

Kuznetsov I.V., Zobkova A.Yu., Kalenova M.Yu., Shchepin A.S., Budin O.N., Stepanov V.A., Melnikova I.M., Stefanovskaya O.I., Klemazov K.V. A study of the mechanical and thermophysical properties of crystal matrices for the immobilization of high-level wastes. *Tonk. Khim. Tekhnol. = Fine Chem. Technol.* 2024;19(2):149–162. https://doi.org/10.32362/2410-6593-2024-19-2-149-162

НАУЧНАЯ СТАТЬЯ

Исследование механических и теплофизических свойств кристаллических матриц для иммобилизации высокоактивных отходов

И.В. Кузнецов[1],✉, А.Ю. Зобкова[1], М.Ю. Каленова[1], А.С. Щепин[1], О.Н. Будин[1], В.А. Степанов[2], И.М. Мельникова[1], О.И. Стефановская[3], К.В. Клемазов[2]

[1] *Ведущий научно-исследовательский институт им. Б.Н. Ласкорина, Москва, 115524 Россия*

[2] *Обнинский институт атомной энергетики, Национальный исследовательский ядерный университет «МИФИ», Обнинск, Калужская область, 249039 Россия*

[3] *Институт физической химии и электрохимии им. А.Н. Фрумкина, Российская академия наук, Москва, 119071 Россия*

✉ *Автор для переписки, e-mail: ivan7501966@mail.ru*

Аннотация

Цели. Целью работы являлось подтверждение соответствия механических и теплофизических свойств титанатно-цирконатных минералоподобных матриц, предназначенных для иммобилизации редкоземельно-актинидной фракции высокоактивных отходов (ВАО) российским требованиям, предъявляемым к конечным формам радиоактивных отходов, направляемых на захоронение. Матрицы имеют структуры пирохлора (Nd_2ZrTiO_7) и орторомбического титаната редкоземельных элементов ($Nd_4Ti_9O_{24}$+TiO_2). Применительно к фракционированным радиоактивным отходам данный тип матриц более предпочтителен по сравнению с консервативными алюмофосфатными и боросиликатными стеклами благодаря большей емкости и лучшей химической, термической и радиационной устойчивости.

Методы. Синтез минералоподобных матриц осуществляли путем переплавки гранулированного прекурсора, состоящего из минералообразующих оксидов металлов и раствора, имитирующего редкоземельно-актинидную фракцию ВАО, в индукционном плавителе с холодным тиглем. Исследование температуропроводности проводили методом лазерной вспышки; теплоемкость образцов матриц измеряли методом дифференциальной сканирующей калориметрии; пределы прочности на изгиб и сжатие определяли с помощью универсальных испытательных машин; модули упругости (Юнга) измеряли акустическим методом. Температурные коэффициенты линейного расширения находили с помощью высокотемпературного дилатометра.

Результаты. Установлено, что пределы прочности матриц (Nd_2ZrTiO_7) и ($Nd_4Ti_9O_{24}$+TiO_2) составляют 150–179 и 20.6–57.8 МПа при сжатии и изгибе соответственно. Модули Юнга варьируются от $3.7 \cdot 10^7$ до $2.15 \cdot 10^8$ кН/м^2. Значения теплопроводности при повышении температуры от 50 до 500°C имеют выраженную тенденцию к уменьшению от 1.71 до 0.91 Вт/(м·К). Температурные коэффициенты линейного расширения увеличиваются от $6.96 \cdot 10^{-6}$ до $1.01 \cdot 10^{-5}$ К$^{-1}$ в том же температурном интервале.

Выводы. Комплексные исследования титанатно-цирконатных минералоподобных матриц показали, что их механические и теплофизические свойства в ряде случаев существенно превосходят минимальные требования нормативной документации, предъявляемые к конечным формам ВАО.

Ключевые слова

высокоактивные отходы, пирохлор, орторомбический титанат, прочность, теплопроводность

Поступила: 28.04.2023
Доработана: 29.05.2023
Принята в печать: 11.03.2024

Для цитирования

Кузнецов И.В., Зобкова А.Ю., Каленова М.Ю., Щепин А.С., Будин О.Н., Степанов В.А., Мельникова И.М., Стефановская О.И., Клемазов К.В. Исследование механических и теплофизических свойств кристаллических матриц для иммобилизации высокоактивных отходов. *Тонкие химические технологии*. 2024;19(2):149–162. https://doi.org/10.32362/2410-6593-2024-19-2-149-162

INTRODUCTION

The generation of significant amounts of high-level waste (HLW) during spent nuclear fuel (SNF) reprocessing (variants of the PUREX process[1]) is an obstacle to the large-scale development of modern nuclear power [1, 2]. According to The International Atomic Energy Agency recommendations[2] and the current regulations of countries operating nuclear power plants, liquid HLW must be conditioned in order to reduce its volume. It then must be converted into a final form suitable for environmentally safe long-term storage and burial in geological formations at a depth of at least 500 m [1–5]. The resulting matrix must be chemically, thermally and radiation resistant and retain its insulating capacity for at least 1000 years.[3]

Two technological approaches to immobilization of liquid HLW into matrix materials are currently industrially implemented in the world. At *Mayak Production Association*, universal aluminophosphate glass matrix (AGM) is used. This is characterized by a relatively low synthesis temperature of 900–1050°C and a unique ability to include a wide range of elements and compounds in its composition. This includes significant amounts of molybdenum and aluminum oxide, the source of which is the fuel of mobile power plants [6–8]. On average, the Russian Federation annually generates up to 74 m^3/year of vitrified HLW sent for temporary storage.[4]

France and Great Britain use more specialized final forms as borosilicate glasses which have a slightly higher radionuclide capacity of up to 18.8 wt % [8–9]. Their matrix density is about 2.85 t/m^3. However, even when such relatively high values are achieved, the volume of HLW sent for storage and/or disposal is significant and amounts to 0.1–0.11 m^3/t of SNF [10].

Fractionation may perhaps be the only solution acceptable from the point of view of ensuring relative economic efficiency and environmental safety when handling liquid HLW [11–18]. The process implies maximum extraction of energy nuclides with the purpose of returning to the nuclear fuel cycle and afterburning in fast or liquid salt reactors. At the same time, unclaimed fission products can be divided into several fractions based on the principle of similarity of chemical properties, making it possible to select the optimal composition of the final form. Fractionation scenarios which are more realistic for industrial realization require the separation of HLW from solution:

- rare-earth actinide (REE-actinide) fraction, formed after extraction of uranium, plutonium and neptunium, containing mainly lanthanides, americium and curium (up to 3.5 and 0.44 wt % of the total amount of metals in solution), as well as traces of U, Pu, and Np [11–18];
- cesium-strontium fraction, saturated with active and stable isotopes of Cs and Sr, as well as Ba, the share of which can be up to 26% of the total mass of metals [11–19].

One of the promising forms for immobilization of REE-actinide fraction are crystalline matrices [11]. These have high radionuclide capacity, density, thermal, chemical, and radiation stability [20–22]. Their long-term stability is confirmed by the long-term existence of structurally identical minerals in the harsh conditions of the Earth's crust [23]. To date, there have been many fundamental studies confirming the above-mentioned advantages. However, a coherent, comprehensive and structured justification of their applicability is lacking. In this regard, there is no regulatory framework governing the quality of crystalline matrices. This also limits their industrial development.

Current regulations require cured HLW to be buried in geological formations up to several hundred meters deep [24]. The mechanical and thermophysical properties are the most important qualitative characteristics of the final forms. Strength limits in bending and compression determine the preservation of matrix integrity during transportation operations and the impact of pressure of the geological environment at the point of final disposal. Insufficient strength of matrix blocks can lead to the formation of cracks and fractures in the developed surface, thus reducing the materials resistance to leaching.

The thermal conductivity of the matrix determines its resistance to overheating as a result of to the decay of incorporated radionuclides. This also affects the maximum fraction of incorporated HLW, as well as the ingot dimensions which provide an acceptable level of matrix heating. Low thermal conductivity can lead to local matrix overheating, accompanied by mechanical stress and, can eventually lead to matrix failure.

The linear expansion temperature coefficient (LETC) affects the change in the dimensions of the matrix ingot in the process of its heat release drop. This is due to the decay of short-lived radionuclides. The indicator is critical at the stage of container selection. The values

1 Plutonium-Uranium Recovery by Extraction.

2 https://www.iaea.org/ru. Accessed March 25, 2023.

3 Federal Standards and Rules in the Field of Atomic Energy. Criteria for Accepting Radioactive Waste for Disposal. NP-093-14. *Nuclear and Radiation Safety*. 2015;77:(3):59–82. https://docs.secnrs.ru/documents/nps/НП-093-14/НП-093-14.pdf. Accessed March 23, 2023.

4 Semyonov M.A. Issues of preparation of class 2 radioactive waste for disposal. Proceedings of the Scientific and Technical Seminar "SNF and RW Management at ZNFC," May 27, 2021; Moscow, Russia. A.A. Bochvar VNIINM; 2021. https://bochvar.ru/materialy-konferentsiy/06%20Семенов%20М.А.%20(ФГУП%20ПО%20Маяк)%20-%20Презентация.pdf. Accessed March 27, 2023.

of LETC of the final mold and its packaging material should not differ significantly.

The aim of the study was to confirm the compliance of the mechanical and thermophysical properties of titanate-zirconate mineral-like matrices intended for immobilization of REE-actinide fraction of HLW with the current Russian requirements for the final forms of radioactive wastes sent for disposal.

MATERIALS AND METHODS

The following types of crystalline matrices for immobilization of REE-actinide fraction were tested in the present study:

- structure of titanate-zirconate pyrochlore Ln_2ZrTiO_7 (up to 62 wt % of Ln_2O_3);
- phase of orthorhombic REE titanate and rutile $Ln_4Ti_9O_{24}$+TiO_2 (up to 33 wt % of Ln_2O_3).

The above crystal matrices were selected due to their versatility, expressed in the ability to include REE-actinide fraction with different An : Ln (actinides and lanthanides) ratios. This solution is convenient from a technological point of view, since it does not impose strict limitations on the fractionation process.

Matrix materials were synthesized using an original method which includes obtaining a granular precursor from inactive simulant of liquid HLW and solid mineral formers with subsequent cold crucible induction melting (CCIM). The resulting matrices were ingots with a diameter of 120 mm and a height of ~120 mm. Before testing, the material to be studied was inspected for compliance of phase and chemical compositions with those specified using the Vista PRO atomic emission spectrometer with inductively coupled plasma (*Varian*, Australia) and DRON-4M powder X-ray diffractometer *(Burevestnik*, USSR). X-ray diffraction data decoding and phase identification were performed using the Match! software package (*Crystalimpact GmbH*, Germany) and ICDD-2 database.[5]

Crystalline matrices with confirmed characteristics were cut into samples to study the mechanical and thermophysical properties. Material fragmentation and surface treatment were performed using the following precision machines: Mecatome T210 cutting machine (*Presi SAS*, France) and Mecatech 234 grinding and polishing machine (*Presi SAS*, France), respectively. The configurations of the specimens and references to the test methods according to the manufacturing requirements are presented in Table 1.

Figure 1 shows the appearance of the samples, Fig. 2 shows the diffraction pattern of matrices with pyrochlore (a) and orthorhombic titanate (b) structures.

The compressive and flexural strengths were determined using a universal testing machine LFM-50 (*Walter+Bai*, Switzerland). The final values of the parameters were calculated as arithmetic averages in a series of measurements. Young's moduli were measured acoustically by recording the time of passing through the sample ultrasonic signal with a frequency of 2.5 MHz. The propagation velocity (v_l) of ultrasonic longitudinal waves was determined by Eq. (1):

$$v_l = \frac{l}{t_2 - t_1}, \quad (1)$$

wherein l—sample length, m; t_1—travel time of ultrasonic waves with the sample, s; t_2—travel time of ultrasonic waves without sample, s.

Young's modulus (E) was calculated by Eq. (2):

$$E = v_l^2 \times \rho, \quad (2)$$

wherein ρ—density, kg/m^3.

Thermal conductivity was determined by calculation method on the basis of measured values of heat capacity and thermal diffusivity by the Eq. (3):

$$\lambda = 1000000 \times a \times c \times \rho, \quad (3)$$

wherein a—diffusivity, m^2/s; c—specific heat capacity, J/(g·K); λ—heat transfer coefficient, W/(m·K); ρ—material density, t/m^3.

Heat capacity was determined using a differential scanning calorimeter DSC 404 F1 (*Netzsch*, Germany). The temperature conductivity was determined using a LFA 457 (*Netzsch*, Germany) solid state thermophysical parameter meter by the laser flash principle [25, 26]. In both types of tests, three parallel measurements were performed for each matrix type in the range of 50–500°C with a step of 50°C at a furnace heating rate of 3°C/min for each type of matrix.

LETC was determined using a DIL 402 horizontal pusher dilatometer (*Netzsch*, Germany) at a temperature range of 20 to 500°C in 20°C increments, with a furnace heating rate of 3°C/min.

RESULTS AND DISCUSSION

As mentioned earlier, the only certified final form for immobilization of HLW in the Russian Federation is AGM. The requirements for its quality are given in state standard GOST R 50926-96[6]. The initial data for the drafting of this legislative document was based on the parameters of glass produced at *Mayak*. This was done during solidification of the collective flow of liquid HLW generated during reprocessing of SNF of different

[5] International Center for Diffraction Data. https://www.icdd.com/. Accessed March 10, 2023.

[6] GOST R 50926-96. State Standard of the Russian Federation. High level solidified waste. General technical requirements. Moscow: Gosstandart Rossii; 1997.

genesis. In the case of matrices with a crystalline structure, the above standard is applicable in only a very limited way. This is due to the fundamentally different nature of the materials under study. The assumption can be made that promising matrix materials will be introduced, if they achieve comparable or superior values to those presented in the standard document. In this regard, the indicators of physical properties given in state standard GOST R 50926-96 are chosen as reference values for comparison. The results of tests with reference values of the standard are presented in Table 2.

The data in Table 2 shows that Young's modulus values of crystalline matrices with pyrochlore and orthorhombic REE titanate structures reach values of $2.15 \cdot 10^8$ kN/m^2. This significantly exceeds the requirements for vitrified HLW ($5.4 \cdot 10^7$ kN/m^2). It also eliminates the issues of stacking during containerization, intermediate storage and disposal.

The compressive strengths fall within the range of common technical oxide ceramics: from 30 MPa for construction ceramics to 300 MPa for technical corundum. The tensile strengths for pyrochlore and

Table 1. Nomenclature of mineral-like matrices (MLMs) samples made for the mechanical and thermophysical properties study

Properties		Sample sizes, mm	Regulatory act	Number of prepared samples, pcs	
				Pyrochlore structure	Orthorhombic titanate structure
Flexural strength, flexural modulus		Square beam 4.5 × 4.5 × 35.0	GOST R 24409-80[7]	14	15
Compressive strength, Young's modulus in compression		Cube with a side of 10	GOST R 57606-2017 (ISO 20504:2006)[8]	21	19
Thermal conductivity	Thermal diffusivity	Rectangular parallelepiped 10.0 × 10.0 × 2.5	GOST R 24409-80 ASTM E1461-13[9]	3	4
	Heat capacity	Square plate 3.4 × 3.4 × 1.0	GOST R 24409-80 ASTM E1269-11[10]	3	3
Linear expansion temperature coefficient (LETC)		Square beam 4 × 4 × 30	GOST R 57743-2017 (ISO 17139:2014)[11]	5	3

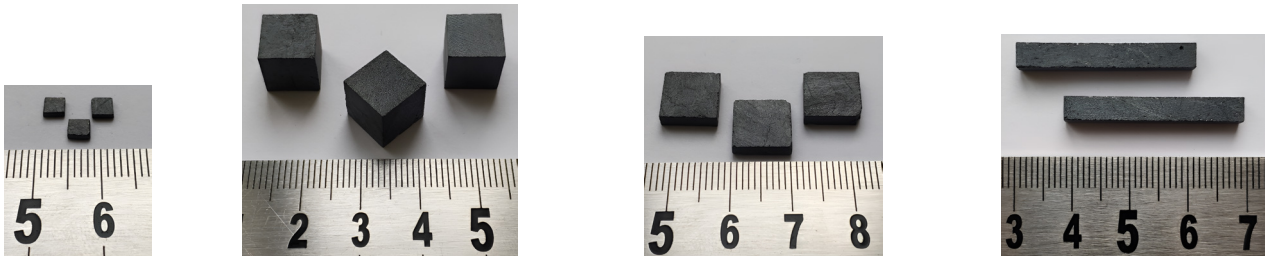

(a) (b) (c) (d)

Fig. 1. Appearance of MLMs samples of various sizes: (a) heat capacity determining samples; (b) compressive strength determining samples; (c) thermal diffusivity determining samples; (d) ultimate strength in bending determining samples

7 GOST 24409-80. Interstate Standard. Ceramic electrotechnical materials. Methods of testing. Moscow: Standartinform; 2005.

8 GOST R 57606-2017 (ISO 20504:2006). National Standard of the Russian Federation. Fine ceramics. Test method for compressive behavior of continuous fiber-reinforced composites at room temperature, MOD. Moscow: Standartinform; 2017.

9 ASTM E1461-13. Standard Test Method for Thermal Diffusivity by the Flash Method. https://www.astm.org/e1461-13.html. Accessed January 15, 2023.

10 ASTM E1269-11. Standard Test Method for Determining Specific Heat Capacity by Differential Scanning Calorimetry.

11 GOST R 57743-2017 (ISO 17139:2014). National Standard of the Russian Federation. Fine ceramics. Thermophysical properties of ceramic composites — Determination of thermal expansion, MOD. Moscow: Standartinform; 2017.

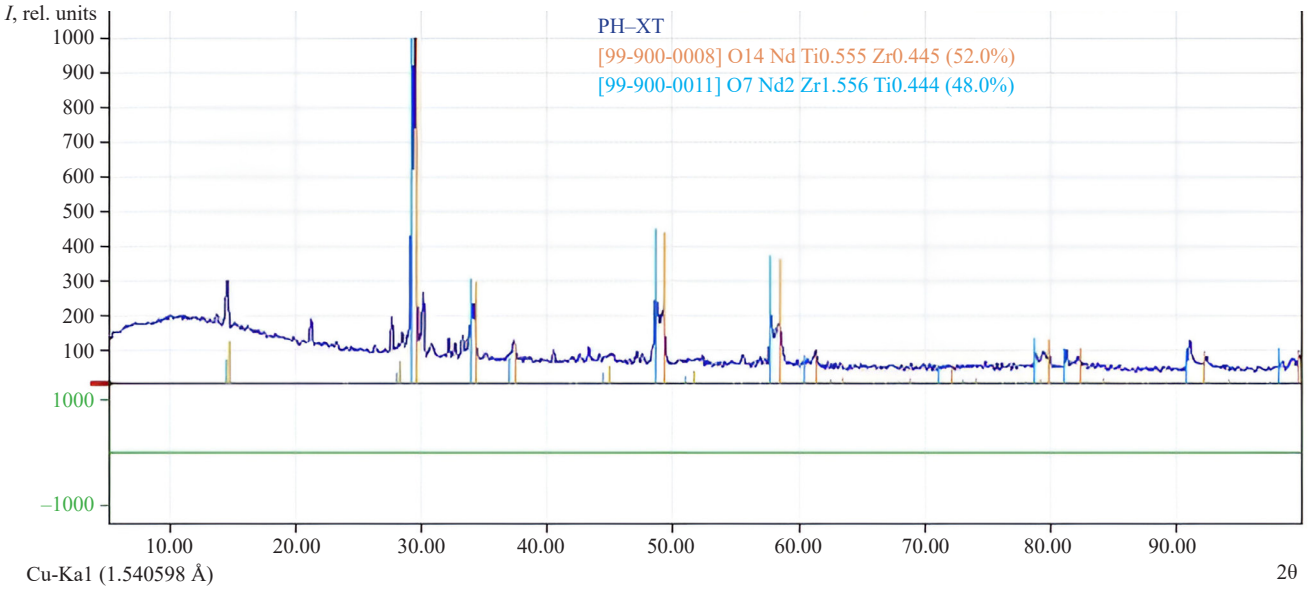

(a)

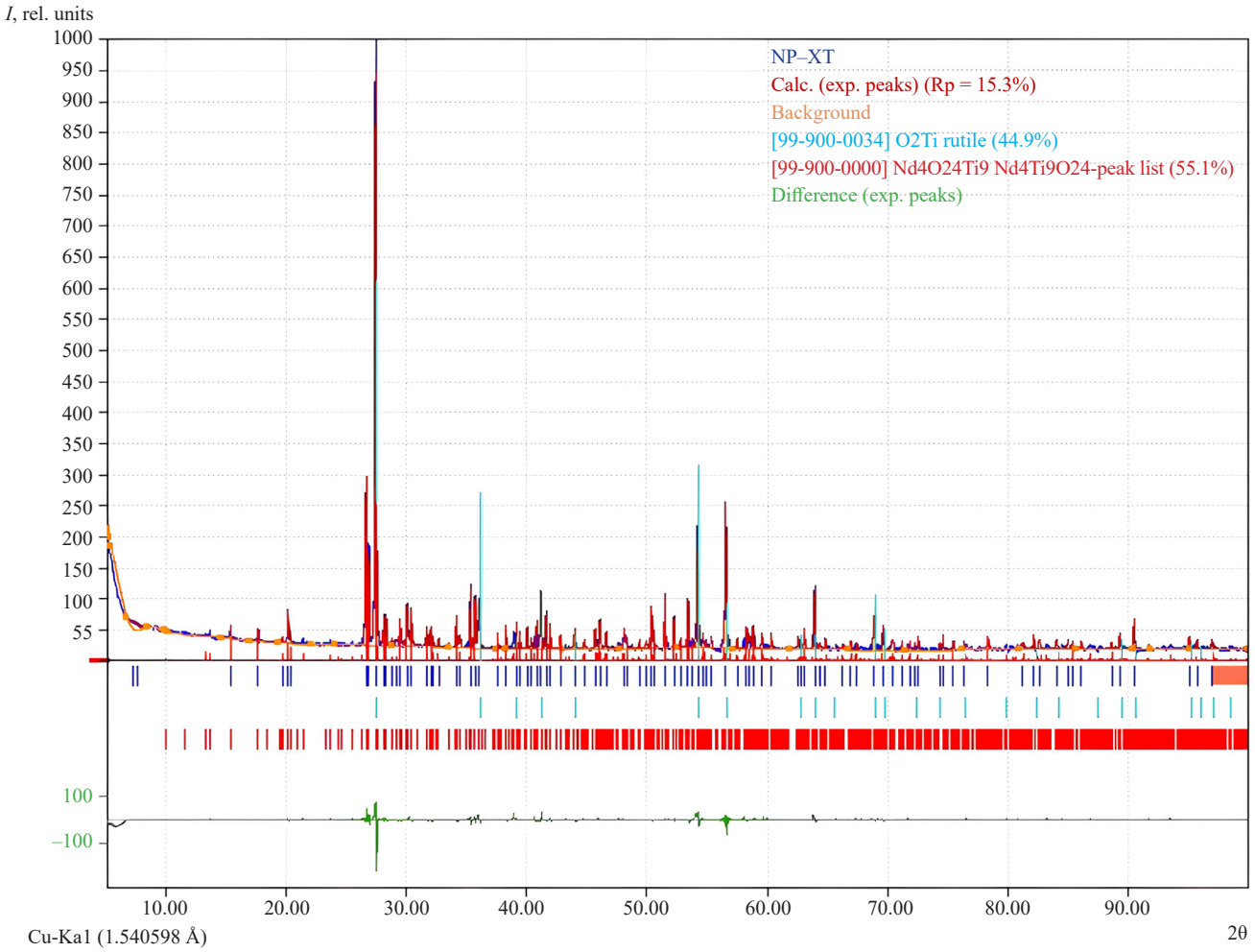

(b)

Fig. 2. Synthesized matrices X-ray diffraction patterns:
(a) titanate-zirconate matrix with the pyrochlore structure; (b) matrix with the structure of orothorhombic REE titanate

Table 2. Results of the study of mechanical and thermophysical properties

Type of test	GOST R 50926-96 requirements	Measured values	
		Pyrochlore Ln_2TiZrO_7	Pyrochlore Ln_2TiZrO_7
Thermal conductivity in the temperature range from 20 to 500°C, W/(m·K)	1–2	0.91–1.18	1.54–1.71
LETC in the temperature range from 20 to 500°C, $K^{-1} \cdot 10^{-6}$, no more than	9	9.12–10.10	6.96–7.88
Young's modulus in compression, kN/m^2, no less than	$5.4 \cdot 10^7$	$1.78 \cdot 10^8$	$2.15 \cdot 10^8$
Ultimate compressive strength, MPa, no less than	9	179 ± 26	150 ± 10
Bending strength, MPa, no less than	41	57.8 ± 3.9	20.6 ± 4.0

orthorhombic REE titanate were 179 and 150 MPa, respectively, while for AGM this index was 9 MPa.

The compressive strength of ceramic material and Young's modulus are usually characterized by values of the same order. The multiple differences observed in the case of the matrices studied is due to the presence of a certain number of pores in the samples. The averaged bending strength values amounted to 20.6 and 57.8 MPa for crystalline matrices with pyrochlore and orthorhombic REE titanate structures, respectively. The values obtained are 4–7 times lower than the values measured under compressive loads. This is typical for structural ceramics. Bending is a special case of simultaneous compression and tension [27]. The expectedly low index is also due to the crystalline structure which is comparatively poor in absorbing bending loads. At the stage of engineering barrier design this feature must be leveled. Package rigidity must be provided by the side wall of the non-returnable container used for intermediate storage and burial.

The results of heat capacity of the MLM samples in the temperature range of 50–500°C are presented in Fig. 3.

The diffusivity coefficients were obtained by comparing the experimental thermogram with the theoretical model. The determination results averaged over three parallel measurements of matrix samples of each type are presented in Fig. 4.

The dependencies of matrix thermal conductivities on temperature obtained by calculation are shown in Fig. 5.

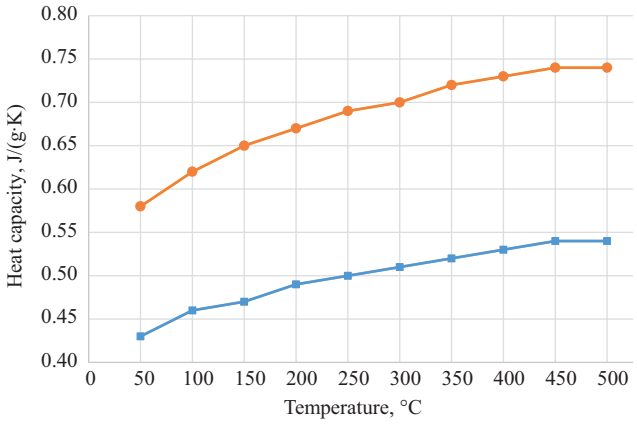

Fig. 3. Dependencies of the crystalline matrices heat capacity on temperature (squares, blue line—a matrix with a pyrochlore structure; circles, red line—a matrix with structure of an orthorhombic REE titanate)

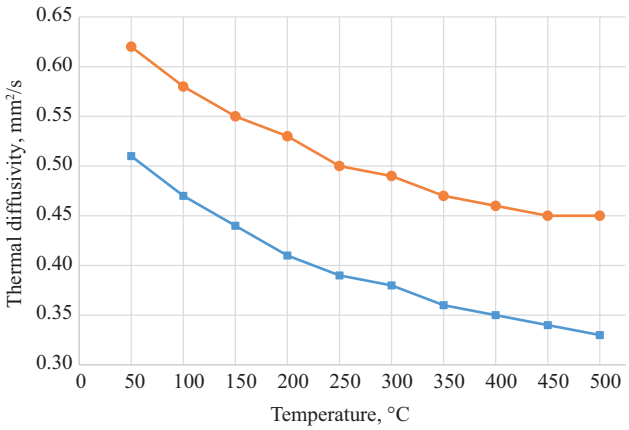

Fig. 4. Dependencies of the crystalline matrices thermal diffusivity on temperature (squares, blue line—a matrix with a pyrochlore structure; circles, red line—a matrix with structure of an orthorhombic REE titanate)

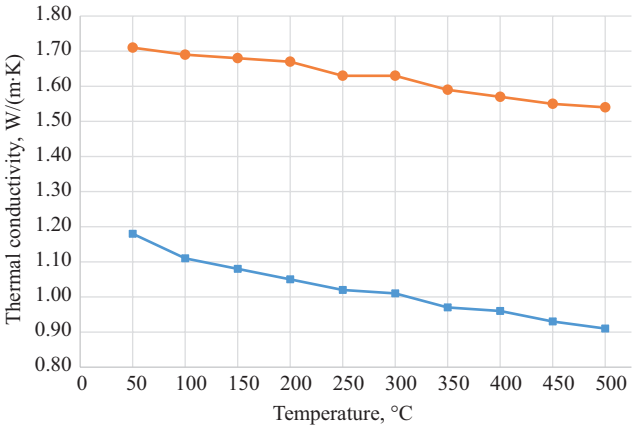

Fig. 5. Dependencies of the thermal conductivity coefficients of crystalline matrices on temperature (squares, blue line—a matrix with a pyrochlore structure; circles, red line—a matrix with structure of anorthorhombic REE titanate)

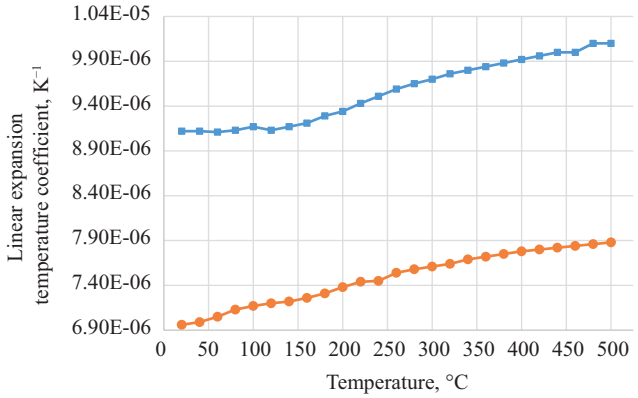

Fig. 6. Dependence of the matrices thermal expansion coefficient on temperature (squares, blue line—a matrix with a pyrochlore structure; circles, a red line—a matrix with an orthorhombic REE titanate structure)

As seen from the above dependencies, the thermal conductivity of the material is significantly affected by its chemical composition. The thermal conductivity of the matrix with orthorhombic REE titanate structure is higher in the whole range of investigated temperatures. This is apparently due to the contribution of the rutile phase with a very high intrinsic index, reaching reaches 5.3 W/(m·K) at 473 K [31]. The values of the matrices tested can vary from 0.9 to 1.7 W/(m·K) and almost completely fit into the range of 1–2 W/(m·K), as regulated by Russian state standard GOST R 50926-96. In general, the values of thermal conductivity of both matrices are close to the range of 0.8–1.5 W/(m·K). This is characteristic for oxide ceramics with variations caused by differences in chemical composition and porosity of the materials. Known exceptions include ceramics based on Al_2O_3, where the thermal conductivity in the range of 100–1000°C can range from 30 to 6 W/(m·K). The decrease in the level of thermal conductivity is also typical for non-metallic materials. An increase in the index can only be observed in the temperature region above 600°C for quartz glass and several types of translucent materials for thermal radiation.

The LETC was determined to be in the temperature range from 20 to 500°C in steps of 20°C at a heating rate of 3°C/min. The pyrochlore structure matrix was tested for five parallel samples, with the structure of orthorhombic REE titanate—for three samples. The measurement results are presented graphically in Fig. 6.

As seen from Fig. 6, there is a smooth growth of LETC in both cases with increasing temperature. This is typical for the vast majority of technical ceramics [29]. The increase of the index with increasing temperature is common for most solids. In the case of the materials being studied herein, this indicates the absence of allotropic transformations in the heating process where decrease in volume is possible. Fluctuations observed at 100 and 240°C on the curves of matrices with pyrochlore and orthorhombic REE titanate structures are apparently caused by measurement errors.

It should be noted that thermophysical and mechanical properties of the matrices being studied here are close to typical parameters of technical ceramics. They mainly correspond or exceed the characteristics of AGM used for immobilization of HLW.

Thus, we can tentatively conclude that crystalline matrices are able to fully perform the function of final forms for immobilization of the corresponding HLW fractions. The application of materials of this type will allow the long-term safety of intermediate storage sites and deep burial sites of conditioned wastes to be enhanced. The specific features of the matrices due to their crystalline structure are not a limitation to their application. Indeed, they are leveled out by the qualities of engineering barriers, especially primary packaging.

CONCLUSIONS

The study established the mechanical and thermophysical properties of crystalline matrices in the immobilization of REE-actinide fraction obtained on an enlarged scale using the method combining granular precursor and CCIM.

The compressive strength limits of matrices with pyrochlore and orthorhombic REE titanate structures were found to be 17–20 times higher than the index regulated for AGM. This fact indicates the possibility of safe handling of the final product during manipulations during *in situ* handling, transportation to the disposal site and during actual disposal.

The bending strength is lower than that of glass by up to 50%, due to the nature of the crystalline material which is poorly able to absorb tensile loads. However, this feature can be offset by the stiffness of the primary packaging.

The values of thermal conductivity coefficients in the temperature range of 50–500°C range from 0.91 to 1.71 W/(m·K) depending on the matrix composition. LETC is characterized by quite low values $(7–10) \cdot 10^{-6}$ K^{-1}. This is comparable to the values of corundum $(8 \cdot 10^{-6} K^{-1})$ and quartz glass $(8.5 \cdot 10^{-6} K^{-1})$.

In general, the mechanical and thermophysical properties of MLMs are comparable or superior to the regulated parameters of preserved final forms. This, in addition to other advantages, confirms the potential for their application in the immobilization of fractionated wastes.

When implementing the technology for the immobilization of fractionated HLW, attention must be paid to the development of specialized non-returnable containers taking into account the LETC of crystalline matrices and the relatively small bending strength limits.

Acknowledgments

The project was undertaken under the Unified Industry Thematic Plan of Rosatom State Corporation EOTP-TTsPM-25.

Authors' contributions

M.Yu. Kalenova, I.V. Kuznetsov, O.I. Stefanovskaya, V.A. Stepanov—study concept and methodological support.

M.Yu. Kalenova, I.V. Kuznetsov, A.Yu. Zobkova—draft manuscript preparation.

I.M. Melnikova, A.S. Shchepin, K.V. Klemazov—data collection.

O.N. Budin, V.A. Stepanov, K.V. Klemazov, I.M. Melnikova—analysis and interpretation of results.

A.S. Shchepin, O.N. Budin—specimen synthesis and sample preparation.

The authors declare no conflict of interest.

REFERENCES

1. Putilov A.V., Vorobiev A.G., Bugaenko M.V. The strategy and practice of radioactive waste management and their geological disposal. *Gornyi Zhurnal = Mining J.* 2015;10:6–10 (in Russ.). https://doi.org/10.17580/gzh.2015.10.01
2. Gupalo T.A., Chistyakov V.N., Feshchenko A.I., Suvorova A.A., Shadrin A.Yu., Schmidt O.V. Kormilitsyn M.V., Osipenko A.G. Technical and economic modeling of technological schemes of preparation of high level wastes from processing of spent nuclear fuel for final isolation. *Voprosy radiatsionnoi bezopasnosti = Issues of Radiation Safety.* 2012;4(68):38–48 (in Russ.).
3. Linge I.I., Utkin S.S., Kulagina T.A., Trokhov N.N. Underground research laboratory in "the Yenisei" section of the Nizhnekansky massif of the Krasnoyarsk Region. *Zhurnal Sibirskogo federal'nogo universiteta. Seriya: Tekhnika i tekhnologii = Journal of the Siberian Federal University. Series: Technics and Technologies*. 2019;12(7):830–841 (in Russ.).
4. Dorofeev A.N., Bolshov L.A., Linge I.I., Utkin S.S., Savelyeva E.A. Strategic master plan for R&D demonstrating the safety of construction, operation and closure of a deep geological disposal facility for radioactive waste. *Radioaktivnye otkhody = Radioactive Waste.* 2017;1(1):34–43 (in Russ.).
5. Kochkin B.T., Bogatov S.A. Borehole RW disposal concept and prospects of its implementation in Russia. *Radioaktivnye otkhody = Radioactive Waste.* 2022;2(19):85–99 (in Russ). https://doi.org/10.25283/2587-9707-2022-2-85-99
6. Kudryavtsev E.G. Khaperskaya A.V. Problems of SNF handling in Russia and prospects for their solution. *Rossiiskii khimicheskii zhurnal = Russ. Chem. J.* 2010;54(3):8–11 (in Russ.).
7. Glagolenko Yu.V., Dzekun E.G., Drozhko E.G. Medvedev G.M., Rovnyi S.I., Suslov A.P. Strategy for handling radioactive waste at the Mayak production association. *Voprosy radiatsionnoi bezopasnosti = Issues of Radiation Safety.* 1996;2:3–10 (in Russ.).
8. Ozhovan M.I., Poluektov P.P. Glasses for immobilization of nuclear waste. *Priroda J.* 2010;3(1135):3–11 (in Russ.).
9. Aloy A.S., Blokhin A.I., Blokhin P.A., Kovalev N.V. Radiation characteristics of borosilicate glass containing high-level waste. *Radioaktivnye otkhody = Radioactive Waste.* 2020;3(12):93–100 (in Russ.). https://doi.org/10.25283/2587-9707-2020-3-93-100
10. Aloy A.S., Trofimenko A.V., Koltsova T.I., Nikandrova M.V. Physico-chemical characteristics of vitrified simulated HLW at EDC MCC. *Radioaktivnye otkhody = Radioactive Waste.* 2018;4(5):67–75 (in Russ.).
11. Logunov M.V., Voroshilov Yu.A., Babain V.A., Skobtsov A.S. Experience of Mastering, Industrial Exploitation, and Optimization of the Integrated Extraction–Precipitation Technology for Fractionation of Liquid High-Activity Wastes at Mayak Production Association. *Radiochemistry*. 2020;62(6):700–722. https://doi.org/10.1134/S1066362220060028
[Original Russian Text: Logunov M.V., Voroshilov Yu.A., Babain V.A., Skobtsov A.S. Experience of Mastering, Industrial Exploitation, and Optimization of the Integrated Extraction–Precipitation Technology for Fractionation of Liquid High-Activity Wastes at Mayak Production Association. *Radiokhimiya*. 2020;62(6):463–484 (in Russ.). https://doi.org/10.31857/S0033831120060027]
12. Tananaev I.G., Myasoedov B.F. Commercial recovery of valuable radionuclides from spent nuclear fuel: Methods and approaches. *Radiochemistry.* 2016;58(3):257–264. https://doi.org/10.1134/S1066362216030061
[Original Russian Text: Tananaev I.G., Myasoedov B.F. Commercial recovery of valuable radionuclides from spent nuclear fuel: Methods and approaches. *Radiokhimiya*. 2016;58(3):222–228 (in Russ.).]

СПИСОК ЛИТЕРАТУРЫ

1. Путилов А.В., Воробьев А.Г., Бугаенко М.В. Стратегия и практика обращения с радиоактивными отходами и их геологического захоронения. *Горный журнал.* 2015;10:6–10. https://doi.org/10.17580/gzh.2015.10.01
2. Гупало Т.А., Чистяков В.Н., Фещенко А.И., Суворова А.А., Шадрин А.Ю., Шмидт О.В. Кормилицын М.В., Осипенко А.Г. Технико-экономическое моделирование технологических схем подготовки высокоактивных отходов от переработки отработавшего ядерного топлива для окончательной изоляции. *Вопросы радиационной безопасности.* 2012;4(68):38–48.
3. Линге И.И., Уткин С.С., Кулагина Т.А., Трохов Н.Н. Подземная исследовательская лаборатория на участке «Енисейский» Нижнеканского массива Красноярского края. *Журнал Сибирского федерального университета. Серия: Техника и технологии*. 2019;12(7):830–841.
4. Дорофеев А.Н., Большов Л.А., Линге И.И., Уткин С.С., Савельева Е.А. Стратегический мастер-план исследований в обоснование безопасности сооружения, эксплуатации и закрытия пункта глубинного захоронения радиоактивных отходов. *Радиоактивные отходы.* 2017;1(1):34–43.
5. Кочкин Б.Т., Богатов С.А. Перспективы использования скважинной концепции для удаления РАО в России. *Радиоактивные отходы.* 2022;2(19):85–99. https://doi.org/10.25283/2587-9707-2022-2-85-99
6. Кудрявцев Е.Г. Хаперская А.В. Проблемы обращения с отработавшим ядерным топливом в России и перспективы их решения. *Российский химический журнал.* 2010;54(3):8–11.
7. Глаголенко Ю.В., Дзекун Е.Г., Дрожко Е.Г. Медведев Г.М., Ровный С.И., Суслов А.П. Стратегия обращения с радиоактивными отходами на производственном объединении «Маяк». *Вопросы радиационной безопасности.* 1996;2:3–10.
8. Ожован М.И., Полуэктов П.П. Стекла для иммобилизации ядерных отходов. *Природа*. 2010;3(1135):3–11.
9. Алой А.С., Блохин А.И., Блохин П.А., Ковалев Н.В. Радиационные характеристики боросиликатного стекла, содержащего высокоактивные отходы. *Радиоактивные отходы*. 2020;3(12):93–100. https://doi.org/10.25283/2587-9707-2020-3-93-100
10. Алой А.С., Трофименко А.В., Кольцова Т.И., Никандрова М.В. Физико-химические характеристики остеклованных модельных ВАО ОДЦ ГХК. *Радиоактивные отходы.* 2018;4(5):67–75.
11. Логунов М.В., Ворошилов Ю.А., Бабаин В.А., Скобцов А.С. Опыт освоения, промышленной эксплуатации и оптимизации комплексной экстракционно-осадительной технологии фракционирования жидких высокоактивных отходов на ПО «МАЯК». *Радиохимия.* 2020;62(6):463–484. https://doi.org/10.31857/S0033831120060027
12. Тананаев И.Г., Мясоедов Б.Ф. Методы и подходы к технологическому выделению ценных радионуклидов из отработавшего ядерного топлива. *Радиохимия.* 2016;58(3):222–228.
13. Баторшин Г.Ш., Кириллов С.Н., Смирнов И.В., Сарычев Г.А. Тананаев И.Г., Фёдорова О.В., Мясоедов Б.Ф. Комплексное выделение ценных компонентов из техногенных радиоактивных отходов как вариант создания рентабельного ЗЯТЦ. *Вопросы радиационной безопасности.* 2015;3(79):30–36.
14. Salvatores M., Palmiotti G. Radioactive waste partitioning and transmutation within advanced fuel cycles: Achievements and challenges. *Progress in Particle and Nuclear Physics.* 2011;66(1):144–166. https://doi.org/10.1016/j.ppnp.2010.10.001

13. Batorshin G.Sh., Kirillov S.N., Smirnov I.V., Sarychev G.A. Tananaev I.G., Fedorova O.V., Myasoedov B.F. Complex extraction of valuable components from anthropogenic waste as an option of establishing cost-effective closed nuclear fuel cycle. *Voprosy radiatsionnoi bezopasnosti = Issues of Radiation Safety.* 2015;3(79):30–36 (in Russ.).
14. Salvatores M., Palmiotti G. Radioactive waste partitioning and transmutation within advanced fuel cycles: Achievements and challenges. *Progress in Particle and Nuclear Physics.* 2011;66(1):144–166. https://doi.org/10.1016/j.ppnp.2010.10.001
15. Mamchich M.V., Goletsky N.D., Tkachenko L.I., Vyznyi A.N., Naumov A.A., Puzikov E.A., Zil'berman B.Y., Belova E.V. Development and Verification of a Scheme for Fractionation of HAWs with TODGA Extractive Agent in a "Light" Diluent. *Radiochemistry.* 2021;63(4):462–469. https://doi.org/10.1134/S1066362221040093
[Original Russian Text: Mamchich M.V., Goletsky N.D., Tkachenko L.I., Vyznyi A.N., Naumov A.A., Belova E.V., Puzikov E.A., Zil'berman B.Y. Development and Verification of a Scheme for Fractionation of HAWs with TODGA Extractive Agent in a "Light" Diluent. *Radiokhimiya*. 2021;63(4):372–380 (in Russ.). https://doi.org/10.31857/S0033831121040092]
16. Wei Y.Z., Wang X.P., Liu R.Q., Wu Y., Usuda S., Arai T. An advanced partitioning process for key elements separation from high level liquid waste. *Sci. China Chem*. 2012;55:(9):1726–1731. https://doi.org/10.1007/s11426-012-4697-4
17. Iqbal M., Waheed K., Rahat S.B., Lee T.M., Lee M.S. An overview of molecular extractants in room temperature ionic liquids and task specific ionic liquids for the partitioning of actinides/lanthanides. *J. Radioanal. Nuclear Chem.* 2020;325(1):1–31. https://doi.org/10.1007/s10967-020-07199-1
18. Nayak P.K., Kumaresan R, Venkatesan K.A., Antony M.P., Vasudeva Rao P.R. A New Method for Partitioning of Trivalent Actinides from High-Level Liquid Waste. *Sep. Sci. Technol.* 2013;48(9):1409–1416. https://doi.org/10.1080/01496395.2012.737401
19. Awwad N.S. Introductory Chapter: From the Cradle to the Grave for the Nuclear Fuel Cycle. In: Awwad N.S. (Ed.). *Nuclear Power Plants – The Processes from the Cradle to the Grave*. London: IntechOpen; 2021. 168 p. https://doi.org/10.5772/intechopen.87697
20. Bogdanov R.V., Kuznetsov R.A., Epimakhov V.N., Oleinik M.S., Epimakhov T.V. *Method for immobilization of strontium-cesium fraction of highly active wastes by incorporation into geo-ceramic matrices*: Pat. RU2561508C1. Publ. 27.08.2015 (in Russ.).
21. Yudintsev S.V., Nikolskii M.S., Nikonov B.S., Malkovskii V.I. Matrices for isolation of actinide wastes in a deep well repository. *Dokl. Earth Sci.* 2018;480(1):631–636. https://doi.org/10.1134/S1028334X18050203
[Original Russian Text: Yudintsev S.V., Nikolskii M.S., Nikonov B.S., Malkovskii V.I. Matrices for isolation of actinide wastes in a deep well repository. *Doklady Akademii Nauk*. 2018;480(2):217–222 (in Russ.). https://doi.org/10.7868/S0869565218140177]
22. Alekseeva L.S., Nokhrin A.V., Karazanov K.O., *et al.* Mechanical Properties and Thermal Shock Resistance of Fine-Grained Nd:YAG/SiC Ceramics. *Inorg. Mater*. 2022;58(2):199–204. https://doi.org/10.1134/S0020168522020017
[Original Russian Text: Alekseeva L.S., Nokhrin A.V., Karazanov K.O., Orlova A.I., Boldin M.S., Lantsev E.A., Murashov A.A., Chuvildeev V.N. Mechanical Properties and Thermal Shock Resistance of Fine-Grained Nd:YAG/SiC Ceramics. *Neorganicheskie Materialy*. 2022;58(2):209–214 (in Russ.).]
15. Мамчич М.В., Голецкий Н.Д., Ткаченко Л.И., Визный А.Н., Наумов А.А., Белова Е.В., Пузиков Е.А. Зильберман Б.Я. Разработка и проверка схемы фракционирования ВАО с использованием экстрагента TODGA в «легком» разбавителе. *Радиохимия*. 2021;63(4):372–380. https://doi.org/10.31857/S0033831121040092
16. Wei Y.Z., Wang X.P., Liu R.Q., Wu Y., Usuda S., Arai T. An advanced partitioning process for key elements separation from high level liquid waste. *Sci. China Chem*. 2012;55:(9):1726–1731. https://doi.org/10.1007/s11426-012-4697-4
17. Iqbal M., Waheed K., Rahat S.B., Lee T.M., Lee M.S. An overview of molecular extractants in room temperature ionic liquids and task specific ionic liquids for the partitioning of actinides/lanthanides. *J. Radioanal. Nuclear Chem.* 2020;325(1):1–31. https://doi.org/10.1007/s10967-020-07199-1
18. Nayak P.K., Kumaresan R, Venkatesan K.A., Antony M.P., Vasudeva Rao P.R. A New Method for Partitioning of Trivalent Actinides from High-Level Liquid Waste. *Sep. Sci. Technol.* 2013;48(9):1409–1416. https://doi.org/10.1080/01496395.2012.737401
19. Awwad N.S. Introductory Chapter: From the Cradle to the Grave for the Nuclear Fuel Cycle. In: Awwad N.S. (Ed.). *Nuclear Power Plants – The Processes from the Cradle to the Grave*. London: IntechOpen; 2021. 168 p. https://doi.org/10.5772/intechopen.87697
20. Богданов Р.В., Кузнецов Р.А., Епимахов В.Н., Олейник М.С., Епимахов Т.В. *Способ иммобилизации стронций-цезиевой фракции высокоактивных отходов включением в геокерамические матрицы*: Пат. RU 2561508C1. Заявка № 2014117398/07, заявл. 29.04.2014; опубл. 27.08.2015. Бюл. № 24.
21. Юдинцев С.В., Никольский М.С., Никонов Б.С., Мальковский В.И. Матрицы для изоляции актинидных отходов в глубоком скважинном хранилище. *Доклады Академии наук*. 2018;480(2):217–222. https://doi.org/10.7868/S0869565218140177
22. Алексеева Л.С., Нохрин А.В., Каразанов К.О., Орлова А.И., Болдин М.С., Ланцев Е.А., Мурашов А.А., Чувильдеев В.Н. Исследование механических свойств и стойкости к термоудару мелкозернистой керамики YAG:ND/SIC. *Неорганические материалы*. 2022;58(2):209–214.
23. Юдинцев С.В. Изоляция фракционированных отходов ядерной энергетики. *Радиохимия.* 2021;63(5):403–430. https://doi.org/10.31857/S0033831121050014
24. Юдинцев С.В. Титанаты лантанидов – потенциальные матрицы для иммобилизации актинидных отходов. *Доклады Академии наук.* 2015;460(4):453–458. https://doi.org/10.7868/S0869565215040192
25. Баранов В.Г., Тенишев А.В., Лунёв А.В., Покровский С.А., Хлунов А.В. Высокотемпературные измерения температуропроводности реакторных материалов методом лазерной вспышки. *Ядерная физика и инжиниринг.* 2011;2(4):291–302.
26. Головин Ю.И., Тюрин А.И., Головин Д.Ю., Самодуров А.А. Определение коэффициента температуропроводности прозрачных материалов модифицированным методом лазерной вспышки. *Известия Российской академии наук. Серия физическая.* 2020;84(7):1004–1009. https://doi.org/10.31857/S036767652007011X
27. Межецкий Г.Д., Загребин Г.Г., Решетник Н.Н. *Сопротивление материалов*. 5-ое изд. М.: Дашков и К; 2016. 432 с.
28. Охотин А.С. *Теплопроводность твердых тел*. М.: Энергоатомиздат; 1984. 312 с.
29. Толкачева А.С., Павлова И.А. *Общие вопросы технологии тонкой керамики*. Екатеринбург: Изд-во УрФУ; 2018. 184 с.

23. Yudintsev S.V. Isolation of Separated Waste of Nuclear Industry. *Radiochemistry.* 2021;63(5):527–555. https://doi.org/10.1134/S1066362221050015
[Original Russian Text: Yudintsev S.V. Isolation of Separated Waste of Nuclear Industry. *Radiokhimiya*. 2021;63(5): 403–430 (in Russ.). https://doi.org/10.31857/S0033831121050014]
24. Yudintsev S.V. Lanthanide titanates as promising matrices for immobilization of actinide wastes. *Dokl. Earth Sci.* 2015;460(2):130–136. https://doi.org/10.1134/S1028334X15020051
[Original Russian Text: Yudintsev S.V. Lanthanide titanates as promising matrices for immobilization of actinide wastes. *Doklady Akademii Nauk*. 2015;460(4):453–458 (in Russ.). https://doi.org/10.7868/S0869565215040192]
25. Baranov V.G., Tenishev A.V., Lunev A.V., Pokrovskii S.A., Khlunov A.V. High-temperature measurements of thermal conductivity of reactor materials by laser flash. *Yadernaya fizika i inzhiniring = Nuclear Physics and Engineering*. 2011;2(4): 291–302 (in Russ.).
26. Golovin Yu.I., Tyurin A.I., Golovin D.Yu., *et al*. Determining the Temperature Diffusivity of Transparent Materials via a Modified Laser Flash Technique. *Bull. Russ. Acad. Sci.: Physics.* 2020;84(7):829–834. https://doi.org/10.3103/S1062873820070114
[Original Russian Text: Golovin Yu.I., Tyurin A.I., Golovin D.Yu., Samodurov A.A. Determining the Temperature Diffusivity of Transparent Materials via a Modified Laser Flash Technique. *Izvestiya Rossiiskoi Akademii Nauk. Seriya Fizicheskaya*. 2020;84(7):1004–1009 (in Russ.). https://doi.org/10.31857/S036767652007011X]
27. Mezhetskii G.D., Zagrebin G.G., Reshetnik N.N. *Soprotivlenie materialov* (*Strength of Materials*). Moscow: Dashkov i K; 2016. 432 p. (in Russ.).
28. Okhotin A.S. *Teploprovodnost' tverdykh tel* (*Thermal Conductivity of Solids*). Moscow: Energoatomizdat; 1984. 312 p. (in Russ.).
29. Tolkacheva A.S., Pavlova I.A. *Obshchie voprosy tekhnologii tonkoi keramiki* (*General issues of fine ceramics technology*). Yekaterinburg: UrFU; 2018. 184 p. (in Russ.).

About the authors

Ivan V. Kuznetsov, Cand. Sci. (Eng.), Head of the Laboratory of Methods of Handling Spent Nuclear Fuel and Radioactive Waste, Laskorin Leading Research Institute of Chemical Technology "VNIIHT" (2-1, Electrodnaya ul., Moscow, 115524, Russia). E-mail: ivan7501966@mail.ru. RSCI SPIN-code 4266-0115, https://orcid.org/0000-0002-0904-6959

Anna Yu. Zobkova, Cand. Sci. (Eng.), Leading Engineer, Laboratory of High-Temperature Chemistry and Electrochemistry, Laskorin Leading Research Institute of Chemical Technology "VNIIHT" (2-1, Electrodnaya ul., Moscow, 115524, Russia). E-mail: anna-zobkova@mail.ru

Maya Yu. Kalenova, Cand. Sci. (Eng.), Head of the Department "Chemical Technologies of Closed Nuclear Fuel Cycle," Laskorin Leading Research Institute of Chemical Technology "VNIIHT" (2-1, Electrodnaya ul., Moscow, 115524, Russia). E-mail: kalenovamu@yandex.ru. https://orcid.org/0000-0003-4093-7589

Andrey S. Shchepin, Leading Engineer, Laboratory of Methods of Handling Spent Nuclear Fuel and Radioactive Waste, Laskorin Leading Research Institute of Chemical Technology "VNIIHT" (2-1, Electrodnaya ul., Moscow, 115524, Russia). E-mail: a.s.schepin@gmail.com. RSCI SPIN-code 8370-7976, https://orcid.org/0000-0002-8712-043X

Oleg N. Budin, Leading Engineer, Laboratory of Methods of Handling Spent Nuclear Fuel and Radioactive Waste, Laskorin Leading Research Institute of Chemical Technology "VNIIHT" (2-1, Electrodnaya ul., Moscow, 115524, Russia). E-mail: o.n.budin@gmail.com. RSCI SPIN-code 5910-6649, https://orcid.org/0000-0002-8712-043X

Vladimir A. Stepanov, Dr. Sci. (Phys.-Math.), Professor, Head of the Department of Laser and Plasma Technologies (LaPlaz Department), Obninsk Institute for Nuclear Power Engineering – The Branch of National Research Nuclear University MEPhI (1, Studgorodok, Obninsk, Kaluga oblast, 249039, Russia). E-mail: stepanov@iate.obninsk.ru. Scopus Author ID 7402659774, ResearcherID C-8683-2018, RSCI SPIN-code 7646-7744, https://orcid.org/0000-0003-0869-6711

Irina M. Melnikova, Junior Researcher, Testing Analytical Center, Laskorin Leading Research Institute of Chemical Technology "VNIIHT" (2-1, Electrodnaya ul., Moscow, 115524, Russia). E-mail: irina.sokolova95@yandex.ru. RSCI SPIN-code 3683-3317, https://orcid.org/0000-0002-3666-084X

Olga I. Stefanovskaya, Cand. Sci. (Eng.), Senior Researcher, Laboratory of Radioecological and Radiation Problems, A.N. Frumkin Institute of Physical Chemistry and Electrochemistry, Russian Academy of Sciences (31, Leninskii pr., Moscow, 119071, Russia). E-mail: olga-stef@yandex.ru. Scopus Author ID 14623103700, https://orcid.org/0000-0002-3079-8637

Kirill V. Klemazov, Lecturer, Institute of Laser and Plasma Technologies (LaPlaz Department), Obninsk Institute for Nuclear Power Engineering – The Branch of National Research Nuclear University MEPhI (1, Studgorodok, Obninsk, Kaluga oblast, 249039, Russia). E-mail: klemazov_kirill@mail.ru. Scopus Author ID 57212564605, RSCI SPIN-code 3642-0455, https://orcid.org/0000-0002-4959-3244

Об авторах

Кузнецов Иван Владимирович, к.т.н., начальник лаборатории методов обращения с отработавшим ядерным топливом и радиоактивными отходами, АО «Ведущий научно-исследовательский институт химической технологии им. Б.Н. Ласкорина» (АО «ВНИИХТ им. Б.Н. Ласкорина») (115524, Россия, Москва, ул. Электродная, д. 2, стр. 1). E-mail: ivan7501966@mail.ru. SPIN-код РИНЦ 4266-0115, https://orcid.org/0000-0002-0904-6959

Зобкова Анна Юрьевна, к.т.н., ведущий инженер лаборатории высокотемпературной химии и электрохимии, АО «Ведущий научно-исследовательский институт химической технологии им. Б.Н. Ласкорина» (АО «ВНИИХТ им. Б.Н. Ласкорина») (115524, Россия, Москва, ул. Электродная, д. 2, стр. 1). E-mail: anna-zobkova@mail.ru

Каленова Майя Юрьевна, к.т.н., начальник отделения «Химические технологии замкнутого ядерного топливного цикла», АО «Ведущий научно-исследовательский институт химической технологии им. Б.Н. Ласкорина» (АО «ВНИИХТ им. Б.Н. Ласкорина») (115524, Россия, Москва, ул. Электродная, д. 2, стр. 1). E-mail: kalenovamu@yandex.ru. https://orcid.org/0000-0003-4093-7589

Щепин Андрей Станиславович, ведущий инженер лаборатории методов обращения с отработавшим ядерным топливом и радиоактивными отходами, АО «Ведущий научно-исследовательский институт химической технологии им. Б.Н. Ласкорина» (АО «ВНИИХТ им. Б.Н. Ласкорина») (115524, Россия, Москва, ул. Электродная, д. 2, стр. 1). E-mail: a.s.schepin@gmail.com. SPIN-код РИНЦ 8370-7976, https://orcid.org/0000-0002-8712-043X

Будин Олег Николаевич, ведущий инженер лаборатории методов обращения с отработавшим ядерным топливом и радиоактивными отходами, АО «Ведущий научно-исследовательский институт химической технологии им. Б.Н. Ласкорина» (АО «ВНИИХТ им. Б.Н. Ласкорина») (115524, Россия, Москва, ул. Электродная, д. 2, стр. 1). E-mail: o.n.budin@gmail.com. SPIN-код РИНЦ 5910-6649, https://orcid.org/0000-0002-8712-043X

Степанов Владимир Александрович, д.ф.-м.н., профессор, начальник отделения лазерных и плазменных технологий (Отделение ЛаПлаз), Обнинский институт атомной энергетики – филиал ФГАОУ ВО Национальный исследовательский ядерный университет «МИФИ» (249039, Россия, Калужская область, Обнинск, тер. Студгородок, д. 1). E-mail: stepanov@iate.obninsk.ru. Scopus Author ID 7402659774, ResearcherID C-8683-2018, SPIN-код РИНЦ 7646-7744, https://orcid.org/0000-0003-0869-6711

Мельникова Ирина Михайловна, младший научный сотрудник испытательного аналитического центра, АО «Ведущий научно-исследовательский институт химической технологии им. Б.Н. Ласкорина» (АО «ВНИИХТ им. Б.Н. Ласкорина») (115524, Россия, Москва, ул. Электродная, д. 2, стр. 1). E-mail: irina.sokolova95@yandex.ru. SPIN-код РИНЦ 3683-3317, https://orcid.org/0000-0002-3666-084X

Стефановская Ольга Ивановна, к.т.н., старший научный сотрудник лаборатории радиоэкологических и радиационных проблем, ФГБУН Институт физической химии и электрохимии им. А.Н. Фрумкина Российской академии наук (ИФХЭ РАН) (119071, Россия, Москва, Ленинский проспект, д. 31, корп. 4). E-mail: olga-stef@yandex.ru. Scopus Author ID 14623103700, https://orcid.org/0000-0002-3079-8637

Клемазов Кирилл Валерьевич, преподаватель Института лазерных и плазменных технологий (Отделение ЛаПлаз), Обнинский институт атомной энергетики – филиал ФГАОУ ВО Национальный исследовательский ядерный университет «МИФИ» (249039, Россия, Калужская область, Обнинск, тер. Студгородок, д. 1). E-mail: klemazov_kirill@mail.ru. Scopus Author ID 57212564605, SPIN-код РИНЦ 3642-0455, https://orcid.org/0000-0002-4959-3244

Translated from Russian into English by H. Moshkov
Edited for English language and spelling by Dr. David Mossop

Tonkie Khimicheskie Tekhnologii = Fine Chemical Technologies.
2024;19(2):163–173 ISSN 2686-7575 (Online)

UDC 661.665.1:66.096.5
https://doi.org/10.32362/2410-6593-2024-19-2-163-173

RESEARCH ARTICLE

Effect of leakage of volatile synthesis products on silicon carbide yield in an electrothermal fluidized bed reactor

Vyacheslav S. Kuzevanov[1], Sergey S. Zakozhurnikov[2], Galina S. Zakozhurnikova[3,✉]

[1] *National Research University "MPEI", Volzhsky Branch, Volzhsky, Volgograd oblast, 404110 Russia*

[2] *MIREA — Russian Technological University, Moscow, 119454 Russia*

[3] *Volgograd State Technical University, Volgograd, 400005 Russia*

✉ *Corresponding author, e-mail: galya.vlz@mail.ru*

Abstract

Objectives. To calculate the effect of leakage of volatile synthesis products on silicon carbide yield in an electrothermal fluidized bed reactor, as well as to develop a general model of the synthesis of finely divided silicon carbide. This will be achieved by particularizing a mathematical model of leakage of volatile products of chemical reactions from the reaction volume of the reactor with the fluidizing inert gas.

Methods. As a method to produce silicon carbide, synthesis in an electrothermal fluidized bed was studied. The model of leakage of volatile products was validated by comparing the calculation results with existing experimental data on the SiC synthesis in a high-temperature fluidized bed reactor. The comparison parameters were: mass yield of silicon carbide, and the total synthesis time in a reactor with batch loading of silicon dioxide into the reaction volume.

Results. The value of the parameter p in the general model of SiC synthesis in a fluidized bed was established. The parameter p is equal to the ratio of the number of carbon-containing particles involved in the formation of SiO, to the total number of silicon dioxide particles. It also characterizes the composition of stable complexes of particles of the charge at various operating temperatures of the fluidized bed. The discrepancy between the calculated and experimental values of the masses of the synthesized silicon carbide was shown not to exceed 15.5% at a high temperature of the fluidized bed (T = 1800°C) and decreases with a decrease in the operating temperature to 4.7% at T = 1450°C.

Conclusions. The general computational model for silicon carbide synthesis with a built-in procedure for calculating the leakage of volatile products of chemical reactions enables the variants of SiC production in electrothermal fluidized bed reactors to be analyzed. In this case, it is important to establish an energy-efficient working cycle without preliminary expensive experimental studies.

Keywords

synthesis, silicon carbide, fluidized bed, charge, volatile reaction products, model, SiO leakage

Submitted: 12.01.2023
Revised: 13.11.2023
Accepted: 07.03.2024

For citation

Kuzevanov V.S., Zakozhurnikov S.S., Zakozhurnikova G.S. Effect of leakage of volatile synthesis products on silicon carbide yield in an electrothermal fluidized bed reactor. *Tonk. Khim. Tekhnol. = Fine Chem. Technol.* 2024;19(2):163–173. https://doi.org/10.32362/2410-6593-2024-19-2-163-173

НАУЧНАЯ СТАТЬЯ

Влияние утечки летучих продуктов синтеза на выход карбида кремния в реакторе электротермического кипящего слоя

В.С. Кузеванов[1], С.С. Закожурников[2], Г.С. Закожурникова[3],✉

[1] *Национальный исследовательский университет «МЭИ», филиал в г. Волжском, Волжский, Волгоградская область, 404110 Россия*

[2] *МИРЭА — Российский технологический университет, Москва, 119454 Россия*

[3] *Волгоградский государственный технический университет, Волгоград, 400005 Россия*

✉ *Автор для переписки, e-mail: galya.vlz@mail.ru*

Аннотация

Цели. Рассчитать влияние утечки летучих продуктов реакций карботермического синтеза карбида кремния на массовый выход конечного продукта и развить общую модель синтеза мелкодисперсного карбида кремния в части конкретизации математической модели утечки летучих продуктов химических реакций из реакционного объема установки с ожижающим инертным газом.

Методы. В качестве способа получения SiC рассмотрен процесс его производства в электротермическом кипящем слое. Верификация модели утечки летучих продуктов проведена путем сравнения результатов расчета с имеющимися экспериментальными данными по синтезу SiC в реакторе высокотемпературного кипящего слоя. Параметрами сравнения являлись массовый выход карбида кремния и суммарное время синтеза при последовательных вводах порций диоксида кремния в реакционный объем реактора.

Результаты. Конкретизировано значение параметра p общей модели синтеза SiC в кипящем слое — параметр p равен отношению числа углеродосодержащих частиц, участвующих в образовании SiO, к общему числу частиц диоксида кремния и характеризует состав устойчивых комплексов частиц шихты при разных рабочих температурах псевдоожиженного слоя. Показано, что отклонение расчетных и экспериментальных значений масс карбида кремния, получаемого в результате синтеза, не превышает 15.5% при высокой температуре кипящего слоя (T = 1800°C) и уменьшается при снижении рабочей температуры: 4.7% при T = 1450°C.

Выводы. Общая расчетная модель синтеза карбида кремния с встроенной процедурой расчета утечки летучих продуктов химических реакций позволяет проводить анализ вариантов производства SiC в реакторах электротермического кипящего слоя. Важным при этом является организация энергоэффективного рабочего цикла без предварительных дорогостоящих экспериментальных исследований.

Ключевые слова

синтез, карбид кремния, кипящий слой, шихта, летучие продукты реакций, модель, утечка SiO

Поступила: 12.01.2023
Доработана: 13.11.2023
Принята в печать: 07.03.2024

Для цитирования

Кузеванов В.С., Закожурников С.С., Закожурникова Г.С. Влияние утечки летучих продуктов синтеза на выход карбида кремния в реакторе электротермического кипящего слоя. *Тонкие химические технологии*. 2024;19(2):163–173. https://doi.org/10.32362/2410-6593-2024-19-2-163-173

INTRODUCTION

Analysis of complex high-temperature processes in heterogeneous systems with chemically reacting components is efficient, if it combines experimental and analytical research methods [1–6]. Mitrofanov *et al*. [7, 8] carried out an experimental and theoretical study of the formation of a fluidized bed of dispersed material, in order to determine patterns and relationships between hydrodynamic processes and the electrical conductivity of the bed. A mathematical model was constructed to predict the structure of the region of fluidized particles in the presence of internal local heat sources. However, in those works [7, 8], the area under study was not reactive; i.e., neither conversion of components was considered, nor the yield of any product.

Borodulya *et al.* [9–11] studied the patterns of formation of silicon carbide in an electrothermal fluidized bed (ETFB) [12] and performed experiments to find process parameters that ensure the necessary properties of the resulting product; however, no theoretical analysis of physicochemical processes in the synthesis of SiC in the ETFB reactor was made in those works.

In our previous works [13–15], we developed a model of the synthesis of finely divided silicon carbide in a high-temperature fluidized bed of components of chemical reactions. This reaction volume consists of randomly moving solid particles, a fluidizing gas, and volatile products of chemical reactions. Together with the fluidizing neutral gas, volatile reaction products are also removed from the reaction volume, which undoubtedly affects the efficiency of the reactor.

In this work, we proposed a model of the process of leakage of SiO, the most important component of the SiC synthesis reaction, which significantly affects the yield of silicon carbide.

Basic provisions of the synthesis model

An ETFB reactor with electrical energy supply was considered, where the reaction volume was designed as a fluidized bed. The solid components of the reaction volume (charge) after loading into the reactor were particles of carbon-containing material (coal or coke, Rexyl) and particles of silicon dioxide (river or quartz sand) [16].

The maximum operating temperature in the fluidized bed was 1800°C. The pressure in the working volume remained close to atmospheric pressure. The SiC synthesis process comprised several stages:

- loading of carbon-containing particles, and their fluidization and heating of the entire reaction volume to the operating temperature;
- batch loading of SiO_2 particles until the full consumption of their entire amount provided for the SiC synthesis.

In the model, the following approximations and assumptions were made:

- in the reaction volume, the gas pressure and temperature do not change during the synthesis of silicon carbide;
- the mixture of gases in the reaction volume is a mixture of ideal gases;
- the only volatile synthesis products are CO and SiO; the gas mixture consists of CO, SiO, and the fluidizing gas (N_2);
- the mass flow rate of the fluidizing gas does not change during the synthesis process;
- the synthesis process is represented in a quasi-stationary approximation.

Mathematical model of SiO leakage

As previously [13–15], we used a phenomenological approach and took into account only two main chemical reactions of the synthesis of silicon carbide:
for particles c_2,

$$C + SiO_2 = SiO + CO; \quad (1)$$

and for particles c_1,

$$2C + SiO = SiC + CO. \quad (2)$$

Herein, c_1 are carbide-forming carbon-containing particles and c_2 are carbon-containing particles reacting with SiO_2 in the gaseous phase.

Since the temperature of melting and intense evaporation of SiO_2 is lower than the temperature of the beginning of carbide formation, c_2 particles are cooled and do not participate in reaction (2).

The amounts of the gaseous product SiO in the same reaction volume in reactions (1) and (2) are different because of the leakage of SiO. Let us define the mass leakage of SiO as:

$$\frac{dm_{SiO}^{leak}}{d\tau} = V_{rem} M_{SiO} C_{SiO}. \quad (3)$$

Herein, m is mass; τ is time; V is volume flow rate; M is molar mass; C is concentration. The subscript *SiO* refers to silicon oxide; the superscript *leak*, to leakage; and the subscript *rem*, to the removal of a mixture of gases from the reaction volume. Then, it follows from reactions (1) and (2) that:

$$-\dot{m}_{c_2} = -\frac{1}{2}\dot{m}_{c_1} + V_{rem} M_c C_{SiO}, \quad (4)$$

where the subscripts c, c_1, and c_2 refer to carbon and carbon-containing particles c_1 and c_2, respectively; $\dot{m}_{c_1} = \frac{dm_{c_1}}{d\tau}$; and $\dot{m}_{c_2} = \frac{dm_{c_2}}{d\tau}$.

Let us take into account that, for the mixture of ideal gases:

$$C_{N_2} + C_{CO} + C_{SiO} = \frac{P}{\tilde{R}T}. \quad (5)$$

Herein, P is the pressure of the gas mixture; T is the temperature of the mixture; $\tilde{R}$ is the universal gas constant; the subscripts N_2 and CO refer to the fluidizing gas and carbon monoxide, respectively.

Transforming the molar balance equation at the outlet of the reaction volume $\dot{V}_{\text{r.v.}}$, where the gas mixture leaves it, and taking into account Eq. (5) for the relationship between the concentrations of volatile products in this volume, we obtain the following equation for the relationship between the concentration C_{SiO} and V_{rem}:

$$V_{\text{rem}} = \frac{\frac{1}{M_{\text{N}_2}} V_{\text{in}} \rho_{\text{in}} - \frac{1}{M_c}\left(\dot{m}_{c_2} + \frac{1}{2}\dot{m}_{c_1}\right)}{a_1 - C_{\text{SiO}}}, \qquad (6)$$

wherein the subscript *in* refers to the fluidizing gas at the inlet of the reaction volume, ρ is the density, and $a_1 = \frac{P}{\tilde{R}T}$.

Equation (4) describes the effect of SiO leakage on the changes in the masses of particles c_1 and c_2 in the reaction volume and, therefore, also shows the relationship between the SiO leakage and the yield of silicon carbide. The integration of Eq. (4) gives the following value of the period Δτ of reactor operation with a single SiO_2 load:

$$\Delta r_{c_2}^3 = \frac{1}{2}\frac{\tilde{n}_{c_1}}{\tilde{n}_{c_2}}\Delta r_{c_1}^3 + \left(\frac{1}{3}a_2\right)^{-1} m_{\text{SiO}}, \qquad (7)$$

wherein $m_{\text{SiO}} = \int_{\Delta\tau}\left\{\dot{m}_{\text{in}} - \dot{m}_{c_2} - \frac{1}{2}\dot{m}_{c_1}\right\}\theta d\tau$;

$$\theta = \frac{C_{\text{SiO}}}{\left(a_1 - C_{\text{SiO}}\right)};\quad \Delta r_{c_2}^3 = \left(r_{c_2}^{\text{act}}\right)^3 - \left(r_{c_2}^{\text{cr}}\right)^3;$$

$$\Delta r_{c_1}^3 = \left(r_{c_1}^{\text{act}}\right)^3 - \left(r_{c_1}^{\text{cr}}\right)^3;\quad \dot{m}_{\text{in}} = \frac{M_c}{M_{\text{N}_2}} V_{\text{in}}\rho_{\text{in}};$$

r is the current radius of the particle, the superscript *act* (actual) refers to the parameters at the moment of loading a batch of SiO_2, the superscript *cr* (critical) refers to the time of loading the next batch or the end of the SiC production process, $a_2 = 4\pi\rho_c\tilde{n}_{c_2}$, and $\tilde{n}$ is the number of particles in the reaction volume.

The main difficulty in resolving the problem of the effect of SiO leakage on the yield of silicon carbide is to integrate the right-hand side of Eq. (7) for m_{SiO}. Let us use a model proposal, in order to describe the change in the radii of particles c_1 and c_2 [14, 15] in the representation of the components $\dot{m}_{c_1}$ and $\dot{m}_{c_2}$ of integrand (7). As a result, we have a function which when integrated gives the product of the beta function and the hypergeometric series [17, 18]. After transformations, we obtain the following:

$$\Delta r_{c_2}^3 = \frac{1}{2}\frac{\tilde{n}_{c_1}}{\tilde{n}_{c_2}}\Delta r_{c_1}^3 + a_{\text{I}}\ln\frac{1}{1-\beta^*} + a_{\text{II}}\left\{\left(r_{c_2}^{\text{cr}}\right)^2 S_1 + 2r_{c_2}^{\text{cr}}\Delta r_{c_2} S_2 + \left(\Delta r_{c_2}\right)^2 S_3\right\} + a_{\text{III}}\left\{\left(r_{c_1}^{\text{cr}}\right)^2 S_4 + 2r_{c_1}^{\text{cr}}\Delta r_{c_1} S_5 + \left(\Delta r_{c_1}\right)^2 S_6\right\}. \qquad (8)$$

Herein, $\beta^* = \frac{C_{\text{SiO}}^{\max}}{a_1}$; $a_{\text{I}} = \dot{m}_{\text{in}}\frac{R_c^3}{m_{c_2}^0 L_{c_1}}$; $a_{\text{II}} = 3l\Delta r_{c_2}\beta^*$;

$a_{\text{III}} = \frac{3}{2}\frac{\tilde{n}_{c1}}{\tilde{n}_{c2}}\Delta r_{c_1}\beta^*$; $\Delta r_{c_1} = r_{c_1}^{\text{act}} - r_{c_1}^{\text{cr}}$; $\Delta r_{c_2} = r_{c_2}^{\text{act}} - r_{c_2}^{\text{cr}}$;

and Sj (j = 1, …, 6) are the hypergeometric series with the general form

$$S_j = \sum_{i=1}^{\infty}\frac{\left(\beta^*\right)^{i-1}}{k_j + i}, \qquad (9)$$

wherein $k_1 = l$, $k_2 = 2l$, $k_3 = 3l$, $k_4 = 1$, $k_5 = 2$, $k_6 = 3$, $l = \frac{L_{c_2}}{L_{c_1}}$. The subscript *0* in the definition of a_{I} means the time at which the synthesis begins after the reaction volume has been heated to the operating temperature of the process. R is the initial average radius of particles loaded into the reactor, $L_{c_1} = \psi_{C_1}^*\frac{C_{\text{SiO}}^{\max}}{\Delta r_{c_1}}$, and $L_{c_2} = \psi_{C_2}^*\frac{C_{\text{SiO}_2}^{\max}}{\Delta r_{c_2}}$. The functions $\psi_{C_1}^*$ and $\psi_{C_2}^*$ describe the rates of chemical reactions (2) and (1), respectively [19, 20][1]. The maximum concentration $C_{\text{SiO}_2}^{\max}$ of SiO_2 vapor is calculated according to the data from [14]. The definition of the concentration $C_{\text{SiO}}^{\max}$ of the volatile product of the SiC synthesis immediately after loading the next batch of silicon dioxide into the reaction volume should be refined in accordance with the mathematical model of SiO leakage.

Determination of the maximum SiO concentration in the reaction volume

Let $\dot{m}_{\text{SiO}}$ and $\dot{m}_{\text{CO}}$ be the mass flow rates (generations) of SiO and CO, respectively, in $\dot{V}_{\text{r.v.}}$ at the time of

[1] Feng N. *Kinetics of the reaction between quartz and silicon carbide in different gas atmospheres*: Master Thesis. Norwegian University of Science and Technology (NTNU). Trondheim. 2015. 90 p.

loading a batch of SiO_2 ($\tau = 0$). Then it follows from reactions (1) and (2) that

$$\frac{C_{SiO}^{max}}{C_{CO}^{max}} = \left(1 + \frac{1}{2}\frac{\dot{m}_{c_1}}{\dot{m}_{c_2}}\right)^{-1}\Bigg|_{\tau=0}. \quad (10)$$

Equation (5) at $\tau = 0$ taking into account relation (10) takes the form

$$a_1 = C_{N_2}\Big|_{\tau=0} + C_{SiO}^{max}\left(2 + \frac{1}{2}\frac{\dot{m}_{c_1}}{\dot{m}_{c_2}}\right)\Bigg|_{\tau=0}. \quad (11)$$

The established concentration $C_{N_2}\big|_{\tau=0}$ of the fluidizing gas after loading a batch of SiO_2 particles into the reaction volume is found through the concentration C_{SiO}^{max} from the relationship of the generations of the volatile products:

$$\frac{C_{N_2}}{C_{SiO}^{max}}\Bigg|_{\tau=0} = -\frac{\dot{m}_{вх}}{\dot{m}_{c_2}}\frac{M_c}{M_{N_2}}. \quad (12)$$

The mass flow rates $\dot{m}_{c_1}$ and $\dot{m}_{c_2}$ are calculated using the general model of the synthesis of silicon carbide [14, 15]. As a result, from Eqs. (10)–(12) and the expressions for $\dot{m}_{c_1}$ and $\dot{m}_{c_2}$, we obtain the following equation and solution, which are quadratic in the intended parameter C_{SiO}^{max}.

$$C_{SiO}^{max} = \frac{\tilde{\rho}}{2}\left[\left(1 + \frac{4\tilde{q}}{\tilde{\rho}^2}\right)^{\frac{1}{2}} - 1\right], \quad (13)$$

where $\tilde{\rho} = \dfrac{2b_2 + b_3}{b_1}$; $\tilde{q} = a_1\dfrac{b_2}{b_1}$; $b_1 = M_{N_2}\sigma_{c_1}$;

$b_2 = M_{N_2}\sigma_{c_2}C_{SiO_2}^{max}$; $b_3 = \dfrac{1}{3}V_{in}\rho_{in}R_C^3\rho_c$;

$\sigma_{c_1} = m_{c_1}^0\left(r_{c_1}^{act}\right)^2\alpha_{c_1}k_{c_1}$; $\sigma_{c_2} = m_{c_2}^0\left(r_{c_2}^{act}\right)^2\alpha_{c_2}k_{c_2}$; α is the fraction of the surface of a particle that participates in the chemical reaction; and k_{c_1} and k_{c_2} are the rate constants for reactions (2) and (1), respectively.

General scheme of calculations

As in our previous works [14, 15], the general model of silicon carbide synthesis was used to calculate all the main process parameters, in order to determine the change in the characteristics of the charge over time. These are: the size of solid particles, the concentration of volatile components in the reaction volume and the yield of the final synthesis product. However, unlike those works, each variant calculation of the masses m_{SiC} of the synthesized silicon carbide was carried out for two cases: with SiO leakage in the working process; and without such leakage. The effect of SiO leakage was determined by comparing the values of the following dimensionless parameter:

$$Y = \frac{m_{SiC}^{max} - m_{SiC}^{p}}{m_{SiC}^{*}}, \quad (14)$$

where the superscript * refers to the absence of SiO leakage in the synthesis process. The superscripts *max* and *p* indicate the mass yield of the synthesis product with minimum leakage and various values of the parameter *p*, respectively. In this case, the maximum yield of silicon carbide, m_{SiC}^{max}, is always observed at the minimum *p* value. This depends on the physical properties of carbon-containing particles and SiO_2 particles. For example, for Rexyl and river sand, $p^{min} \simeq 0.2$.

The variable parameters in the calculations were the mass m_{ch}^0 and composition of the initial charge; the operating temperature of the synthesis; the number δ of loaded batches of SiO_2; and the relative number of particles c_2 entering into reaction (1), $p = \dfrac{\tilde{n}_{c_2}}{\tilde{n}_{SiO_2}}$. Since the parameter *p* cannot be determined within the framework of phenomenological approaches when modeling processes with a multiple number of particles, this parameter was determined by comparing the integral characteristics found in the experiments [11] and calculations. These characteristics were the mass yield of silicon carbide and the synthesis time under the same initial data of the experiments and calculations.

RESULTS AND DISCUSSION

General initial data

All calculations were carried out at three values of δ (δ = 2, 5, and 10). The weights of batches of SiO_2 particles loaded into the reaction volume were assumed to be equal. The carbon-containing particles were Rexyl (ρ_C = 500 kg/m^3). Silicon dioxide as a component of the initial charge was coarse river sand. The processes at different operating temperatures *T* in the reaction volume (1450, 1600, and 1800°C were considered separately). The particles of the charge component in the initial state in all calculations had the same average size: $R_C = 10.75 \cdot 10^{-5}$ m and $R_{SiO_2} = 6.5 \cdot 10^{-5}$ m. The mass flow rate of the fluidizing gas was calculated according to Wallis' monograph [21].

Calculation at variable values of the parameter *p*

Table 1 shows the results of calculations of the yield of silicon carbide in the synthesis processes in the case of SiO leakage, and in the hypothetical situation when there is no such leakage and the product yield is maximum. The initial masses of solid components of the charge are m_c^0 = 0.32 kg and $m_{SiO_2}^0$ = 0.3 kg. The operating temperature of the process was T = 1600°C.

Similar calculations were made at other operating temperatures of silicon carbide synthesis: T = 1450°C and T = 1800°C. The results are presented in Fig. 1. Table 1 and Fig. 1 show that, at the considered operating temperatures of SiC synthesis, an increase in the parameter p is accompanied by a decrease in the yield of the final product.

The explanation for this effect is quite simple. An increase in the parameter p means the formation of stable complexes of particles c_2 + SiO_2 at a lower temperature

Table 1. The main characteristics of the SiC synthesis process and the particle sizes of the residual charge

m_{SiC}, kg	Mass yield, %	Time, s	$r_{c_1}^{yield} \cdot 10^5$, m	δ	p	m_{SiC}, kg	Mass yield, %	Time, s	$r_{c_1}^{yield} \cdot 10^5$, m	$r_{c_2}^{yield} \cdot 10^5$, m
With SiC leakage				–	–	Without SiC leakage				
0.108	35.724	10589	6.685	10	0.6	0.195	57.716	32127	5.708	9.413
0.114	37.381	9146	7.626	10	0.5	0.195	57.770	19876	7.216	9.095
0.119	38.713	8025	8.264	10	0.4	0.195	57.796	14733	7.980	8.572
0.124	39.958	7531	8.734	10	0.3	0.195	57.812	11962	8.460	7.523
0.132	42.222	7202	8.952	10	0.2	0.195	57.822	10574	8.795	2.595
0.124	40.152	9836	6.724	5	0.6	0.195	57.563	31079	5.779	9.413
0.130	41.602	8694	7.975	5	0.5	0.195	57.639	16792	7.244	9.095
0.136	43.109	7538	8.308	5	0.4	0.195	57.688	11746	7.995	8.572
0.142	44.703	6377	8.865	5	0.3	0.195	57.719	9446	8.470	7.523
0.147	46.005	5741	9.009	5	0.2	0.195	57.739	8187	8.802	2.595
0.141	44.637	7870	7.121	2	0.6	0.195	57.490	30146	5.883	9.413
0.142	44.816	6881	8.002	2	0.5	0.195	57.439	12467	7.297	9.095
0.144	45.295	5523	8.586	2	0.4	0.195	57.492	8461	8.026	8.572
0.148	46.315	4865	8.929	2	0.3	0.195	57.535	6745	8.491	7.523
0.163	50.036	4606	9.185	2	0.2	0.195	57.566	5618	8.817	2.595

Note: The yield (%) is calculated as $\left(\frac{m_{SiC}}{m_{ch}}\right) \cdot 100\%$; the subscript *yield* refers to the time at which the synthesis is completed.

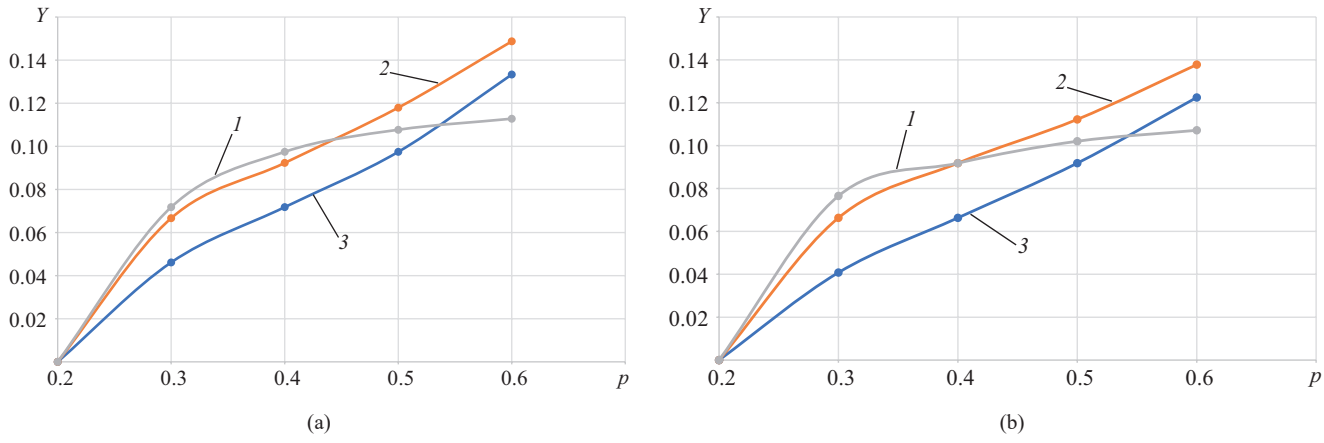

Fig. 1. Effect of SiO leakage on silicon carbide yield at operating temperatures of (a) 1450 and (b) 1800°C. Function $Y = Y(p)$: (*1*) δ = 2; (*2*) δ = 5; (*3*) δ = 10

with an increasing number of particles c_2. In the case of a constant initial number of carbon-containing particles, the number of carbide-forming particles c_1 decreases, and the thickness of the silicon carbide layer formed on the core of c_1 increases with the inevitable increase in diffusion resistance and decrease in the rate of main reaction (2). The synthesis process becomes longer with an increased loss of SiO, an important volatile component of chemical reaction (2).

Figure 2 illustrates the relationship between the SiO leakage and the time of the synthesis process as the dependence of Y on the relative time X of additional SiO leakage. This corresponds to the increase in the parameter p from its minimum value:

$$X = \frac{\tau^p - \tau^{\max}}{\tau^*}. \quad (15)$$

In definition (15), τ^p, $\tau^{\max}$, and τ^* are the times at which the yields of the final product are m^p_{SiC}, $m^{\max}_{SiC}$, and m^*_{SiC}, respectively. The dependencies shown in Fig. 2 also characterize the effect of both the number δ of loadings of equal-mass batches of SiO_2 into the reaction volume, as well as the operating temperature of the working process on the loss of the component of chemical reactions in the synthesis of silicon carbide.

Validation of calculation results

The variables X (Eq. (15)) and Y (Eq. (14)), which are the argument and the calculation function in Fig. 2 respectively, are convenient for analyzing the effect of SiO leakage on the loss of the final product in the synthesis of SiC. This effect largely depends on the synthesis time. This in turn, is determined by the ratio of reacting particles p in the resulting stable complexes c_2 + SiO_2 and the number δ of loadings of batches of SiO_2 particles during the entire process.

Albeit not in the calculated (virtual) but in the real silicon carbide production process, the parameter p takes a very specific value, related to the model representation of the physicochemical process. However, this value cannot be detected directly in the reaction volume in the experiment due to the lack of workable techniques for the corresponding measurements. In turn, at a given composition of the charge, with known constants for chemical reactions (1) and (2), a specific operating temperature of the synthesis, and a specified number of loadings of batches of silicon dioxide into the reaction volume, the parameter p and the time of synthesis of the final product are uniquely related. This can be seen from a comparison of Figs. 1 and 2.

As show by experiments [9–11], in an electrothermal fluidized bed reactor during the high-temperature synthesis of silicon carbide, the changes in the following parameters of the reaction medium, in particular, were measured: operating temperature of the fluidized bed, fluidizing gas flow rate, and CO concentration (at the reactor outlet). At the end of each experiment, the mass of the residual charge was measured. Then, after

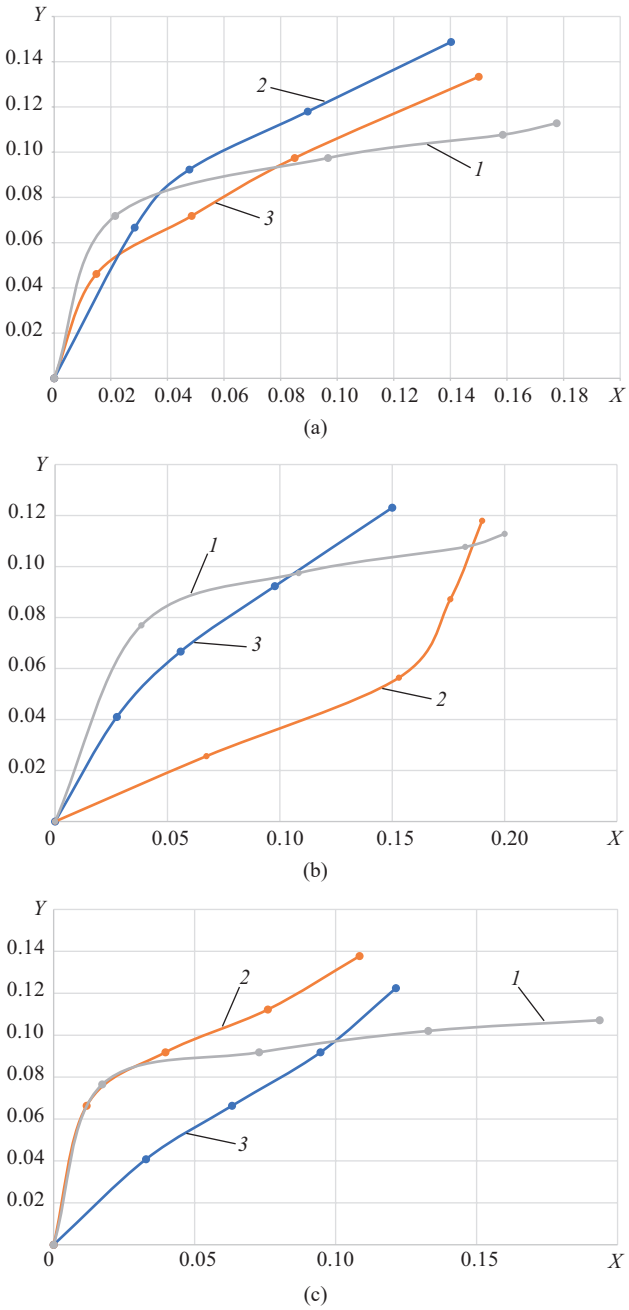

Fig. 2. Effect of synthesis time on silicon carbide yield at operating temperatures of
(a) 1450,
(b) 1600, and
(c) 1800°C.
$Y_1 = Y_1(p)$:
(*1*) δ = 2,
(*2*) δ = 5,
(*3*) δ = 10

annealing, the mass of the resulting final product was measured. A thorough morphological analysis was also carried out. The data [11] was taken as the basis for validating the calculation results in this study with the simultaneous determination of the model value of the parameter p.

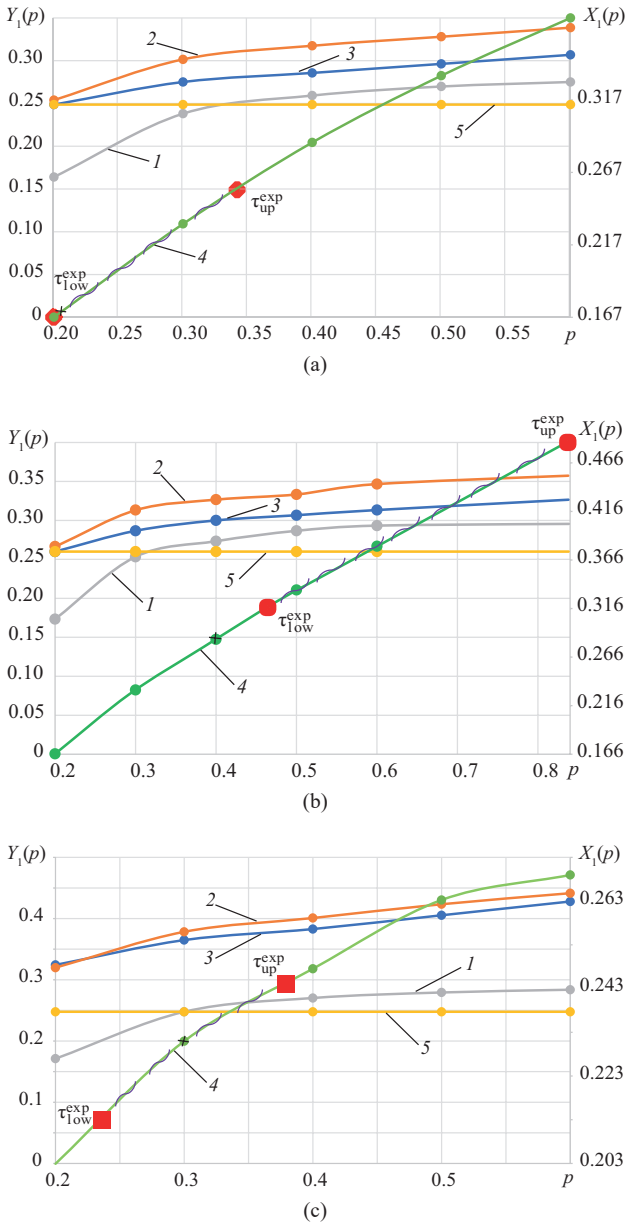

Fig. 3. Relative loss of end product (SiC) because of SiO leakage:
(a) T = 1450°C, m_c^0 = 0.570 kg, $m_{SiO_2}^0$ = 0.290 kg;
(b) T = 1600°C, m_c^0 = 0.500 kg, $m_{SiO_2}^0$ = 0.230 kg;
(c) T = 1800°C, m_c^0 = 0.400 kg, $m_{SiO_2}^0$ = 0.340 kg;
(⁓) range of experimental value of synthesis time;
(+) calculated synthesis time, δ = 10. Function $Y_1 = Y_1(p)$: (*1*) δ = 2; (*2*) δ = 5; (*3*) δ = 10; (4) function $X_1 = X_1(p)$ at δ = 10; (*5*) experimental data [11]

Figure 3 compares the experimental and calculated values of SiC yield and synthesis time at the experimental initial parameters. The calculated graphs in Fig. 3 are plotted in relative coordinates $Y_1 = Y_1(p)$ and $X_1 = X_1(p)$, where

$$\begin{cases} X_1 = \dfrac{\tau^* - \tau^p}{\tau^*} \\ Y_1 = \dfrac{m_{SiC}^* - m_{SiC}^p}{m_{SiC}^*} \end{cases}. \qquad (16)$$

The horizontal lines represent experimental data and are constructed by the elementary change of τ^p and m_{SiC}^p by the experimental (superscript *exp*) values τ^{exp} и m_{SiC}^{exp} in definition (16).

Estimates of synthesis time in experiments were made according to the following two criteria:

- according to the time during which the operating temperature in the reaction volume exceeded the value assigned in a specific experiment;
- according to the time during which CO as a volatile product of reactions (1) and (2) was detected at the outlet of the reaction volume.

Since the estimates do not coincide, in the graphs $X_1 = X_1(p)$ in Fig. 3, both upper (τ_{up}^{exp}) and lower (τ_{low}^{exp}) estimates of the synthesis time are indicated for each experiment. The experimental data was compared with the calculation results at δ = 10. This is due to the number of pulse changes in the operating temperature and CO concentration in the experimental curves [9–11].

Table 2 analyzes the agreement between the results of experiments and calculations.

The right hand column of Table 2 shows the parameter p values averaged over the synthesis time, which were taken to compare the results of experiments and calculations. We assessed the efficiency of our model taking into account the leakage of SiO in the calculations of SiC synthesis at $\bar{p}$ = 0.2 at T = 1450°C, $\bar{p}$ = 0.4 at T = 1600°C, and $\bar{p}$ = 0.3 at T = 1800°C in terms of the discrepancy between the calculated and experimental values of the masses of the synthesized silicon carbide, $\left(1 - \dfrac{m_{SiC}^{\bar{p}}}{m_{SiC}^{exp}}\right) \cdot 100\%$, to obtain 4.7% ($T$ = 1450°C), 5.4% (T = 1600°C), and 15.5% (T = 1800°C). Note that the SiC loss calculated by the leakage model is somewhat higher than that observed in experiments. This is quantitatively demonstrated by the discrepancy $\left(1 - \dfrac{m_{SiC}^{\bar{p}}}{m_{SiC}^{*}}\right) \cdot 100\%$ which is 3.6% (T = 1450°C), 3.9% (T = 1600°C), and 11.5% (T = 1800°C).

Table 2. Calculated and experimental parameters of SiC synthesis

T, °C	m_{ch}, kg	m_{ch}^{exp}, kg	$m_{SiC}^{\overline{p}}$, kg	m_{SiC}^{exp}, kg	$\tau_{low}^{exp} \cdot 10^{-4}$, s	$\tau_{up}^{exp} \cdot 10^{-4}$, s	$\tau^{\overline{p}} \cdot 10^{-4}$, s	$\overline{p}$
1450	0.589	0.565*	0.142	0.149*	1.00	1.20	1.13	0.2
1600	0.523	0.509*	0.105	0.111*	1.23	1.38	1.20	0.4
1800	0.382	0.418*	0.141	0.167*	1.25	1.40	1.31	0.3

*Impurities in the charge are ignored [22].

CONCLUSIONS

The process of SiC formation at variable parameters of chemically reacting media in a high-temperature fluidized bed is very complex. The yield of the final product is not determined by the volumetric balance of the interacting components of the closed system and significantly depends on the loss of any reacting component from the reaction volume. This work demonstrated the adequacy of the first model, as well as the calculation algorithm for the leakage of a volatile product of silicon carbide synthesis.

The leakage of SiO, an intermediate volatile product of the synthesis of silicon carbide, from the reaction volume of the ETFB reactor ultimately leads to the loss of the final product, SiC. However, a decrease in the amount of SiO as a reagent is accompanied by a decrease in the synthesis time of silicon carbide, i.e., a decrease in energy costs for the production of a unit of product.

A computational model of the synthesis of silicon carbide with a validated procedure for calculating the leakage of volatile products of chemical reactions, presented in this work in the form of the SiO leakage model, will allow for computational studies aimed at optimizing the SiC production process in ETFB reactors. In turn, this will determine the validity of recommendations on the composition of the initial charge, the number of loadings of SiO_2 batch into the reaction volume, and the operating temperature of the production process. In this case, it is of the utmost importance to design an energy-efficient operating cycle without preliminary expensive experimental studies.

Authors' contributions

V.S. Kuzevanov—developing the research concept and methodology and writing the text of the manuscript.

S.S. Zakozhurnikov—software and validation.

G.S. Zakozhurnikova—carrying out calculations, analyzing literature sources, and searching and analyzing experimental data.

All authors have read and agreed to the published version of the manuscript.

The authors declare no conflict of interest.

REFERENCES

1. Vasil'eva E.V., Cherkasova T.G., Nevedrov A.V., Papin A.V., Subbotin S.P. The possibility of modernizing coke chemical production using a computer program for predicting the yield of chemical coking products. In: *Chemistry and Chemical Technology: Achievements and Prospects: Proceedings of the Fifth All-Russian Conference*. 2020. P. 83.1–83.3 (in Russ).
2. Ryabov G.A., Folomeev O.M. Problems of Hydrodynamics and Heat Transfer in Interconnected Bed Reactors for CO_2 Capture and Obtaining Hydrogen. *Therm. Eng*. 2023;70(4):311–322. https://doi.org/10.1134/S0040601523040055
3. Prado D.S., Vilarrasa-García E., Sampronha E., *et al*. Multiple approaches for large-scale CO_2 capture by adsorption with 13X zeolite in multi-stage fluidized beds assessment. *Adsorption*. 2023. https://doi.org/10.1007/s10450-023-00422-x
4. Sun L., Yin F., Cao J., *et al*. Numerical Study on the Process of Chemical Looping Hydrogen Production with Multiple Circulating Fluidized Bed Reactors. *J. Therm. Sci*. 2023;32(5):1945–1954. https://doi.org/10.1007/s11630-023-1872-1
5. Ryabov G.A. A Review of the Research Results into the Technologies of Solid-Fuel Combustion in a Circulating Fluidized Bed Conducted Abroad and in Russia. *Therm. Eng*. 2021;68(2): 117–135. https://doi.org/10.1134/S0040601521020051
6. Semeiko K.V., Kustovskyi S.S., Kupriyanchuk S.V., *et al.* Dependence of the Pyrocarbon Structure on the Parameters of the Process of Pyrolysis of Hydrocarbon Gases in an Electrothermal Fluidized Bed. *J. Eng. Phy. Thermophys.* 2020;93(3):677–684. https://doi.org/10.1007/s10891-020-02166-9
7. Mitrofanov A.V., Mizonov V.E., Vasilevich S.V., Mal'ko M.V. Experimental-calculated study of hydro-mechanical processes within electrothermal fluidized bed. *Kosygin International Forum. MNTS Planovsky*-2021. 2021. V. 1. P. 54–57 (in Russ.).
8. Mitrofanov A.V., Vasilevich S.V., Mal'ko M.V., Ovchinnikov L.N., Shpeinova N.S. Development of a mathematical model of fluidization of particles in presence of internal heat sources. *Vestnik Ivanovskogo gosudarstvennogo energeticheskogo universiteta* (*Vestnik IGEU*) = *Vestnik of Ivanovo State Power Engineering University* (*Vestnik IGEU*). 2022;6:49–57 (in Russ.).
9. Borodulya V.A., Vinogradov L.M., Greben'kov A.Zh., Mikhailov A.A., Sidorovich A.M. Carbide-thermal reduction of SiO_2 and formation of silicon carbide in an electrothermal fluidized bed. In: *Teplo- i Massoperenos* – 2012. Minsk: A.V. Lykov ITMO, NAS of Belarus; 2013. P. 121–127 (in Russ.).
10. Borodulya V.A., Vinogradov L.M., Greben'kov A.Zh., Mikhailov A.A. Synthesis of silicon carbide in electrothermal reactor with fluidized bed of carbon particles. *Gorenie i Plazmokhimiya*. 2015;13(2):92–102 (in Russ.).
11. Borodulya V.A., Greben'kov A.Zh., Mikhailov A.A. Features of the formation of various structural modifications of silicon carbide during its carbothermal synthesis in an electrothermal fluidized bed reactor. In: *Teplo- i Massoperenos* – 2018. Minsk: A.V. Lykov ITMO, NAS of Belarus; 2019. P. 107–114 (in Russ.).
12. Borodulya V.A., Vinogradov L.M., Greben'kov A.Zh., Mikhailov A.A. *Method and plant for obtaining silicon carbide*: Eur. Pat. 27539. Publ. 31.08.2017 (in Russ.).
13. Kuzevanov V.S., Garyaev A.B., Zakozhurnikov S.S., Zakozhurnikova G.S. Model of continuous production of fine silicon carbid. *IOP Conf. Ser.: Mater. Sci. Eng*. 2019;537(3): 032106. https://doi.org/10.1088/1757-899X/537/3/032106
14. Kuzevanov V.S., Zakozhurnikov S.S., Zakozhurnikova G.S., Garyaev A.B. Finely dispersed silicon carbide synthesis model in the electrothermal reactor with periodic batch loading. *J. Phys.: Conf. Ser.: Hydrodynamics and Heat and Mass Transfer*. 2020;1683: 022054. https://doi.org/10.1088/1742-6596/1683/2/022054

СПИСОК ЛИТЕРАТУРЫ

1. Васильева Е.В., Черкасова Т.Г., Неведров А.В., Папин А.В., Субботин С.П. Возможность модернизации коксохимического производства с применением компьютерной программы прогнозирования выхода химических продуктов коксования. *Химия и химическая технология: достижения и перспективы: сборник материалов V Всероссийской конференции.* 2020. С. 83.1– 83.3.
2. Ryabov G.A., Folomeev O.M. Problems of Hydrodynamics and Heat Transfer in Interconnected Bed Reactors for CO_2 Capture and Obtaining Hydrogen. *Therm. Eng*. 2023;70(4):311–322. https://doi.org/10.1134/S0040601523040055
3. Prado D.S., Vilarrasa-García E., Sampronha E., *et al*. Multiple approaches for large-scale CO_2 capture by adsorption with 13X zeolite in multi-stage fluidized beds assessment. *Adsorption*. 2023. https://doi.org/10.1007/s10450-023-00422-x
4. Sun L., Yin F., Cao J., *et al*. Numerical Study on the Process of Chemical Looping Hydrogen Production with Multiple Circulating Fluidized Bed Reactors. *J. Therm. Sci*. 2023;32(5): 1945–1954. https://doi.org/10.1007/s11630-023-1872-1
5. Ryabov G.A. A Review of the Research Results into the Technologies of Solid-Fuel Combustion in a Circulating Fluidized Bed Conducted Abroad and in Russia. *Therm. Eng*. 2021;68(2): 117–135. https://doi.org/10.1134/S0040601521020051
6. Semeiko K.V., Kustovskyi S.S., Kupriyanchuk S.V., *et al.* Dependence of the Pyrocarbon Structure on the Parameters of the Process of Pyrolysis of Hydrocarbon Gases in an Electrothermal Fluidized Bed. *J. Eng. Phy. Thermophys.* 2020;93(3):677–684. https://doi.org/10.1007/s10891-020-02166-9
7. Митрофанов А.В., Мизонов В.Е., Василевич С.В., Малько М.В. Опытно-теоретическое исследование гидромеханических процессов в электротермическом кипящем слое. *Международный Косыгинский форум. МНТС Плановский*-2021. 2021. Т. 1. С. 54–57.
8. Митрофанов А.В., Василевич С.В., Малько М.В., Овчинников Л.Н., Шпейнова Н.С. Разработка математической модели псевдоожижения частиц при наличии внутренних источников теплоты. *Вестник Ивановского государственного энергетического университета* (*Вестник ИГЭУ*). 2022;6:49–57.
9. Бородуля В.А., Виноградов Л.М., Гребеньков А.Ж., Михайлов А.А., Сидорович А.М. Карбидотермическое восстановление SiO_2 и образование карбида кремния в электротермическом кипящем слое. В сб. трудов: *Тепло- и массоперенос*-2012. Минск: ИТМО им. А.В. Лыкова НАН Беларуси; 2013. С. 121–127.
10. Бородуля В.А., Виноградов Л.М., Гребеньков А.Ж., Михайлов А.А. Синтез карбида кремния в электротермическом реакторе с кипящим слоем углеродных частиц. *Горение и плазмохимия*. 2015;13(2):92–102.
11. Бородуля В.А., Гребеньков А.Ж., Михайлов А.А. Особенности образования различных структурных модификаций карбида кремния при его карботермическом синтезе в реакторе электротермического кипящего слоя. В сб. трудов: *Тепло- и массоперенос* – 2018. Минск: ИТМО им. А.В. Лыкова НАН Беларуси; 2019. С. 107–114.
12. Бородуля В.А., Виноградов Л.М., Гребеньков А.Ж., Михайлов А.А. *Способ и установка для получения карбида кремния*: Евразийский патент 027539. Заявка № 201500555; заявл. 07.05.2015, опубл. 31.08.2017.
13. Kuzevanov V.S., Garyaev A.B., Zakozhurnikov S.S., Zakozhurnikova G.S. Model of continuous production of fine silicon carbid. *IOP Conf. Ser.: Mater. Sci. Eng*. 2019;537(3):032106. https://doi.org/10.1088/1757-899X/537/3/032106

15. Kuzevanov V.S., Zakozhurnikov S.S., Zakozhurnikova G.S. Model and results of a study of the synthesis of finely dispersed silicon carbide in an electro-thermal reactor. *Solid State Phenomena*. 2021;316:147–152. https://doi.org/10.4028/www.scientific.net/SSP.316.147
16. Simeiko K.V., Malinouski A.I., Grebenkov A.Zh., Sayenko S.Yu., Lobach K.V., Kustovskaya A.D., Liaposhchenko O.O., Sklabinskyi V.I. Development of technologies of silicon carbide producing (Review). *Vestnik NYaTs RK = NNC RK Bulletin*. 2021;2:30–41 (in Russ.). https://doi.org/10.52676/1729-7885-2021-2-30-41
17. *Higher Transcendental Function*: in 3 v. V. I. McGraw – Hill Book Company. Inc.; 1953. 395 p.
18. Fikhtengolts G.M. *Kurs differentsial'nogo i integral'nogo ischisleniya* (*Course of Differential and Integral Calculus*): in 3 v. Moscow–Leningrad: Gostekhizdat; 1948. V. 2. 793 p. (in Russ.).
19. Barabanov N.N., Zemskova V.T., Mitrofanov A.D., Ermolaeva E.V. Mathematical modeling of the process of carbidization of syntactic foams. *Izv. Vyssh. Uchebn. Zaved. Khim. Khim. Tekhnol*. = *ChemChemTech*. 1998;41(5):32–34 (in Russ.).
20. Li X., Zhang G., Tronstad R., Ostrovski O. Reduction of quartz to silicon monoxide by methane-hydrogen mixtures. *Metall. Mater. Trans. B: Process Metall. Mater. Processing Sci*. 2016;47(4): 2197–2204. https://doi.org/10.1007/s11663-016-0670-5
21. Wallis G. *Odnomernye dvukhfaznye techeniya* (*One-Dimensional Two-Phase Flows*): transl. from Engl. Moscow: Mir; 1972. 440 p. (in Russ.).
[Wallis G. *One-Dimensional Two-Phase Flows*. NY: McGraw-Hill; 1969. 408 p.]
22. Ageev O.A. *Karbid kremniya: tekhnologiya, svoistva, primenenie* (*Silicon Carbide: Technology, Properties, Applications*). Kharkov: ISMA; 2010. 531 p. (in Russ.). ISBN 978-966-02-5445-9

14. Kuzevanov V.S., Zakozhurnikov S.S., Zakozhurnikova G.S., Garyaev A.B. Finely dispersed silicon carbide synthesis model in the electrothermal reactor with periodic batch loading. *J. Phys.: Conf. Ser.: Hydrodynamics and Heat and Mass Transfer*. 2020;1683:022054. https://doi.org/10.1088/1742-6596/1683/2/022054
15. Kuzevanov V.S., Zakozhurnikov S.S., Zakozhurnikova G.S. Model and results of a study of the synthesis of finely dispersed silicon carbide in an electro-thermal reactor. *Solid State Phenomena*. 2021;316:147–152. https://doi.org/10.4028/www.scientific.net/SSP.316.147
16. Семейко К.В., Малиновский А.И., Гребеньков А.Ж., Саенко С.Ю., Лобач К.В. Кустовская А.Д., Ляпощенко А.А., Склабинский В.И. Разработки технологий получения карбида кремния (обзор). *Вестник НЯЦ РК*. 2021;2:30–41. https://doi.org/10.52676/1729-7885-2021-2-30-41
17. *Higher Transcendental Function*: in 3 v. V. I. McGraw – Hill Book Company. Inc.; 1953. 395 p.
18. Фихтенгольц Г.М. *Курс дифференциального и интегрального исчисления*: в 3-х т. М.–Л.: Гостехиздат; 1948. Т. 2. 793 с.
19. Барабанов Н.Н., Земскова В.Т., Митрофанов А.Д., Ермолаева Е.В. Математическое моделирование процесса карбидизации синтактных пенопластов. *Известия вузов. Химия и химическая технология*. 1998;41(5):32–34.
20. Li X., Zhang G., Tronstad R., Ostrovski O. Reduction of quartz to silicon monoxide by methane-hydrogen mixtures. *Metall. Mater. Trans. B: Process Metall. Mater. Processing Sci*. 2016;47(4): 2197–2204. https://doi.org/10.1007/s11663-016-0670-5
21. Уоллис Г. *Одномерные двухфазные течения*: пер. с англ. М.: Мир; 1972. 440 с.
22. Агеев О.А. *Карбид кремния: технология, свойства, применение*. Харьков: ИСМА; 2010. 531 с. ISBN 978-966-02-5445-9

About the authors

Vyacheslav S. Kuzevanov, Dr. Sci. (Eng.), Professor, Department of Energy, National Research University MPEI, Volzhsky Branch, (69, Lenina pr., Volzhsky, Volgograd oblast, 404110, Russia). E-mail: vyacheslavkuzevanov@gmail.com. Scopus Author ID 57204855036, RSCI SPIN-code 7835-6260.

Sergey S. Zakozhurnikov, Cand. Sci. (Eng.), Associate Professor, Department of Higher Mathematics-3, Institute for Advanced Technologies and Industrial Programming, MIREA – Russian Technological University (78, Vernadskogo pr., Moscow, 119454, Russia). E-mail: jester.vlz@mail.ru. Scopus Author ID 57198768825, ResearcherID ABG-4696-2020, RSCI SPIN-code 1864-0437, https://orcid.org/0000-0003-2354-9656

Galina S. Zakozhurnikova, Cand. Sci. (Eng.), Associate Professor, Department of Heat Engineering and Hydraulics, Volgograd State Technical University, (28, Lenina pr., Volgograd, 400005, Russia). E-mail: galya.vlz@mail.ru. Scopus Author ID 57198782591, ResearcherID HHY-8485-2022, RSCI SPIN-code 7209-9481, https://orcid.org/0000-0002-4870-0749

Об авторах

Кузеванов Вячеслав Семенович, д.т.н, профессор, кафедра энергетики, Филиал ФГБОУ ВО «Национальный исследовательский университет «МЭИ» в г. Волжском (404110, Волгоградская область, г. Волжский, пр-т Ленина, д. 69). E-mail: vyacheslavkuzevanov@gmail.com. Scopus Author ID 57204855036, SPIN-код РИНЦ 7835-6260.

Закожурников Сергей Сергеевич, к.т.н., доцент, кафедра высшей математики-3, Институт перспективных технологий и индустриального программирования, ФГБОУ ВО «МИРЭА – Российский технологический университет» (119571, Россия, Москва, пр-т Вернадского, д. 86). E-mail: jester.vlz@mail.ru. Scopus Author ID 57198768825, ResearcherID ABG-4696-2020, SPIN-код РИНЦ 1864-0437, https://orcid.org/0000-0003-2354-9656

Закожурникова Галина Сергеевна, к.т.н., доцент, кафедра теплотехники и гидравлики, ФГБОУ ВО «Волгоградский государственный технический университет» (400005, Россия, Волгоград, пр-т им. В.И. Ленина, д. 28). E-mail: galya.vlz@mail.ru. Scopus Author ID 57198782591, ResearcherID HHY-8485-2022, SPIN-код РИНЦ 7209-9481, https://orcid.org/0000-0002-4870-0749

Translated from Russian into English by V. Glyanchenko
Edited for English language and spelling by Dr. David Mossop

MIREA – Russian Technological University
78, Vernadskogo pr., Moscow, 119454, Russian Federation.
Publication date *April 30, 2024.*
Not for sale

МИРЭА – Российский технологический университет
119454, РФ, Москва, пр-т Вернадского, д. 78.
Дата опубликования *30.04.2024.*
Не для продажи

www.finechem-mirea.ru